

Targeting host cell ion channels to treat herpesvirus infections

Holli Carden

Submitted in accordance with the requirements for the degree of

Doctor of Philosophy

The University of Leeds

Faculty of Biological Sciences

School of Molecular and Cellular Biology

May 2021

The candidate confirms that the work submitted is her own and that appropriate credit has been given where reference has been made to the work of others.

This copy has been supplied on the understanding that it is copyright material and that no quotation from the thesis may be published without proper acknowledgement.

© The University of Leeds and Holli Carden

This thesis is dedicated to my late grandfather, who inspired my life-long enthusiasm for learning at a very young age, without which I would not have embarked upon this endeavour.

Acknowledgements

My PhD study has been a life-changing experience, which would not have been possible without the support and guidance of several important people.

Firstly, I would like to thank my supervisor, Professor Adrian Whitehouse, for his consistent support throughout my PhD study. His advice and experience have guided me during my academic research.

I would also like to thank the Whitehouse, Hewitt and Aspden laboratory group members, both past & present for providing a wonderful working environment, and occasional social outing, particularly Dr Nnenna Nwogu and Dr Eleanor Walton, for their encouragement and friendship.

I am grateful for the funding received towards my PhD from Rosetrees Trust. Additionally, many thanks to the NHS Pathology department at the LGI, for welcoming me with open arms as a new colleague, while my PhD was put on hold during the COVID-19 pandemic.

The support of my family and friends has sustained my perseverance and self-belief, and I would like to express my gratitude to them all. Particular thanks go to my mother for sharing commutes to and from campus; where she listened to the recap of my day even though it was littered with technical jargon, and friend, Krysten, who understood the pressures of PhD study from her own investigation into American History and was willing to escape for educational trips abroad when proper laboratory planning allowed time away.

Last but by no means least, I would like to thank my fiancé Steve, for providing unwavering support and faith in me over the last four years.

Abstract

The *Herpesviridae* are associated with life-long persistent infections. The nine human herpesviruses cause a range of acute and chronic diseases, ranging from cold sores to cancer. There is an urgent need for the development of novel anti-herpesvirus drugs; targeting host ion channels, which are manipulated during various viral replication cycles, present a novel avenue for pan-herpes antiviral treatments.

Investigation utilising potassium channel inhibitors led to identification of K_v1.3 as essential during lytic KSHV replication. Both RNA and protein levels of K_v1.3 during KSHV reactivation were increased; overexpression causes increased channel activity and membrane hyperpolarisation in cells hosting lytic replication, this was measured through patch clamping techniques and flow cytometry. Experiments into the cause of K_v1.3 upregulation found a virally mediated mechanism, requiring both viral Rta and host Sp1 transcription factor activity.

As channel blockade is sufficient to prevent this hyperpolarisation mechanism; K_v1.3 knockdown cell lines were generated using a lentiviral system, thus reducing levels of lytic replication. However, reactivation can be rescued with the use of a calcium ionophore, bypassing the membrane hyperpolarisation which leads to calcium influx. To confirm this influx, a ratiometric dye was used to detect calcium levels throughout the first 24 hours of reactivation from latency. This influx activates the calcium signalling pathway via NFAT1 nuclear localisation, and various NFAT-mediated genes are upregulated 24 hours post-reactivation.

Additional research into the effects of K⁺ channel blockers on HSV-1 infection has shown a conservation of cell membrane hyperpolarisation, followed by calcium influx in cells infected with HSV-1.

Given the abundance of ion channel inhibitors currently in clinical trials; this viral driven, hyperpolarisation mediated, calcium influx mechanism presents a novel avenue for pan-herpes antiviral treatments.

Contents

Targeting host cell ion channels to treat herpesvirus infections	ii
Acknowledgements.....	iv
Abstract	v
Abbreviations	xiv
1 Introduction	2
1.1. <i>Herpesviridae</i>	2
1.1.1. Structure.....	3
1.1.2. Life cycle.....	4
1.1.3. <i>Alphaherpesvirinae</i>	7
1.1.4. <i>Betaherpesvirinae</i>	9
1.1.5. <i>Gammaherpesvirinae</i>	10
1.2. Treatment of <i>Herpesviridae</i> infections.....	24
1.3. Ion Channels	27
1.3.1. K ⁺	29
1.3.2. Ca ²⁺	32
1.3.3. Other channels	36
1.4. Viral dependence on host ion channels	41
1.2.1. Host ion channel modification by <i>Herpesviridae</i>	42
1.5. Ion channel inhibitors.....	46
1.5.1. Ion channel inhibitors as therapeutics	47
1.5.2. Ion channel inhibitors as antivirals	48
1.6. Thesis aim	50
2 Materials and Methods.....	52
2.1. Materials.....	52
2.1.1. Cell lines	52
2.1.2. Antibodies.....	52
2.1.3. Oligonucleotides	53
2.1.4. Compounds	54
2.1. Methods.....	55
2.2.1. Cell culture.....	55
2.2.2. Cell Proliferation Assay (MTS)	55
2.2.3. Plasmid preparation.....	56
2.2.4. Transfection.....	56

2.2.5. Patch Clamping	57
2.2.6. Confocal Microscopy.....	57
2.2.7. RNA extraction.....	58
2.2.8. Quantitative real-time polymerase chain reaction (qRT-PCR)	59
2.2.9. Chromatin Immunoprecipitation	59
2.2.10. Subcellular Fractionation	59
2.2.11. Western Blotting	60
2.2.12. Flow Cytometry.....	61
2.2.13. Statistical analysis	61
3 Investigating the role of host K⁺ channels during KSHV lytic replication	63
3.1. Introduction.....	63
3.2. General K ⁺ inhibition affects KSHV lytic replication	64
3.3. K _v activity is required for KSHV lytic replication.....	65
3.4. K _v 1.3 is required for KSHV lytic replication.....	66
3.5. K _v 1.3 expression is induced during KSHV lytic replication.....	67
3.6. KSHV Rta protein induces K _v 1.3 expression	68
3.7. K _v 1.3 activity is increased during KSHV lytic replication	70
3.8. KSHV lytic replication causes cell membrane hyperpolarisation	70
3.9. K _v 1.3 is essential for KSHV lytic replication.....	72
3.10. Channel activity in K _v 1.3 knockdown is decreased.....	72
3.11. K _v 1.3 knockdown inhibits KSHV lytic replication.....	73
3.12. Discussion	75
4 Investigating the role of hyperpolarisation-induced calcium influx in KSHV lytic replication	79
4.1. Introduction.....	79
4.2. Calcium ionophores can override K _v 1.3 depletion to activate KSHV lytic replication	80
4.3. A calcium influx is induced during KSHV lytic replication	80
4.4. KSHV lytic replication is suppressed by Ca _v inhibition.....	82
4.5. Ca _v 3 inhibition is sufficient to suppress KSHV lytic replication	84
4.6. Ca _v 3 expression during KSHV lytic replication	85
4.7. Ca _v 3.2 activity is required during KSHV lytic replication	85
4.8. Calcineurin-NFAT inhibition prevents KSHV lytic replication	86
4.9. NFAT1 is localized in the nucleus during KSHV lytic replication.....	87
4.10. NFAT-responsive gene expression is induced by KSHV lytic replication	88

4.11. Discussion	90
5 Investigating the conservation of K⁺ channel mediated hyperpolarisation-induced calcium influx in HSV-1 and HCMV lytic replication cycles	93
5.1. Introduction.....	93
5.2. Both HSV-1 and HCMV successfully infect HFF cells	94
5.3. K ⁺ inhibitors reduce HSV-1 and HCMV lytic replication	95
5.4. HSV-1 lytic replication requires K _{Ca} 3.1 channel activity.....	96
5.5. HCMV lytic replication requires K _v 3.4 channel activity.....	98
5.6. Membrane hyperpolarisation occurs during both HSV-1 and HCMV lytic replication cycles	100
5.7. Calcium influx occurs during HSV-1 and HCMV lytic replication	101
5.8. Calcineurin activity is required during HSV-1 and HCMV lytic replication.....	102
5.9. Discussion	104
6 Discussion	107
6.1. Future work.....	115
References.....	117
Appendix.....	125

Table of Figures

Figure 1.1 Schematic representing human <i>Herpesviridae</i> phylogeny.....	2
Figure 1.2 Structure of <i>Herpesviridae</i>	3
Figure 1.3 Schematic of <i>Herpesviridae</i> cell entry, showing both receptor binding mediated cell fusion (left) and endocytosis (right).....	4
Figure 1.4 Schematic of <i>Herpesviridae</i> lytic replication cycle.	7
Figure 1.5 VZV rash, presenting as varicella (left) and zoster (right).....	8
Figure 1.6 Schematic of Epstein Barr virus infection.	11
Figure 1.7 KSHV seroprevalence worldwide.	13
Figure 1.8 The KSHV genome codes for temporal expression of open reading frames.	14
Figure 1.9 Schematic showing the biphasic lifecycle of KSHV.....	15
Figure 1.10 Schematic displaying temporal cascade of KSHV lytic gene expression and DNA replication.	17
Figure 1.11 Various clinical manifestations of Kaposi's Sarcoma.....	19
Figure 1.12 KS incidence rates in males worldwide..	20
Figure 1.13 Computed Tomography (CT) scan of a patient with PEL (left), and post-treatment scan lacking pleural effusions (right).....	22
Figure 1.14 CT scans of a patient with MCD, showing the abdomen (left), pelvis (centre) and lungs (d).	23
Figure 1.15 Schematic of acyclovir chain termination mechanism of action during lytic HSV-1 replication.....	25
Figure 1.16 Other <i>Herpesviridae</i> treatments in clinical use and development with different targets.	26
Figure 1.17 Schematic showing different types of ion channels in their closed and open states.	28
Figure 1.18 Schematic of K _v channel domains.....	30
Figure 1.19 Schematic of monomeric BK _{Ca} channel domains within the cell membrane, showing both α - and β - subunits.....	31
Figure 1.20 Schematic showing calcium signalling of NFAT pathway.	33
Figure 1.21 Schematic of Ca _v channel domains within the cell membrane, showing α - $\alpha_2\sigma$ - and β - subunits.....	34
Figure 1.22 Schematic of SOCE pathway.	36
Figure 1.23 Schematic of CFTR channel (left) and LRCC8A monomer (right).	39
Figure 1.24 Schematic of viral lifecycle showing stages at which various viroporins are utilised by each virus.	40
Figure 1.25 Schematic displaying various host ion channel families required during viral replication, along with respective viruses.....	42

Figure 1.26 Schematic displaying host ion channel families affected during HSV-1 replication.	43
Figure 1.27 Schematic of channel dysregulation seen during VZV or HCMV replication cycles.	45
Figure 1.28 Schematic displaying effect of LMP-1 on Orai1 during EBV latency.	46
Figure 3.1 Cell viability of TREx BCBL1-Rta in the presence of KCl (a), Qn (b) or TEA (c).....	64
Figure 3.2 Effect of general potassium inhibitors on KSHV lytic replication.....	65
Figure 3.3 Effect of K _v inhibitor, 4AP, on KSHV lytic replication.....	65
Figure 3.4 Effect of K _v 1.3 inhibitors on KSHV lytic replication.	66
Figure 3.5 Effect of K _{Ca} 3.1 inhibitor, TRAM-34, on KSHV lytic replication.....	67
Figure 3.6 K _v 1.3 expression in TREx BCBL1-Rta cells.	67
Figure 3.7 Expression levels of K _v 1.3 after transfection of GFP-viral constructs.....	68
Figure 3.8 K _v 1.3 and IL-6 expression in transfected U87 cells, pre-treated with Mith A or DMSO.	69
Figure 3.9 ChIP analysis of proteins binding the K _v 1.3 promoter region in latent and lytically infected cells.....	69
Figure 3.10 K _v 1.3 channel activity as seen via patch clamping in TREx BCBL1-Rta cells.	70
Figure 3.11 Mean fluorescence caused by serial dilutions of DiBAC ₄ (3).	71
Figure 3.12 DiBAC ₄ (3) mean fluorescence of TREx BCBL1-Rta cells, as measured by flow cytometry.	71
Figure 3.13 RNA and protein levels of K _v 1.3 in knockdown cell lines, compared to the control scramble cell line.	72
Figure 3.14 K _v 1.3 channel activity and hyperpolarisation as seen via patch clamping.....	73
Figure 3.15 DiBAC ₄ (3) mean fluorescence, measured via flow cytometry.	73
Figure 3.16 Viral gene expression in scramble and ΔK _v 1.3 cell lines.....	74
Figure 3.17 Schematic of Rta-mediated, K _v 1.3 dependent hyperpolarisation mechanism.....	77
Figure 4.1 Effect of A23187 on KSHV lytic replication in scramble and ΔK _v 1.3 cell lines.	80
Figure 4.2 Emission and excitation spectra of calcium bound and calcium free Fura Red.	81
Figure 4.3 Emission and excitation spectra of calcium bound and calcium free Fura Red.	81
Figure 4.4 Calcium ratio in wild-type TREx BCBL1-Rta cells (a) and scramble or ΔK _v 1.3 cell lines (b), measured via flow cytometry.	82

Figure 4.5 Cell viability of TREx BCBL1-Rta cells after 24-hour treatment with nifedipine or SKF.....	83
Figure 4.6 Dose-dependent effect of general voltage-gated calcium channel inhibitors, nifedipine (a) and SKF-96365 (b), on KSHV reactivation.....	83
Figure 4.7 Cell viability of TREx BCBL1-Rta cells after 24-hour treatment with flunarizine (a), mibefradil (b) or pimoziide (c).....	84
Figure 4.8 Dose-dependent effect of Ca _v 3 inhibitors; flunarizine (a), mibefradil (b) and pimoziide (c), on KSHV lytic replication.	84
Figure 4.9 Ca _v 3 expression in HFB and TREx BCBL1-Rta cells (a) and Ca _v 3.2 expression in TREx BCBL1-Rta cells during a reactivation time-course (b).....	85
Figure 4.10 PNG and A23187 treatment in TREx BCBL1-Rta cells.	86
Figure 4.11 Dose-dependent effect of CsA on lytic KSHV replication.	86
Figure 4.12 Subcellular fractionation of TREx BCBL1-Rta cells during latency and KSHV lytic replication.	87
Figure 4.13 Confocal microscopy images showing the localisation of NFAT1 in TREx BCBL1-Rta cells during latent or KSHV lytic replication and after pre-treatment with a variety of drugs.....	88
Figure 4.14 NFAT-mediated gene expression during latency and KSHV lytic replication in the presence and absence of ShK or PNG in TREx BCBL1-Rta cells (a) and in scramble and ΔK _v 1.3 cell lines (b)..	89
Figure 4.15 Schematic of hyperpolarisation-mediated calcium influx-dependent NFAT relocalisation mechanism, triggered by KSHV lytic replication, along with potential therapeutic targets.....	90
Figure 5.1 Viral proteins from HFFs infected with serial dilutions of HSV-1 stock.....	94
Figure 5.2 UL69 RNA levels in infected HFFs during a timecourse (a) and with varying serial dilutions (b).	94
Figure 5.3 Viral expression levels after pre-treatment with general K ⁺ blockers in HFFs.	95
Figure 5.4 RNA levels of viral genes in general K ⁺ channel inhibitor reinfection assays.	96
Figure 5.5 HSV-1 RNA (a) and protein (b) levels after pre-treatment with CTX or TRAM in HFFs or in a reinfection assay (c)..	97
Figure 5.6 K ⁺ channel expression in mock- and HSV-1 infected HFFs.	97
Figure 5.7 HSV-1 RNA (a) and protein (b) levels after pre-treatment with ShK in HFFs or in a reinfection assay (c).	98
Figure 5.8 HCMV RNA (a) and protein (b) levels after pre-treatment with ShK in HFFs or in a reinfection assay (c).	98
Figure 5.9 K ⁺ channel expression in mock- and HCMV infected HFFs (a) and during an HCMV lytic replication time-course (b).	100
Figure 5.10 HCMV RNA (a) and protein (b) levels after pre-treatment with BDS I in HFFs or in a reinfection assay (c).....	99

Figure 5.11 DiBAC₄(3) mean fluorescence of HFFs, as measured by flow cytometry.	100
Figure 5.12 Calcium ratio in HSV-1 infected (a) and HCMV-infected (b) HFFs, measured via flow cytometry.....	101
Figure 5.13 Viral gene expression after pre-treatment with PNG in HFFs.....	102
Figure 5.14 RNA levels of viral genes in CsA pre-treatment reinfection assays.	103
Figure 5.15 Schematic of hyperpolarisation-mediated calcium influx mechanism, conserved during HSV-1, HCMV or KSHV lytic replication.....	104
Figure 6.1 Schematic of KSHV-specific K_v1.3-mediated hyperpolarisation mechanism which occurs upon reactivation of lytic viral replication.	108
Figure 6.2 Schematic of KSHV-specific hyperpolarisation-mediated calcium influx and signalling mechanism which occurs upon reactivation of lytic viral replication.	110
Figure 6.3 Schematic of general K⁺ efflux and hyperpolarisation-mediated calcium influx and signalling mechanism which occurs during herpesviral lytic replication.	113

List of Tables

Table 2.1 Primary antibodies used.....	52
Table 2.2 Secondary antibodies used.....	53
Table 2.3 Human primer sequences used during qRT-PCR analysis	53
Table 2.4 Viral primer sequences used during qRT-PCR analysis	54
Table 2.5 Drug compounds with solvents and suppliers used	54
Table 2.6 Solutions used during patch clamping experiments.....	57
Table 2.7 Tris-glycine polyacrylamide running gel solutions	60

Abbreviations

AIDS	acquired immunodeficiency syndrome
ANGPT2	angiopoietin 2
AMP	adenosine monophosphate
ATP	adenosine triphosphate
BDS	blood depressing substance
BK _{Ca}	large-conductance calcium activated potassium
BKPyV	BK polyomavirus
BL	Burkitt's lymphoma
BUNV	Bunyamwera orthobunyavirus
Ca _v	voltage-gated calcium
CAEBV	chronic active Epstein-Barr virus infection
CFTR	cystic fibrosis transmembrane conductance regulator
CHIKV	Chikungunya virus
ChIP	chromatin immunoprecipitation
COVID-19	coronavirus disease 2019
COX2	cyclooxygenase 2
CRAC	calcium release activated calcium
CREB	cyclic AMP response element-binding protein
CsA	cyclosporin A
CSF2	granulocyte-macrophage colony-stimulating factor 2
CT	Computed Tomography
CTX	charybdotoxin
CVB3	coxsackievirus B3
DENV	Dengue virus
DiBAC ₄ (3)	bis-(1,3-dibutylbarbituric acid) trimethine oxonol
DLBCL	Diffuse Large B cell Lymphoma
DMEM	Dulbecco's modified Eagle's medium
DMSO	dimethyl sulphoxide
DNA	deoxyribose nucleic acid
Dox	doxycycline hyclate
DTT	dithiothreitol

EBV	Epstein-Barr virus
EGTA	ethylene glycol-bis (β -aminoethyl ether)-N,N,N',N'-tetraacetic acid
ER	endoplasmic reticulum
EV71	enterovirus 71
FBS	foetal bovine serum
FDA	food and drug administration
FGF2	fibroblast growth factor 2
GAPDH	glyceraldehyde 3-phosphate dehydrogenase
GFP	green fluorescent protein
GPCR	G protein-coupled receptor
HAART	highly active antiretroviral therapy
HCMV	human cytomegalovirus
HCN	hyperpolarization-activated cyclic nucleotide-gated
HCV	hepatitis C virus
HEK-293T	human embryonic kidney expressing the SV40 T antigen
HEPES	(4-(2-hydroxyethyl)-1-piperazineethanesulphonic acid
HFB	human foetal brain
HFF	human foreskin fibroblast
HHV	human herpesvirus
HVS	herpesvirus saimiri
HIV	human immunodeficiency virus
HPV16	human papillomavirus 16
HSV	herpes simplex virus
HL	Hodgkin lymphoma
HRP	horseradish peroxidase
IAV	influenza A virus
IBV	influenza B virus
ICV	influenza C virus
ICTV	international committee on taxonomy of viruses
IE	immediate early
IF	immunofluorescence
IFN γ	interferon gamma

IK _{Ca}	intermediate-conductance calcium activated potassium
IM	Infectious mononucleosis
IP ₃	inositol 1,4,5-triphosphate
IRIS	immune reconstitution inflammatory syndrome
JCPyV	JC polyomavirus
K _{Ca}	calcium activated potassium
K _{ir}	inwardly-rectifying potassium
K _v	voltage-gated potassium
K _{2P}	two pore domain potassium
kbp	kilobase pair
KSHV	Kaposi's sarcoma-associated herpesvirus
KS	Kaposi's Sarcoma
LANA	latency associated nuclear antigen
LAT	latency associated transcript
LPM-1	latent membrane protein 1
LRR	leucine-rich repeat
MCD	Multicentric Castleman's Disease
MCPyV	Merkel cell polyomavirus
MERS	Middle Eastern respiratory syndrome coronavirus
MgTX	Margatoxin
Mith A	Mithramycin A
MHV-68	murine γ -herpesvirus
mRNA	messenger ribose nucleic acid
Na _v	voltage-gated sodium
NBD	nucleotide binding domain
NF	nuclear factor
NFAT	nuclear factor of activated T cells
NHL	non-Hodgkin lymphoma
NK	natural killer
NPPB	5-nitro-2-(3-phenyl-propylamino) benzoic acid
ORF	open reading frame
PBL	plasmablastic lymphoma

PBS	phosphate buffered saline
PEL	primary effusion lymphoma
PHN	post-herpetic neuralgia
PNG	(2R/S)-6-prenylnaringenin
Qn	quinine hydrochloride dihydrate
qRT-PCR	quantitative real-time polymerase chain reaction
RCAN1	down syndrome critical region gene 1
RNA	ribose nucleic acid
RRE	Rta-response element
Rta	replication and transcription activator protein
SARS-CoV	severe acute respiratory syndrome coronavirus
SDS	sodium dodecyl sulphate
SK _{Ca}	small-conductance calcium activated potassium
SOCE	store operated calcium entry
Sp1	specificity protein 1
STIM	stromal interaction protein
T _{EM}	effector memory T
TEA	tetraethylammonium chloride
TEMED	tetramethylethylenediamine
TNF α	tumour necrosis factor alpha
TPC	two-pore channels
TRP	transient receptor potential
TRPM8	transient receptor potential melastatin cation channel 8
TTX	tetrodotoxin
vFLIP	viral FLICE inhibitory protein
VRAC	volume-regulated anion channel
VSD	voltage sensor domain
VZV	varicella-zoster virus
4AP	4-114 aminopyridine

Chapter 1

Introduction

1 Introduction

1.1. *Herpesviridae*

Herpesviridae family members belong to the taxonomic order *Herpesvirales* (ICTV, 2021), which comprises three families of viruses; *Alloherpesviridae*, *Herpesviridae* and *Malacoherpesviridae*, and share common structure and life cycles. *Herpesviridae* infect mammals, reptiles, and birds. Notably, nine members of the *Herpesviridae* are known to cause lifelong persistent infections and a range of diseases in humans. *Herpesviridae* is further categorised into three subfamilies; *Alphaherpesvirinae*, *Betaherpesvirinae* and *Gammaherpesvirinae* (Figure 1.1), which share around 25 common open reading frames (ORFs) and around 50 homologues playing vital roles in viral replication (Albà et al., 2001). Classification into subfamilies was initially based on biological properties such as host range, replication strategies and genomic variation. It is thought the subfamilies diverged from a common ancestor around 200 million years ago, as estimated through molecular phylogenetics (Albà et al., 2001).

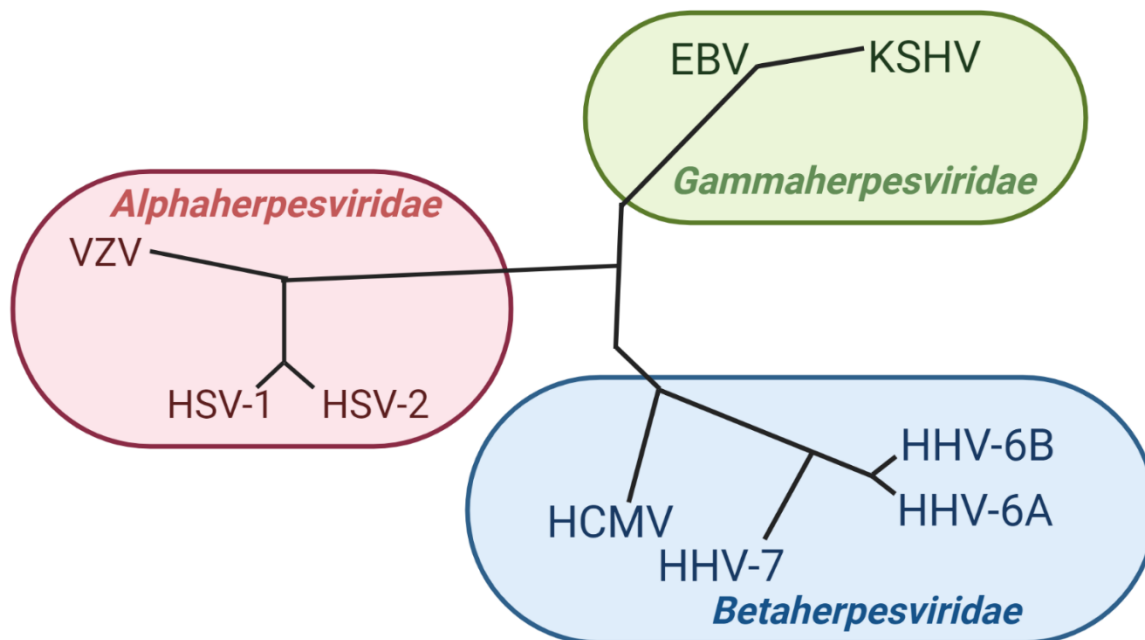


Figure 1.1 Schematic representing human *Herpesviridae* phylogeny. Created with Biorender.com

1.1.1. Structure

The *Herpesviridae* virion structure is unique, which defines them from other viral families (Carter and Saunders, 2008). All herpesvirus virions share four major structural features; the genome, capsid, tegument and envelope (Figure 1.2).

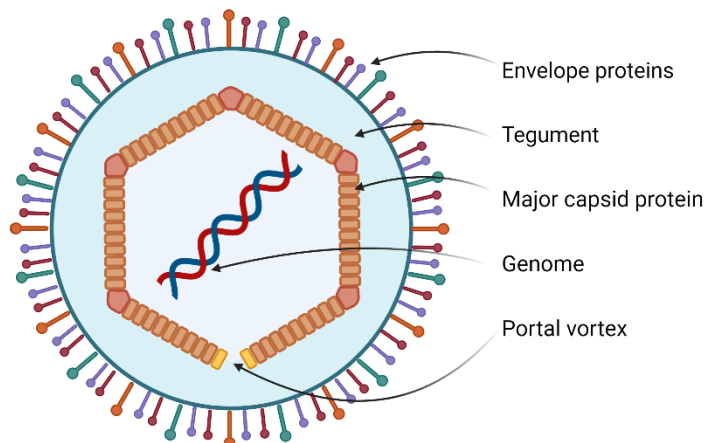


Figure 1.2 Structure of *Herpesviridae*. The tegument layer, located between the capsid and envelope, is unique to *Herpesviridae*. Created with BioRender.com.

Herpesviridae belong to Baltimore class I and the double-stranded DNA genomes vary from 120 to 250 kilobase pairs (kbp), encoding for between 70 to 220 ORFs (Carter and Saunders, 2008; Guo et al., 2010; Grinde, 2013; Arias et al., 2014; Kennedy et al., 2015; Kostopoulou et al., 2017). Herpesviral genomes, particularly *Gammaherpesvirinae*, also contain human homologs which aid in immune evasion; such as KSHV viral interferon response factor which reduces the interferon-mediated antiviral immune response (Choi et al., 2001). An icosahedral capsid with triangulation number 16 symmetry encases the herpesviral genome. The capsid consists of 161 capsomers and is approximately 100-130nm in diameter (Brown and Newcomb, 2011). To complete the capsid, a final protein complex replaces the 162nd capsomer (Brown and Newcomb, 2011). This creates a portal to allow genome exit and entry. The tegument envelops the nucleocapsid and is a proteinaceous layer unique to *Herpesviridae*. Teguments vary between subfamilies and contain between 10 and 40 viral proteins (Guo et al., 2010). These proteins vary in role; some are essential for virion structure, others are vital for infection, immune evasion or viral DNA replication. Host proteins, viral and cellular messenger RNA (mRNA) have also been shown localised within the tegument layer through mass spectrometry of purified virions (Leroy et al., 2016). The entire herpesvirus

particle is contained in a host cell-derived lipid bilayer envelope expressing around 10 viral glycoproteins essential for host cell binding, fusion and entry (Guo et al., 2010), such as the HSV-1 gD-nectin binding, which then enables gH- and gL-mediated viral entry; gB undergoes conformational changes including insertion into the host membrane followed by trimerization and pore formation (Connolly et al., 2021).

1.1.2. Life cycle

Herpesviridae life cycle starts as the virion attaches to receptors on the surface of a host cell (Figure 1.3) (Carter and Saunders, 2008; Grinde, 2013). Most *Herpesviridae* attach via heparan sulphate (O'Donnell and Shukla, 2008). While Epstein-Barr virus (EBV), and other family members, can enter the cell by endocytosis upon endosomal compartment acidification; typically, virus-host cell fusion occurs through interactions with viral envelope glycoproteins (Miller and Hutt-Fletcher, 1992). Three glycoproteins, gH, gB and gL, are conserved throughout *Herpesviridae*. The addition of viral glycoproteins into the host cell membrane causes changes in conformation, leading to pore formation and delivery of viral tegument proteins and the nucleocapsid into the host cytoplasm (O'Donnell and Shukla, 2008). The dynein/dynactin motor protein complex then transports the nucleocapsid along the network of

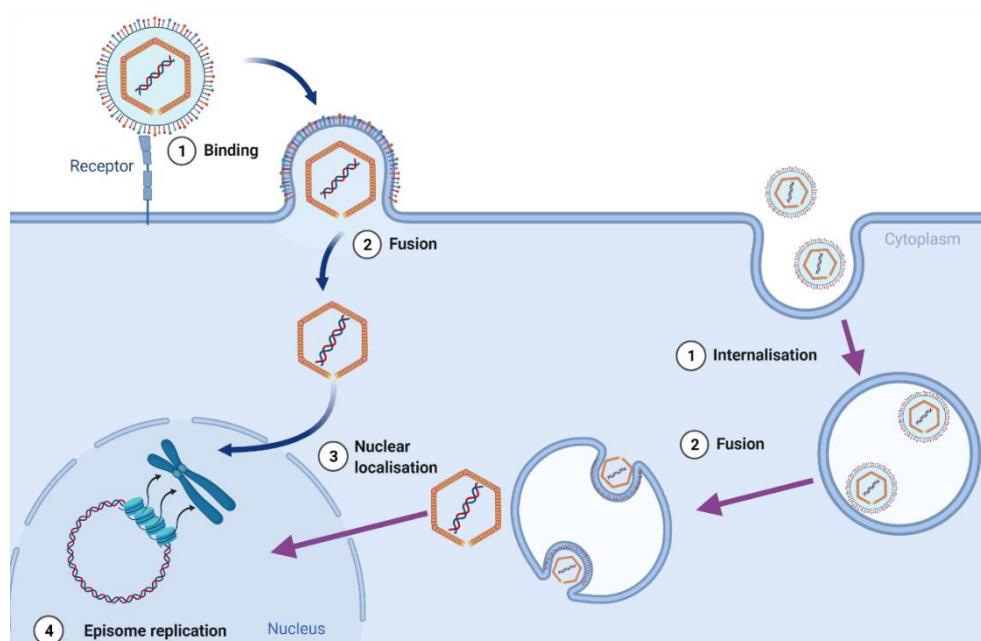


Figure 1.3 Schematic of *Herpesviridae* cell entry, showing both receptor binding mediated cell fusion (left) and endocytosis (right). After viral entry, the genome-containing capsid is transported to the nucleus and the genome is injected into the nucleus via the nuclear pore complex.

host microtubules to the nucleus. Viral DNA enters the nucleus via the nuclear pore complex. Upon nuclear entry, the viral DNA undergoes a conformational change, becoming circular through joining of the GC-rich elements within the genome-flanking terminal repeats (Grinde, 2013). Latent or lytic gene expression cycles can then occur.

1.1.1.1 Latency

Latency is the term given to the transcriptionally dormant phase of *Herpesviridae* replication (Carter and Saunders, 2008; Grinde, 2013; Gershon et al., 2015). During latency, viral gene expression is limited, and production of infectious virions is prevented. Host cell epigenetic silencing machinery allows the viral genome to be maintained as a non-integrated circular episome, which is condensed into chromatin and packaged by histones (Grinde, 2013). A major difference between subfamilies is the ratio of infected cells and types of cells undergoing latent infection. Latency is the default replication programme for *Gammapherpesvirinae* infections, only a small number of cells undergo the process of 'reactivation' into the lytic replication process. However, both *Alpha-* and *Betaherpesvirinae* favour lytic replication, causing cytolysis of the host cells, while a minority of infected cells survive and harbour latent virus.

In *Alphaherpesvirinae* only the latency associated transcripts (LATs), consisting of approximately 5 genes are actively expressed (Gershon et al., 2015; Kennedy et al., 2015). The latent cycle enables evasion of host antiviral mechanisms and immune signalling pathways, which allows the establishment of a lifelong persistent infection characteristic of *Herpesviridae*. The three human *Alphaherpesvirinae* establish latent infections in neuronal cells (Grinde, 2013; Gershon et al., 2015; Kennedy et al., 2015). This is achieved through retrograde transport to neurons, from the initial site of skin infection.

In contrast, *Betaherpesvirinae* and *Gammapherpesvirinae* establish latent infection in cells which undergo mitotic replication. Therefore, when host cells engage in mitosis, the viral genome is replicated by cellular DNA polymerases (Grinde, 2013). While most genes are silenced during latency, a small percentage of latency associated genes are expressed. For

example, latent EBV can follow three separate latency programmes, termed latency I through III. During latency I, only non-coding RNA and EBNA-1 are expressed, whereas in latency III the expression of various EBV proteins encourage B cell proliferation (Grinde, 2013).

1.1.1.2 Lytic replication

Herpesviridae lytic replication follows a regimented chronological flow of gene expression (Figure 1.4) (Carter and Saunders, 2008; Grinde, 2013; Gershon et al., 2015; Kennedy et al., 2015; Aneja and Yuan 2017). Initially the host RNA polymerase II sequentially transcribes viral mRNAs, which then acquire 5' caps and 3' polyadenylated tails to allow translation and prevent degradation of the viral mRNA, respectively. Following nuclear export, translation of the viral transcripts occurs within the host cell cytoplasm.

Immediate early (IE) genes are first to be expressed and encode proteins important for transcriptional control of the early genes (Carter and Saunders, 2008; Grinde, 2013; Kennedy et al., 2015; Aneja and Yuan, 2017). The functions of early gene products vary; with roles including viral genome replication, late gene transcription initiation and viral mRNA accumulation (Grinde, 2013; Kennedy et al., 2015; Aneja and Yuan, 2017). This latter process allows for the amalgamation of internal products present in progeny virions. Lastly, late viral genes are expressed; these encode proteins which play structural roles in newly assembled virions and help with the infection and subversion of a new host cell. Viral DNA replication is carried out by a viral DNA polymerase instead of the host enzyme, unlike latent viral DNA replication (Carter and Saunders, 2008; Grinde, 2013; Kennedy et al., 2015; Aneja and Yuan, 2017; Zarrouk et al., 2017). Viral DNA synthesis produces long repeats of the entire viral genome in head-to-tail concatemers, which are then cleaved into the single full-length genomes (Carter and Saunders, 2008; Grinde, 2013; Kennedy et al., 2015; Aneja and Yuan, 2017). Herpesvirus capsid assembly occurs in the nucleus. Pre-formed capsids are packaged with newly replicated DNA, before budding through the nuclear membrane. Initial envelopment begins at the inner nuclear membrane, allowing entry to the perinuclear space which is followed by outer membrane fusion and release into the cytoplasm. Nucleocapsids then

associate with tegument proteins and bud into vesicles synthesised by the host trans-Golgi network. Within these vesicles, the virions fully mature and nascent infectious virions emerge from the cell following vesicle fusion with the plasma membrane (Carter and Saunders, 2008; Guo et al., 2010; Grinde, 2013; Kennedy et al., 2015; Aneja and Yuan, 2017).

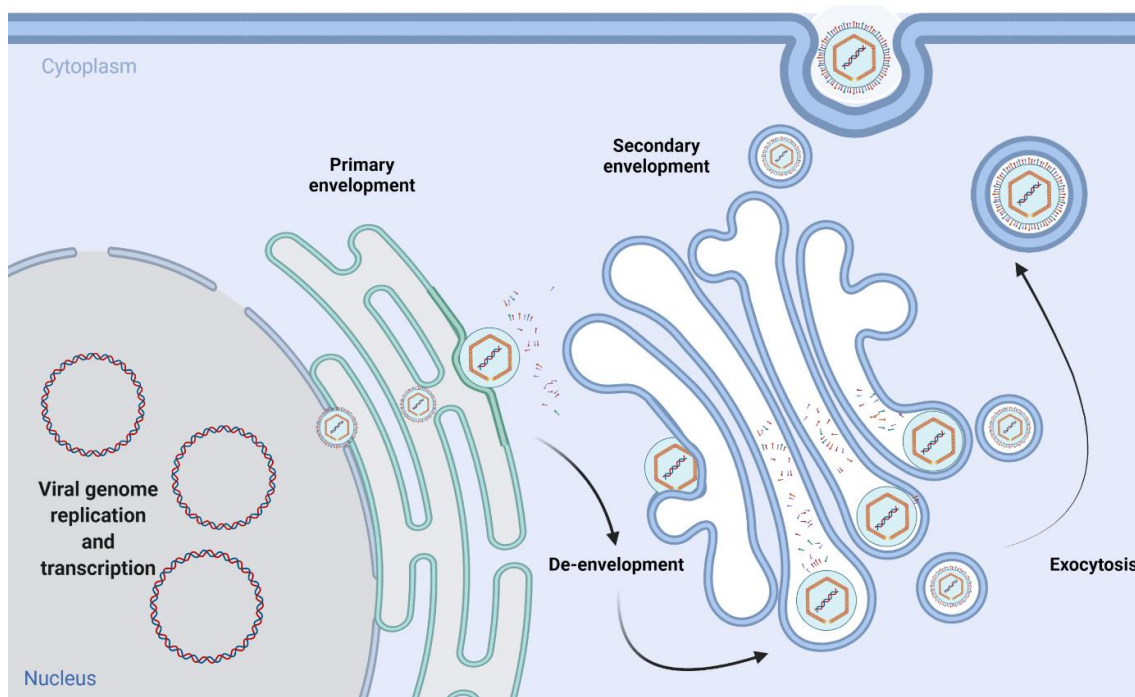


Figure 1.4 Schematic of *Herpesviridae* lytic replication cycle. Upon reactivation or primary infection, lytic replication leads to the production of lytic viral proteins and replication of the viral genome. These are assembled into progeny virions, which are then released from the host cell. Created with BioRender.com

1.1.3. *Alphaherpesvirinae*

Alphaherpesvirinae cause latent infection in neuronal cells (Kennedy et al., 2015; Poole and James, 2018). Upon initial infection, which is most often in epithelial cells, rapid lytic replication results in host cell death, presenting as itchy lesions at the site of infection in humans (Guo et al., 2010; Brown and Newcomb, 2011; Grinde, 2013; Kennedy et al., 2015; Poole and James, 2018). However, asymptomatic infection has been known to occur. The spread of virus to surrounding sensory neurons, most likely through retrograde transport, marks the start of a lifelong persistent infection (O'Donnell and Shukla, 2008; Guo et al., 2010; Kennedy et al., 2015; Poole and James, 2018). *Alphaherpesvirinae* differ from both *Betaherpesvirinae* and *Gammaherpesvirinae* through their short replicative life cycle, which rapidly completes with host cell cytolysis.

Of the *Alphaherpesvirinae* members, three are known for their ability to cause infection in humans; herpes simplex virus type-1 (HSV-1), herpes simplex virus type-2 (HSV-2) and varicella-zoster virus (VZV) (ICTV, 2021; O'Donnell and Shukla, 2008; Guo et al., 2010; Grinde, 2013; Kennedy et al., 2015; Poole and James, 2018). These are also known as human herpesviruses (HHV) 1-3, respectively. HSV-1 and VZV are usually acquired during childhood (Birkmann and Zimmermann, 2016; Ding et al. 2017; Kennedy et al., 2015; Poole and James, 2018; Zheng et al., 2014). All are spread through direct contact with an infected individual, although HSV-2 is typically sexually transmitted. Viral shedding and thus transmission can occur in asymptomatic individuals. Both HSV-1 and HSV-2 can cause sporadic skin lesions; normally around the mouth, genital regions, and the cornea, although infection of the fingers can also occur and is referred to as herpetic whitlow (Birkmann and Zimmermann, 2016; Kennedy et al., 2015; Poole and James, 2018; Zheng et al., 2014). Additionally, both can cause encephalitis in more severe infections, a third of these cases occur upon primary infection (Kennedy et al., 2015). In developed countries, HSV-1 is the most common cause of infection-based blindness. Globally, around two thirds of the world's population are latently infected with HSV-1 (James et al., 2020).

Upon primary infection VZV causes chickenpox, or varicella (Stankus et al., 2000; Grinde, 2013; Kennedy et al., 2013; Gershon et al., 2015; Kennedy et al., 2015; Woodward et al., 2019). This disease is characterized by itchy red lesions located on the trunk and usually



Figure 1.5 VZV rash, presenting as varicella (left) and zoster (right). The varicella rash occurring in an infant is seen throughout the torso, along with both arms and the chin (obtained from Gershon et al., 2015), zoster rash on the torso of an adult is localised to the area around the infected neuron (obtained from Stankus et al., 2000).

occurs during childhood (Figure 1.5). As with HSV infection, VZV primary infection can lead to encephalitis in severe cases. However primary infection can also be complicated by inflammation or damage of the spinal cord, and cranial or spinal nerve roots (Gershon et al., 2015; Kennedy et al., 2015; Woodward et al., 2019). If VZV reactivation occurs, symptoms can present as shingles, also known as zoster; a skin rash contained to the epithelial cells near the infected neuronal cell, localized pain is also more likely to occur with zoster, due to the proximity to neurons (Stankus et al., 2000; Grinde, 2013; Kennedy et al., 2013; Gershon et al., 2015; Kennedy et al., 2015; Woodward et al., 2019).

1.1.4. *Betaherpesvirinae*

Betaherpesvirinae undergo a prolonged life cycle in comparison to *Alphaherpesvirinae*, which progresses over several days (Griffiths et al, 2014; Oberstein and Shenk, 2017). These viruses tend to infect renal monocytes and cells within the reticuloendothelial system and secretory glands (Grinde, 2013; Kostopoulou et al., 2017). HHV-5, HHV-6A, HHV-6B and HHV-7 are the major *Betaherpesvirinae* with tropism for humans (ICTV, 2021). All but HHV-5 belong to the genus *Roseolovirus* and symptomatic lytic *Roseolovirus* infection is characterised by a fever, followed by a pink rash in young infants (Grinde, 2013; Zanella et al. 2020). HHV-6A is the more common cause of primary infection in Africa, while HHV-6B is more predominant in Europe and North America. HHV-6A and HHV-6B are also associated with renal transplant rejection (Zanella et al. 2020).

HHV-5 is also known as human cytomegalovirus, or HCMV, and is the largest of the human *Herpesviridae* (Bakhrarov et al., 1995; Kapoor et al., 2012; Griffiths et al, 2014; Kostopoulou et al., 2017; Oberstein and Shenk, 2017; Hancock et al., 2021). While HCMV infection is common worldwide, the infection is normally asymptomatic in healthy individuals however in the immunocompromised, HCMV can cause severe or sometimes fatal diseases depending on the end-organ infected through HCMV viraemia. This includes hepatitis, retinitis, pneumonitis, and gastrointestinal ulcers (Griffiths et al, 2014). Primary infection or reactivation occurring during pregnancy can lead intrauterine infection of the foetus, causing severe

disease and foetal disabilities, such as sensorineural hearing loss, in 20% of cases (Grinde, 2013; Griffiths et al, 2014; Kostopoulou et al., 2017; Oberstein and Shenk, 2017).

1.1.5. *Gammaherpesvirinae*

As with *Betaherpesvirinae* infections, *Gammaherpesvirinae* display limited host range. *Gammaherpesvirinae* tend to preferentially infect and establish latency within lymphocytes, however productive replication can also occur in both endothelial and epithelial cells (Arias et al., 2014; Aneja and Yuan, 2017; Mesri et al., 2010; Shannon-Lowe and Rickinson, 2019). There are two known human *Gammaherpesvirinae*; Epstein-Barr virus (EBV), or HHV-4, and Kaposi's sarcoma-associated herpesvirus (KSHV), or HHV-8. *Gammaherpesvirinae* are often associated with lymphoproliferative disorders and lymphomas, although KSHV can also cause Kaposi's Sarcoma (KS), a predominantly endothelial cell tumour. EBV is found in all cases of Burkitt's Lymphoma (BL) (Guo et al., 2010; Shannon-Lowe and Rickinson, 2019), whereas KSHV is the causative agent of both Multicentric Castleman's Disease (MCD) and Primary Effusion Lymphoma (PEL) (Arias et al., 2014; Aneja and Yuan, 2017; Mesri et al., 2010). Oncogenic viruses are the root cause of around 10% of the annual cancer incidence globally; over 1% of new cancer cases are EBV-associated annually whereas KSHV-association is less common (Shannon-Lowe and Rickinson, 2019).

1.1.5.1. Epstein-Barr virus (EBV)

Upon initial entry into a new host, EBV infects both epithelial cells and resting B cells in the oropharynx (Shannon-Lowe and Rickinson, 2019). Once B cells are infected, EBV latency can occur, limiting replication to a restricted subset of genes and establishing a lifelong persistent infection (Figure 1.6). Varying expression patterns of these latently expressed genes are thought to contribute to onset of BL and Hodgkin Lymphoma (HL). As with other *Herpesviridae*, reactivation can occur in immunocompromised individuals, such as AIDS patients or transplant recipients.

EBV has been linked to five lymphomas (Dellis et al., 2011; Shannon-Lowe and Rickinson, 2019), BL, HL, Diffuse Large B cell Lymphoma (DLBCL), plasmablastic lymphoma, (PBL) and,

during co-infection with KSHV, PEL (Narkhede et al, 2018). BL was first described to affect African children by Denis Burkitt in 1958, however the correlation between EBV itself was not identified until 1964 by Tony Epstein and Yvonne Barr (Epstein et al., 1967; Shannon-Lowe and Rickinson, 2019). While EBV was found within a BL-derived cell line and present in all BL tumours from equatorial Africa, the association was doubted for years due to the widespread seropositivity of EBV globally. When EBV was also found within all BL tumours from a second geographically distinct region, Papua New Guinea, the link between EBV and BL was accepted (Epstein et al., 1967). In addition to incidences within these geographical regions, BL can also occur sporadically elsewhere, however EBV-positive tumours account for around 10% of cases. AIDS-associated BL became a highly common tumour in HIV-positive individuals during the AIDS epidemic; incidence rates surpassed those seen in endemic regions, of which around 35% are EBV-positive. While links to EBV latency have been detected for several lymphomas, the presence of EBV episomes in tumours varies from around 10% positivity in DLBCLs to 80% in PBL (Delecluse et al., 1997; Cohen et al., 2014).

Furthermore, association between EBV and numerous other cancers not of B cell origin have been shown, including T and NK lymphomas, epithelial gastric carcinoma, and

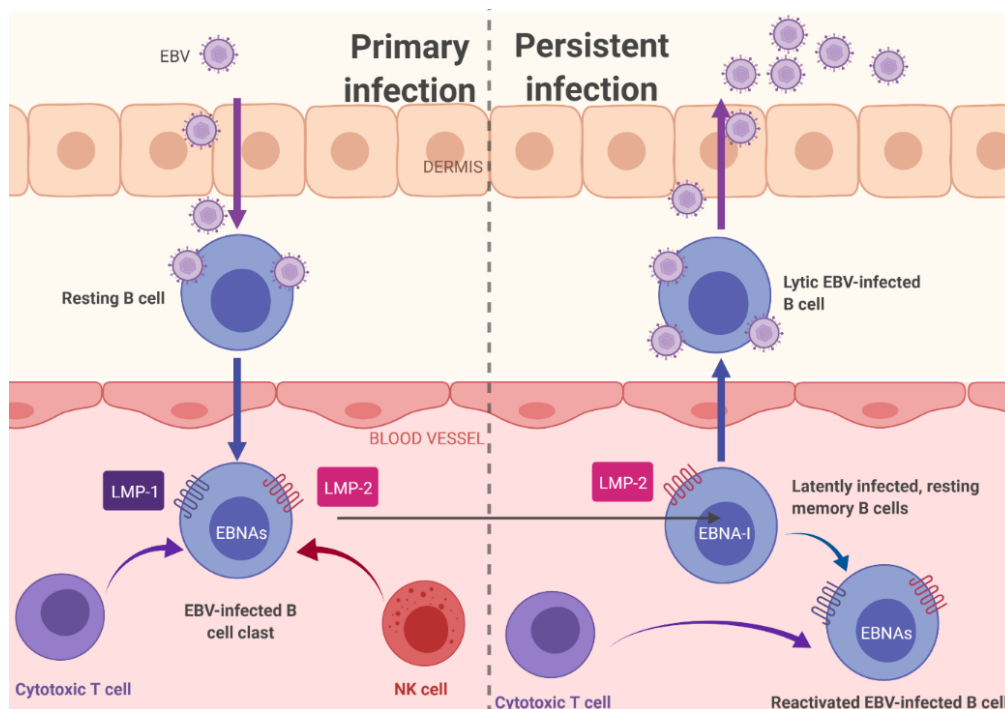


Figure 1.6 Schematic of Epstein Barr virus infection. During latency III expression of EBV genes is limited to LMP-1, LMP-2 and EBNAs, although expression is further reduced in stages until only EBNA-1 is expressed during latency I. Created with BioRender.com

nasopharyngeal carcinoma (Shannon-Lowe and Rickinson, 2019). Rarely, leiomyosarcoma can occur during late-stage AIDS, particularly in children, due to the oncogenic activity of EBV (McClain et al., 1995). This range of tumour types is unique to EBV, as other oncogenic viruses cause cancer within the cell type utilised during viral infection, such as KSHV-association with cancers of B cell or endothelial cell origin, the sites of latent and lytic replication, respectively. In addition to cancers, EBV can cause infectious mononucleosis (IM), also known as glandular fever (Luzuriaga and Sullivan, 2010; Shannon-Lowe and Rickinson, 2019). Most cases of IM occur in childhood or adolescence and IM is common worldwide, with a prevalence of 90%. While most cases of IM are mild, with symptoms including fever and pharyngitis, complications such as hepatitis and rupture of the spleen can occur in rare cases (Luzuriaga and Sullivan, 2010). Both CD4+ and CD8+ T cell populations expand in patients with IM, while this restricts the primary infection, their activity can contribute to IM symptoms. Furthermore, a history of symptomatic IM has been linked to increased risk of both multiple sclerosis (Zivadinov et al., 2019).

IM can infrequently persist as chronic active Epstein-Barr virus infection (CAEBV), most cases occur in East Asian populations, particularly in young children (Luzuriaga and Sullivan, 2010; Kimura and Cohen, 2017; Shannon-Lowe and Rickinson, 2019). However, recently CAEBV has increasingly been reported in adults, with more severe symptoms. CAEBV was first investigated in the 1980s and is defined as severe IM-symptoms which last for more than three months. While CAEBV can be fatal, leading to organ failure or EBV-related lymphomas, some individuals stabilise without treatment; the variation in prognosis is not yet understood (Kimura and Cohen, 2017).

1.1.5.2. Kaposi's Sarcoma-associated Herpes Virus (KSHV)

KSHV belongs to the *Rhadinovirus* genus of *Gammaherpesvirinae* and is closely related to the oncogenic animal herpesviruses; murine γ -herpesvirus (MHV-68), and herpesvirus saimiri (HVS) (Mesri et al., 2010; Arias et al., 2014; Cesarman et al., 2019). Seroprevalence of KSHV varies across geographical regions (Figure 1.7); the highest rates in sub-Saharan Africa with

more than half of the population having seropositivity. One third of individuals in Mediterranean countries display seropositivity. Fewer than ten percent are seropositive in the rest of Europe, Asia, and North America. Incidence of seroprevalence increases among men who have sex with men, and African migrants (Mesri et al., 2010; Cesarman et al., 2019).

The highest levels of KSHV shedding are found in KSHV-infected oral epithelial cells, accounting for the highest levels of virus and spread in saliva, which is likely to be the most common method of KSHV transmission. This transmission route would lead to non-sexual transmission of KSHV between children in endemic areas, thus accounting for the high level of childhood infections in sub-Saharan Africa. Additionally, there is also strong evidence that the virus can be transmitted through sexual contact, especially between men who have sex with men. Other cases point to iatrogenic routes; such as transplantation of infected organs and transfusion of infected blood (Mesri et al., 2010; Cesarman et al., 2019).

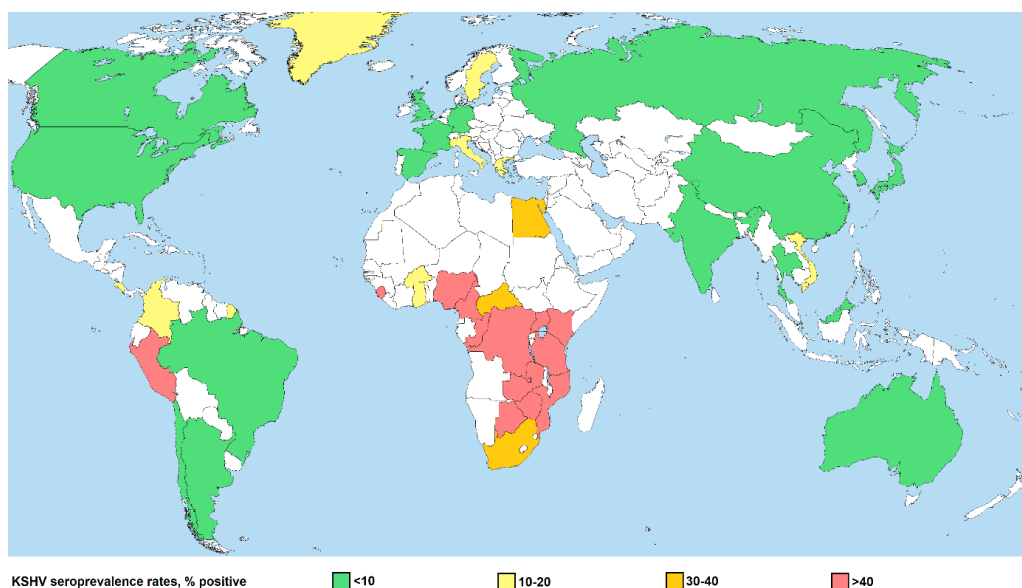


Figure 1.7 KSHV seroprevalence worldwide. Seropositivity varies, with the highest rates occurring in sub-Saharan Africa. Adapted from Mesri et al, 2010.

1.1.5.2.1. KSHV life cycle

As is characteristic of *Herpesviridae*, the KSHV life cycle contains both latent and lytic replication programmes, enabling a lifelong, persistent infection through co-operative phases of both programmes. Upon initial infection, KSHV virions bind to host cell membranes. In addition to the classic *Herpesviridae* receptor heparin sulphate, ephrin A2 and integrins also

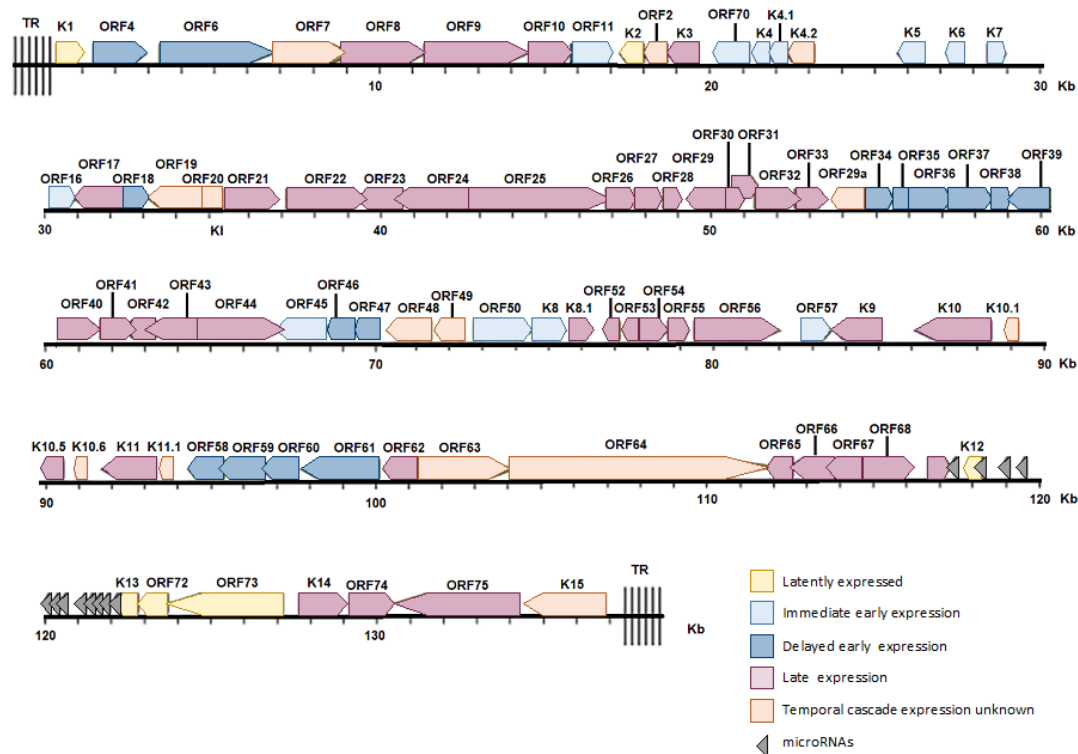


Figure 1.8 The KSHV genome codes for temporal expression of open reading frames. Latently expressed genes are shown in yellow. Immediate early genes are light blue, with delayed early genes in dark blue and late genes are shown in purple. MicroRNAs are shown as grey triangles and genes of unknown temporal expression are orange. Figure generated using information from Arias et al, 2014.

interact with KSHV gB, gH and gL to enable cellular entry (O'Donnell. and Shukla, 2008; Kumar and Chandran, 2016). This entry typically occurs via endocytosis, however KSHV can utilise macropinocytosis and clathrin-mediated endocytosis to enter specific cell types (Kumar and Chandran, 2016). After internalisation of the KSHV virion within a host cell, the nucleocapsid is trafficked to the nuclear pore and the KSHV genome is injected into the nucleus, where either phase of replication can occur. However, latency is thought to be the default phase.

The KSHV genome consists of around 165-70 kb encoding roughly 85 genes (Figure 1.8), including a BCL-2 homolog, v-cyclin, vGPCR and the viral homolog to Flice inhibitory protein (vFLIP), in addition to several proteins that promote DNA synthesis and immune evasion (Choi et al., 2001; Järviluoma and Ojala, 2006).

1.1.5.2.2. KSHV Latency

After nuclear entry, the KSHV genome circularises through joining of terminal repeats and tethers to the host chromatin via latency associated nuclear antigen (LANA), a latent viral

protein (Järviluoma and Ojala, 2006; Mesri et al., 2010; Arias et al., 2014; Aneja and Yuan, 2017). This is achieved through direct binding of LANA to host nucleosomes via its chromatin binding motif, located near the N-terminal domain (Matsumura et al., 2010). The viral genome is then replicated during cell division to maintain a persistent infection as extrachromosomal episomes. Viral gene expression is restricted in latent KSHV-infected cells with only a handful of genes expressed, including LANA, vCyclin, vFLIP, kaposin's A, B and C, and 12 pre-microRNAs (Choi et al., 2001; Järviluoma and Ojala, 2006; Arias et al., 2014). The ORFs of the latency-associated genes are in actively transcribed 'latency regions', which lack nucleosomes and repressive histone modifications (Järviluoma and Ojala, 2006; Arias et al., 2014). Whereas lytic gene expression is hindered by condensed chromatin and thus no infectious virions are produced. LANA is the major regulator of KSHV latency and maintains the chromatinization, replication and segregation of KSHV episomes and thus is vital for long term persistent KSHV infection (Järviluoma and Ojala, 2006;).

Stable maintenance of KSHV episomes is not 100% efficient among any latently infected cell types, this is likely due to errors in replication and segregation during cell division. However,

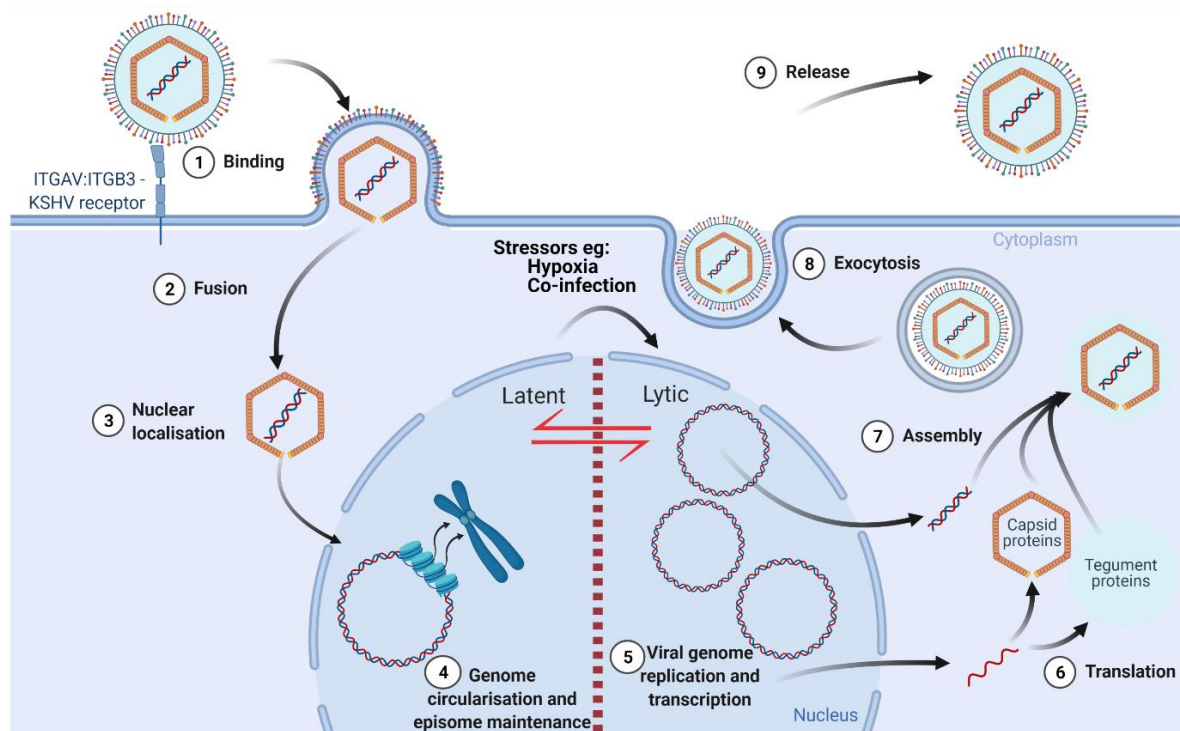


Figure 1.9 Schematic showing the biphasic lifecycle of KSHV. Upon initial infection, KSHV virions bind to integrins, ephrins or heparin sulphate. The genome, within the capsid, is transported to the nucleus and is injected via the nuclear pore. Latent or lytic replication occurs, progeny virions are synthesised and released during lytic replication. Created with BioRender.com

the infection of new cells through virion production in the lytic phase sustains the population of latently infected cells that would otherwise diminish, therefore allowing long term persistence of the virus in an infected individual through the balance of both KSHV replication programmes which are shown in Figure 1.9.

1.1.5.2.3. KSHV Lytic replication

Cells infected with latent KSHV can be reactivated into lytic replication in response to various external factors including stress, hypoxia, viral coinfections, immunosuppression, or inflammation (Mesri et al., 2010; Arias et al., 2014; Aneja and Yuan, 2017; Manners et al., 2018). This reactivation is also necessary to continue persistent infection within the latent B cell reservoir as viral episomes are lost over time during B cell mitosis. While co-infection of several viruses has been shown to encourage KSHV lytic replication, including HIV, HPV, both species of HSV and all human *Betaherpesvirinae*, through inflammatory cytokines induced during immune responses to viral infection; coinfection of EBV hinders KSHV lytic replication (Aneja and Yuan, 2017).

Additionally, latently infected cell culture systems can be induced to undergo lytic replication with treatment of chromatin de-modifying chemicals, such as 5'-azacytidine, sodium butyrate, 12-O-tetradecanoylphorbol-13-acetate and valproic acid. These factors lead to episomal reconfiguration into an active chromatin state, allowing the expression of all KSHV genes in its sequential flow and the mass production of infectious virions (Chang et al., 2000; Aneja and Yuan, 2017).

Several host pathways have also been implicated in promoting lytic replication, including both calcium signalling (Chang et al, 2000; Zoetewij et al., 2001; Aneja and Yuan, 2017) and NF- κ B pathways (Aneja and Yuan, 2017). Some calcium ionophores are sufficient to reactivate KSHV lytic replication, via activity of both calcineurin and NFAT (Chang et al, 2000; Zoetewij et al., 2001). The NF- κ B pathway is hijacked by KSHV to assist in regulating the latent-lytic switch; the latently expressed vFLIP activates the pathway, thus preventing Rta transactivation and AP-1-mediated viral gene expression (Aneja and Yuan, 2017). While, NF- κ B is

subsequently downregulated upon reactivation to prevent the suppression of viral gene expression, downregulation is temporary as the pathway is required to avoid apoptosis of the host cell during KSHV lytic replication (Keller et al., 2000).

Upon induction, expression of the entire viral genome, viral DNA replication, and the assembly of infectious virions occurs in a temporally regulated manner. In contrast to other oncogenic herpesviruses, in which latent gene expression plays a prominent role in tumorigenesis, lytic replication is also required for tumorigenicity and the spread of KSHV infection (Manners et al., 2019). Regulation of the latent to lytic switch is mediated by both viral and cellular factors, however a critical factor is the KSHV-encoded replication and transcription activator protein (Rta) that activates multiple downstream target genes through Rta-responsive elements and autoregulates its own promoter (Aneja and Yuan, 2017; Mesri et al., 2010). The expression of Rta is necessary and sufficient to disrupt latency and trigger the complete lytic cascade (Gradoville et al., 2000). The transactivation domain of Rta is located on the C-terminus and allows binding to numerous Rta-response elements (RREs) within both KSHV and cellular genomes, thus inducing lytic gene expression. Often, these interactions require the cellular transcription factor RBP-J κ which localises Rta to RREs for transactivation (Papp et al., 2018). Several other cellular factors including Oct-1, c-Jun, Sp1, STAT3 and c/EBP α , have also been found to aid Rta-mediated transactivation in a variety of gene promoters (Papp et al., 2018). Furthermore, Rta mediates gene expression through proteasomal degradation of

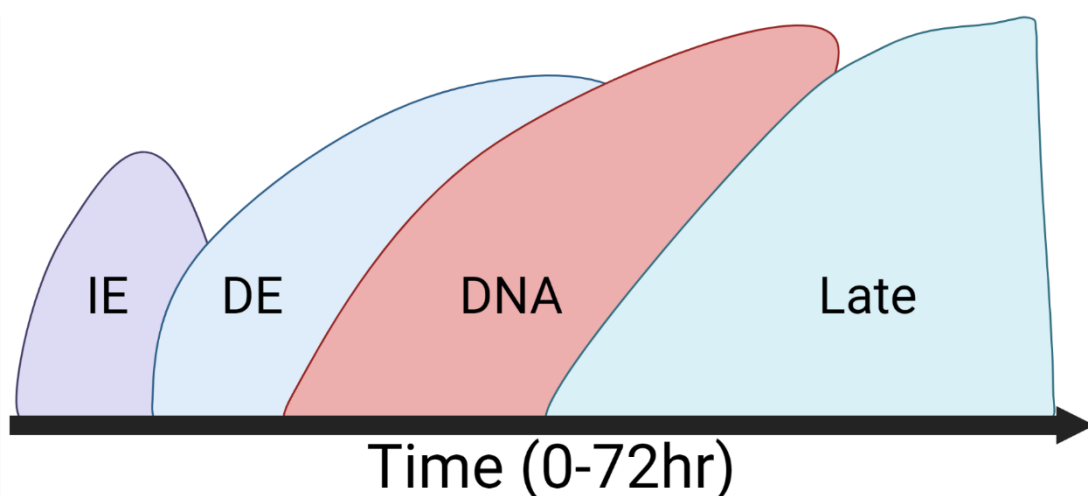


Figure 1.10 Schematic displaying temporal cascade of KSHV lytic gene expression and DNA replication. Immediate early genes replicate first, expression of these can trigger transcription of delayed early genes. Upon sufficient viral DNA replication, late gene expression can occur. Created with BioRender.com

transcriptional repressors. Targets include LANA and the Notch signalling protein Hey-1, via its E3 ubiquitin ligase domain. As the master regulator of KSHV latent and lytic replication programmes respectively, LANA and Rta interactions are strictly controlled. Both can have antagonistic effects on the other, ensuring efficient persistence in the host (Broussard and Damania, 2020).

KSHV gene expression and DNA replication follows a tightly regulated cascade (Figure 1.10) (Aneja and Yuan, 2017). IE genes are the first to be expressed after reactivation and are expressed by the host RNA polymerase. Delayed-early gene expression occurs after IE protein production has begun. DNA replication follows early gene expression and replicates via a rolling circle mechanism, forming concatemers utilising the viral DNA polymerase, unlike the dependence upon host DNA polymerase during latent replication. Cleavage of concatemers occurs during packaging of the genome into the viral capsid. Once KSHV DNA replication has begun, expression of structural proteins begins (Aneja and Yuan, 2017; Mesri et al., 2010). These proteins form the capsid, tegument and envelope layers and are termed late proteins due to their temporally regulated expression, which can be blocked by viral DNA polymerase inhibitors, further indicating late gene expression is dependent upon viral DNA replication. Various delayed-early viral proteins are required to form a preinitiation complex, which then permits late gene expression via binding of ORF24 to the TATA sequence within promoter sequences on late genes. Subsequently, RNA polymerase II is recruited to the complex and gene transcription can occur (Chen et al., 2017). Control of late gene expression is similar in all *Herpesviridae*.

Assembly of newly formed KSHV proteins and packaging of the viral genome occurs in an autocatalytic manner (Aneja and Yuan, 2017; Mesri et al., 2010). The viral genome is encapsidated within the nucleus, with nuclear egress occurring via binding with both layers of the nuclear membrane, encompassing both envelopment and release of the capsid. Within the cytoplasm, tegument proteins are acquired, consisting of both host and KSHV proteins (Leroy et al., 2016). ORF45 promotes transportation of the unenveloped virion to the Golgi complex, where envelopment of the virion occurs. The mature virion can then be transported to the

cellular membrane and released from within Golgi-derived vesicles, through binding of the vesicle and cellular membranes (Aneja and Yuan, 2017).

1.1.5.3. KSHV-associated diseases

Since its discovery, KSHV has been confirmed as the aetiological agent of KS and is associated with two lymphoproliferative disorders, PEL and MCD (Arias et al., 2014; Aneja and Yuan, 2017; Carbone et al., 2015; Mesri et al., 2010; Narkhede et al, 2018). As a result, the International Agency for Research on Cancer has classified KSHV as a group 1 carcinogenic agent.

1.1.5.3.1. Kaposi's Sarcoma

Kaposi's Sarcoma (KS) was first described by Moritz Kaposi over 100 years prior to the identification of KSHV in 1994, after the isolation of herpesvirus DNA from an AIDS-patient KS tumour (Mesri et al., 2010; Arias et al., 2014; Aneja and Yuan, 2017; Cesarman et al., 2019). KSHV is the aetiological agent of KS and it is present in all KS tumours. KS is characterised by dark purple skin or mucosal lesions caused by multifocal angioproliferative neoplasms (Figure 1.11) (Mesri et al., 2010; Cesarman et al., 2019). These can also present within internal organs such as the intestines. KS tumours show a polyclonal makeup, although the most common cell type within these tumours is the spindle cell, which is endothelial in origin (Mesri et al., 2010; Cesarman et al., 2019). KS rarely develops in healthy individuals, however the immunocompromised, especially HIV+ people who have progressed into AIDS symptoms, have a drastically elevated risk. When immunocompetence is restored in patients, for example



Figure 1.11 Various clinical manifestations of Kaposi's Sarcoma. Sites of KS can vary as shown by the lesions on back and nodules on arm (a); KS plaques on legs with tumour-associated oedema (b) and gingival KS nodules (c). All three are from patients with AIDS-associated KS. Obtained from Cesarman et al, 2019.

anti-retroviral AIDS treatment, complete remission of KS tumours can be achieved in 30-50% of cases; however, Kaposi sarcoma-related immune reconstitution inflammatory syndrome (KS-IRIS) can occur with the immune recovery (Bower et al., 2005).

KS-IRIS presents as an exacerbation of KS symptoms, including tumour size and quantity due to immune recovery. In a study of 150 patients with AIDS-associated KS, 6.6% developed KS-IRIS upon initiation of highly active antiretroviral therapy (HAART) (Bower et al., 2005). While patients without KS-IRIS had improved CD4 counts over the course of HAART, those with KS-IRIS had no observed change in their CD4 levels, half also required either chemotherapy or radiotherapy within a year of beginning HAART. Furthermore, KS-IRIS was more likely to occur in patients with higher CD4 counts or those on treatments which combined protease inhibitors and non-nucleoside reverse transcriptase inhibitors (Bower et al., 2005).

KS has four clinical sub-types which vary in disease severity and depend on the extent of immunosuppression: Classic, endemic, iatrogenic, and AIDS-associated (Mesri et al., 2010; Cesarman et al., 2019). Classical KS usually affects older Mediterranean and eastern-European men and is a slow growing tumour. Endemic KS is more aggressive and is widespread in sub-Saharan Africa, it is particularly prevalent in children. Iatrogenic KS usually occurs after transplantation of infected organs, compounded by the immunosuppressive treatment recipients receive to prevent organ rejection. AIDS-associated KS is the most

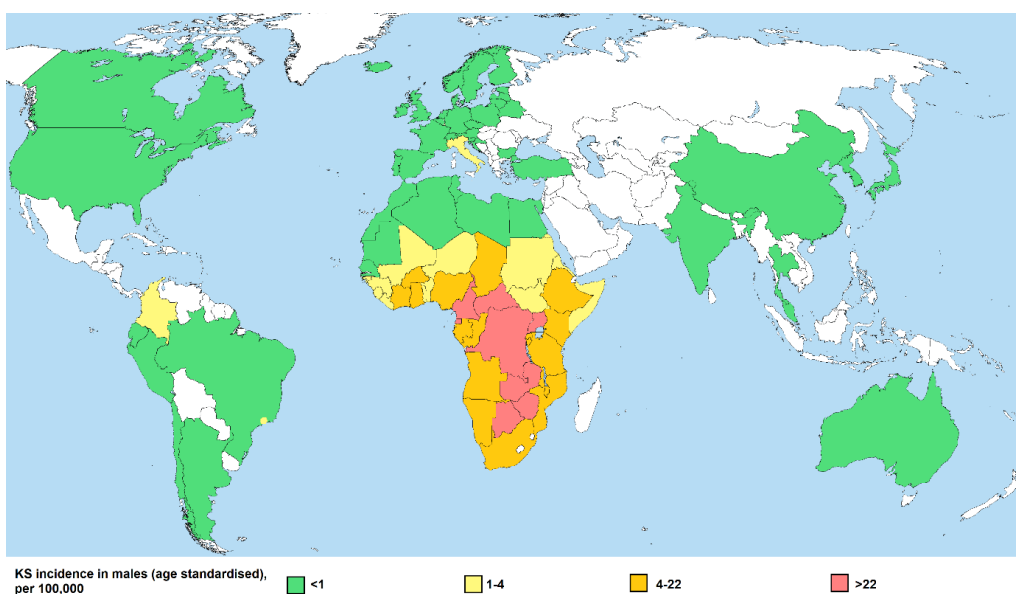


Figure 1.12 KS incidence rates in males worldwide. American, Asian, Australian and European incidence rates are lower than those seen in Sub-Saharan Africa. Adapted from Mesri et al (2010).

recently discovered form of the disease, emerging in 1981; it is also the most severe and causes significant morbidity. AIDS-associated KS is most often seen in men who have sex with men. However, not all AIDS patients with KSHV infection develop KS despite HIV-caused immunosuppression. All subtypes require KSHV infection for tumour development, however evidence suggests that the virus alone is insufficient for tumorigenesis, suggesting that certain cofactors are required (Mesri et al., 2010). Figure 1.12 shows KS incidence rates, globally.

Unlike other oncogenic *Gammaherpesvirinae*, both replication programmes are necessary for KSHV-mediated oncogenesis (Arias et al., 2014; Aneja and Yuan, 2017; Cesarman et al., 2019; Mesri et al., 2010). While the majority of spindle cells within KS tumours are harbouring KSHV latent replication, a proportion of cells undergo spontaneous lytic replication, facilitating the conditions for KSHV-mediated oncogenesis. Upon initial KSHV infection either lytic or latent replication can occur; however, eventually latent replication is favoured. This latent KSHV replication predominantly occurs in B-lymphocytes and a reservoir of latently infected B-cells is established and maintained for life. However, spontaneous reactivation into the lytic replication state occurs in 1-2% of the B-cell reservoir and facilitates infectious virion production, leading to infection of endothelial cells. Viral episomes are rapidly lost in KSHV-infected endothelial cell culture systems unless additional transformational events occur, which suggests KSHV selectively pressures endothelial cell transformation. In addition, spontaneous rounds of lytic replication and infectious virion production repopulate cells within the tumour, where episomes have been lost. Moreover, lytically expressed genes also encode oncogenic proteins required for tumorigenesis. As such the study of both lytic and latent replication programmes are needed to help in the development of novel KS therapeutics.

While AIDS-associated KS can sometimes be directly treated with anti-retroviral therapy, which hinders HIV replication and thus reduces immunosuppression, thereby strengthening the ability to clear KSHV infection, decreasing viral load and reducing KS lesions.

1.1.5.3.2. Primary Effusion Lymphoma

PEL is a rare highly aggressive, non-Hodgkin lymphoma (NHL) (Aneja and Yuan, 2017; Carbone et al., 2015; Narkhede et al, 2018), accounting for around 5% of HIV-associated NHLs and 1% of non-HIV associated lymphomas. Most cases occur in immunocompromised individuals such as AIDS patients or the elderly in KSHV-endemic regions. Men make up the majority of cases in a ratio of 6:1. PEL-transformed B cells invade body cavities, including pleura, peritoneum and pericardium, where they rapidly proliferate. PEL is diagnosed by the presence of CD30, CD38, CD45 and CD138, which are not simultaneously expressed in other aggressive lymphomas, and further confirmation of PEL diagnosis comes from the detection of KSHV; most PEL cases are also co-infected with EBV (Narkhede et al, 2018). The malignancy occurs in B cells persistently infected with KSHV, leading to long term expression of oncogenic viral factors, including LANA, vFLIP, vCyclin and vIL-6. Along with maintaining viral latency, thus contributing to immune evasion, LANA represses both p53 and retinoblastoma proteins, therefore promoting both cell growth and survival. vCyclin activates cyclin-dependent kinase 6, further encouraging proliferation. While vFLIP prevents apoptosis by inhibiting the NF- κ B pathway. Furthermore, apoptosis is hindered by the suppression of cathepsin D, via vIL-6 which is highly concentrated within effusions from PEL cavities (Goto et al., 2014). Figure 1.13 shows scans from a patient with PEL, and post-treatment recovery.

Unlike KS and MCD, PEL has a poor prognosis. However, survival is dependent upon both the number of affected cavities and HIV-status, patients with a single affected body cavity have an overall survival of 1.5 years, whereas those with multiple affected cavities have a survival rate of 4 months (Castillo et al., 2012). While restoration of immunocompetency has no direct effect

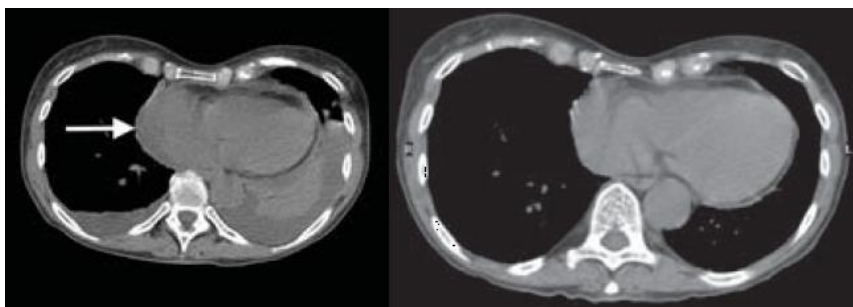


Figure 1.13 Computed Tomography (CT) scan of a patient with PEL (left), and post-treatment scan lacking pleural effusions (right). The arrow in left image shows pericardial effusion. Effusions have shrunk in post-treatment CT scan. Obtained from Patil et al., 2014.

on the disease, the combination of anti-retroviral treatment and chemotherapy in otherwise fit HIV-positive patients can increase survivability for three months, when compared to chemotherapy alone. In patients where chemotherapy successfully causes remission, relapse tends to occur within a year and further treatment is required. Palliative care options to relieve disease burden include radiation and pleurodesis; radiation can alleviate pain in an affected single solid region. Pleurodesis is commonly used as a treatment for mesothelioma, which then causes the fusion of visceral and parietal pleura, to prevent fluid accumulation, this treatment is more likely to be used in elderly or frail individuals who would be unresponsive to more aggressive chemotherapy-based treatments (Birsen et al., 2017).

1.1.5.3.3. Multicentric Castleman's Disease

MCD is a rare lymphoproliferative disorder with various clinical forms (Aneja and Yuan, 2017; Carbone et al., 2015), as with PEL, MCD occurs in B cells with polyclonal origins. The disease can be linked to both KSHV and HIV infection, with KSHV lytic replication more likely to occur than in KS or PEL in HIV-patients. Furthermore, MCD can occur in conjunction to both PEL and KS, along with various other B cell lymphomas. Figure 1.14 shows scans from a patient with MCD.

KSHV is present in almost all HIV-positive MCD patients with the majority of cases exhibiting concurrent KS lesions, however KSHV is less commonly found in HIV-negative MCD patients (Fajgenbaum et al., 2014). IL-6 is highly upregulated in MCD; both human IL-6 and the KSHV-encoded viral homolog. Both HIV and KSHV transcription factors can upregulate IL-6 expression, and synergistically promote replication of both viruses (Thakker and Verma, 2016).

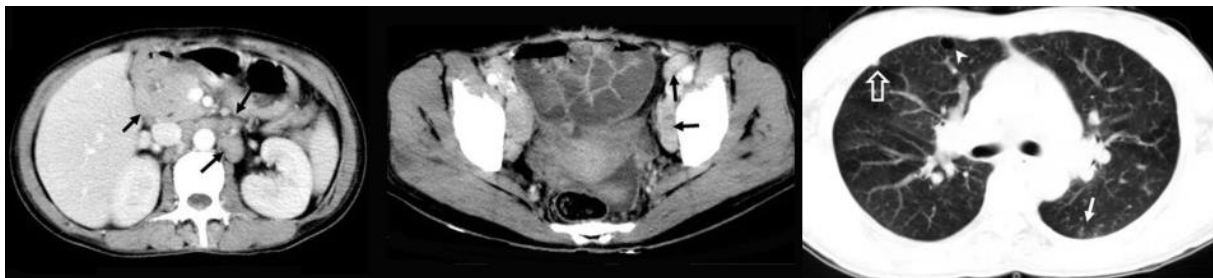


Figure 1.14 CT scans of a patient with MCD, showing the abdomen (left), pelvis (centre) and lungs (d). Enlarged lymph nodes are shown in both the abdomen and pelvis (black arrows). Nodules and cysts are also visible in the lungs (white arrows). Obtained from Zhao et al., 2019.

If left untreated, MCD leads to organ failure, increase susceptibility to infections or lymphoma; all can be fatal (Uldrick et al., 2014). While KSHV-associated MCD is treatable with antiretroviral treatment or chemotherapy, antiretroviral treatment can lead to fatal MCD-IRIS, a similar response to that observed for KS-IRIS. Furthermore, relapses often occur within a month without continued chemotherapy.

1.2. Treatment of *Herpesviridae* infections

As *Herpesviridae* cause persistent life-long infections, there is currently no cure which removes the latent viral reservoir once an individual has been infected with any herpesvirus. However, investigations into CRISPR/Cas9 genome editing have shown both viral replication inhibition and genome eradication of HSV-1, CMV or EBV from infected cells *in vitro* (Poole and James, 2018).

At present, only one vaccine is available for human *Herpesviridae* treatment (Woodward et al, 2019). The vaccine, which targets VZV, has been in use for over 25 years and over 210 million doses have been administered globally. In this time, the yearly incidence rates of primary infection in the United states have decreased from around 4 million prior to vaccine introduction in 1995 to fewer than 350,000 (Woodward et al, 2019). Furthermore, over the same period annual VZV-related hospitalizations and deaths have decreased from over 10,000 and around 150 to around 1700 and fewer than 20, respectively. VZV vaccination safety has also improved, as around 500 adverse effects were recorded per million doses in 1995, whereas around 40 adverse effects per million occurred in 2016 (Woodward et al, 2019). Given the efficacy, and safety, of the VZV vaccine, efforts are continuing to develop vaccines for other human *Herpesviridae*. Additionally, as the tumour virus responsible for highest rates of new cancer cases without an effective vaccine or antiviral, EBV is being targeted for a prophylactic vaccine (Luzuriaga and Sullivan, 2010; Shannon-Lowe and Rickinson, 2019).

However, there are effective antiviral drugs to reduce reactivation or treat a lytically active infection for certain *Herpesviridae* although treatment efficacy varies within subfamilies (De Clercq, 2004; Piret and Boivin, 2011; Coen et al., 2014; Birkmann and Zimmermann, 2016; Poole and James, 2018).

Acyclovir and its derivatives are highly effective anti-herpesvirus agents, specifically for *Alpha-* and *Betaherpesvirinae* subfamilies (De Clercq, 2004; Piret and Boivin, 2011; Birkmann and Zimmermann, 2016; Poole and James, 2018). They act on lytic HSV-1 and HSV-2 infections with a reduced efficacy against VZV. While acyclovir has little effect on the replication of HCMV, some derivatives such as ganciclovir are highly effective (De Clercq, 2004; Poole and James, 2018). Notably, these drugs do not prevent lytic replication in *Gammaherpesvirinae*, EBV or KSHV. Acyclovir functions as a pro-drug which needs to be first phosphorylated by the herpesvirus thymidine kinase (Figure 1.15). Further phosphorylation occurs via host cell kinases, it then functions as a nucleoside analogue, integrating within newly synthesised viral genomes by the viral DNA polymerase in place of deoxyguanosine triphosphate. Acyclovir does not contain a 3' hydroxyl group and thus prevents subsequent nucleotide binding resulting in DNA chain termination. This function means that treatment is restricted to lytic infections, as the viral TK is only functional during lytic replication. EBV and KSHV infections are less susceptible to the activity of acyclovir as their thymidine kinase is less effective at phosphorylating the pro-drug.

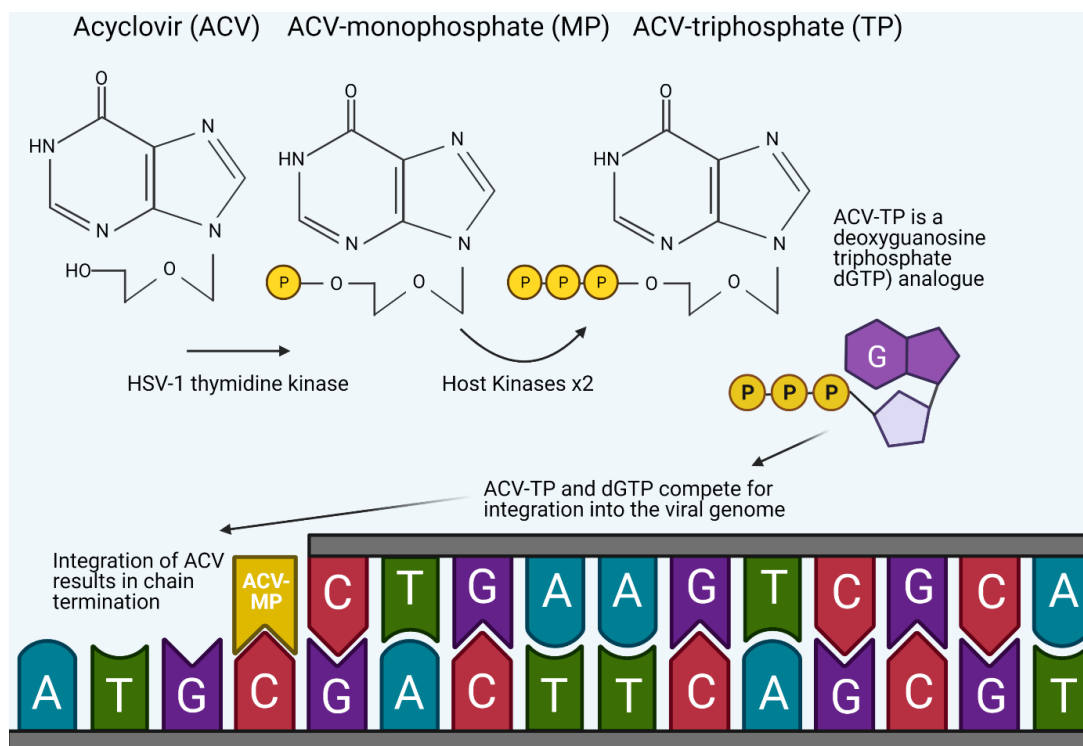


Figure 1.15 Schematic of acyclovir chain termination mechanism of action during lytic HSV-1 replication. The pro-drug acyclovir is phosphorylated by the thymidine kinase of HSV-1, further phosphorylation occurs via host kinases. Acyclovir-triphosphate can then be incorporated into the HSV-1 genome, where it acts as a chain terminator, preventing further genome replication. Created with BioRender.com.

In addition to the lack of pan-herpes treatments, acyclovir resistance is becoming more evident for HSV-1 and HSV-2 infections, particularly in immunocompromised patients (Piret and Boivin, 2011). While acyclovir, and derivatives, can be administered topically, orally or intravenously; oral administration has poor bioavailability. Consequently, there is an urgent requirement for effective anti-herpesvirus drugs. In recent years, more nucleoside and nucleotide analogues have undergone clinical trials with varying levels of success (Poole and James, 2018).

In addition to nucleoside analogues other currently approved for clinical use *Herpesviridae* treatments are available (Figure 1.16). For example, foscarnet is used for the treatment of lytically replicating *Herpesviridae* (De Clercq, 2004; Piret and Boivin, 2011; Coen et al., 2014; Birkmann and Zimmermann, 2016; Poole and James, 2018). However, foscarnet is a pyrophosphate analogue which directly binds to *Herpesviridae* DNA polymerase thus interfering with its activity. This enables its use in acyclovir-resistant strains of HSV-1 or -2 and ganciclovir-resistant CMV although ease of use is hindered by its intravenous administration. Furthermore, foscarnet has been found to hinder KSHV lytic replication in a PEL cell line (Coen et al., 2014; Narkhede et al., 2018). Cidofovir also hinders DNA polymerase activity (De Clercq, 2004; Piret and Boivin, 2011; Coen et al., 2014).

Other sites of antiviral targets which hinder lytic replication include the primase/helicase complex, such as pritelivir (Birkmann and Zimmermann, 2016; Poole and James, 2018). This class of antiviral agents prevent unwinding or priming of the viral DNA template, thus hindering DNA replication. However, these are currently only effective against *Alphaherpesvirinae*

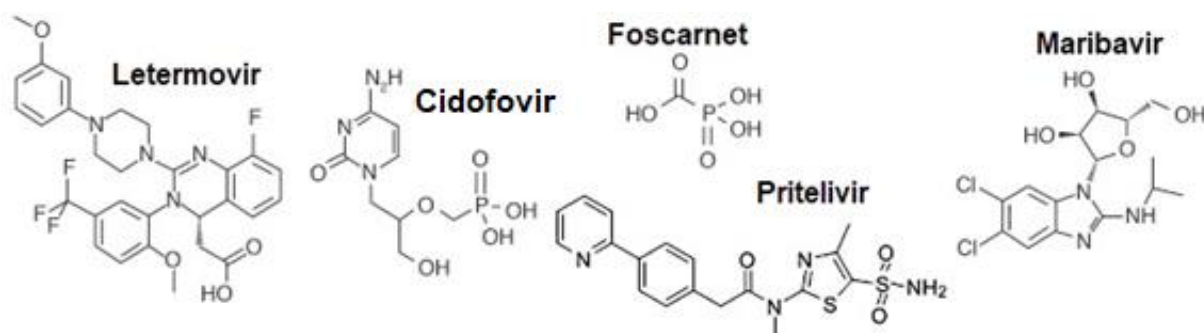


Figure 1.16 Other *Herpesviridae* treatments in clinical use and development with different targets. Foscarnet can be used to treat a variety of *Herpesviridae* infections, including HSV-1, HSV-2, HCMV and KSHV. However, cidofovir, letermovir and maribavir target HCMV only; pritelivir targets both HSV-1 and HSV-2.

infections and clinical trials have not yet completed. Novel treatments of HCMV infection have also been developed, with antivirals letermovir and maribavir developed against either HCMV terminase complex or HCMV UL97 protein kinase, respectively (Poole and James, 2018). Currently, letermovir is approved for use in adult transplant recipients, whereas maribavir is in phase three clinical trials. As with other antiviral agents which directly target viral proteins, resistance could occur.

Therefore, a new approach, for the treatment of *Herpesviridae* infections, could target host cell pathways, which could provide a pan-herpesvirus antiviral treatment, providing broad-spectrum therapeutic research avenues and reducing the possibility of antiviral resistance. Given the abundance of known ion channel modulating drugs, investigations into targeting ion channels as an antiviral therapy is gaining traction (Hover et al., 2017; Charlton et al., 2020). This combines the knowledge of various viral life cycles, which require either host or virally encoded ion channels, with the wide pharmacological information regarding ion channel modulators and physiological data on the plethora of ion channels within humans.

1.3. Ion Channels

Ion channels are highly selective hydrophilic transmembrane pores which permit the transport of ions across the plasma membrane (Alexander et al., 2011). This movement is dependent on the electrochemical gradient, although specific channels cause either ion influx into or efflux out of cells. There are more than three hundred known ion channels, with over 200 cation channels (Brown et al., 2019; Charlton et al., 2020). Each channel has high selectivity, only allowing ions of the appropriate size and charge to pass through, generally transport involves Ca^{2+} , K^+ , Na^+ or Cl^- ions. For example, a positively charged channel pore would only allow anions to pass through, such as Cl^- , whereas negatively charged pores permit cations such as K^+ and Na^+ ions (Brown et al., 2019).

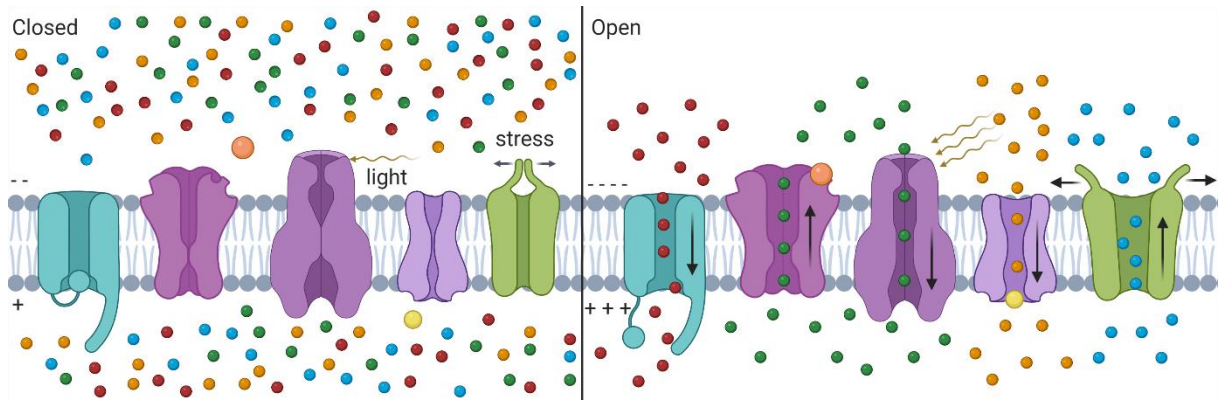


Figure 1.17 Schematic showing different types of ion channels in their closed and open states. Gating of ion channels varies, and there are many methods to induce opening. Voltage-gated channels open due to a change in membrane potential, ligand-gated channels activate after ligand binding, ligands can be extracellular or intracellular. Other changes in cellular environment, such as light levels or stress caused by vibrations or pressure can cause channels to open. Open channels can allow either influx or efflux of ions. Created with BioRender.com.

Channels can exist in three conformational states, closed, open and resting (Figure 1.17)

(Alexander et al., 2011; de Lera Ruiz and Kraus, 2015; Kuang et al., 2015; Brown et al., 2019).

These states are controlled through the attachment of a ligand or an environmental stimulus, such as mechanical stress (mechanically gated), or a change in light (light-gated), or membrane potential (voltage-gated) (Brown et al., 2019). Ligand gated channels can be controlled through the binding of ligands such as ions (ion-gated), neurotransmitters (transmitter-gated), or nucleotides (nucleotide-gated). Once the channel opens, ions of the appropriate size and charge can pass through the channel pore; this flow occurs either into or out of the cell, depending on which channel has opened.

Ion channels are present in all eukaryotic cells and roles include controlling the ion homeostasis of the cell and its organelles, action potential firing, membrane potential and cell volume (Alexander et al., 2011). Additionally, ion channels are required for both autophagy and invasive properties of tumour cells. Given this wide range of functions and ubiquitous nature, dysregulation of ion channels has been implicated in a variety of disorders and diseases known as channelopathies (de Lera Ruiz and Kraus, 2015; Grimm et al, 2017; Hover et al., 2017; Charlton et al., 2020). Research into, and treatment of, these channelopathies has led to the development of multiple ion channel modulators, which have further assisted in the investigation of specific channel function and activity.

1.3.1. K⁺

Potassium ion (K⁺) channels play vital roles in the regulation of important physiological processes such as hormone secretion, calcium signalling, firing of action potentials and cellular homeostasis, including membrane potential and volume (Kuang et al., 2015). The human genome encodes almost 80 K⁺ channels, thus allowing for tight regulation of each process (O'Grady and Lee, 2005). K⁺ channels are grouped based on both their sequence similarity and how many transmembrane domains they consist of; 2, 4, 6, or 7 (Kuang et al., 2015).

K⁺ channels are further categorised into four major classes, voltage-gated (K_v), calcium-activated (K_{Ca}), inwardly-rectifying (K_{ir}), and two-pore-domain (K_{2P}) channels (Kuang et al., 2015). K_v and K_{Ca} channels are discussed further below. K_{ir} channels consists of seven sub-families (K_{ir}1-K_{ir}7) (Kuang et al., 2015; Walsh, 2020). The K_{ir}6 subfamily displays sensitivity to adenosine triphosphate (ATP) and K_{ir}3 members are gated by G protein-coupled receptors (GPCRs); the K_{ir}2 subfamily is primarily expressed in the brain and throughout muscle cells whereas the other four channels, K_{ir}1,4,5 and 7, are responsible for K⁺ secretion via the kidneys (Walsh et al., 2020). Fifteen proteins belong to the K_{2P} class; further categorised into the TWIK, TREK, TASK, TALK, THIK and TRESK families (Mathie et al., 2020). Each of these proteins dimerise to form a K_{2P} channel. These channels consist of either homodimers or heterodimers within families, or on rare occasion within the entire class. These channels regulate several physiological processes, such as hormone secretion and cardiac rhythm.

1.3.1.1. K_v channels

Voltage-gated K⁺ (K_v) channels are found in a wide variety of cells and help to transmit action potentials in plasma membranes, along with stimulating both cellular proliferation and migration, maintaining cell volume and regulating calcium signalling (O'Grady and Lee, 2005). The family contains more than half of the K⁺ channels, consisting 40 members; these are further grouped into 12 sub-families (K_v1.x – K_v12.x). K_v channels are tetrameric and contain six transmembrane segments (S1-S6) and the pore region, formed at the centre of the tetramer

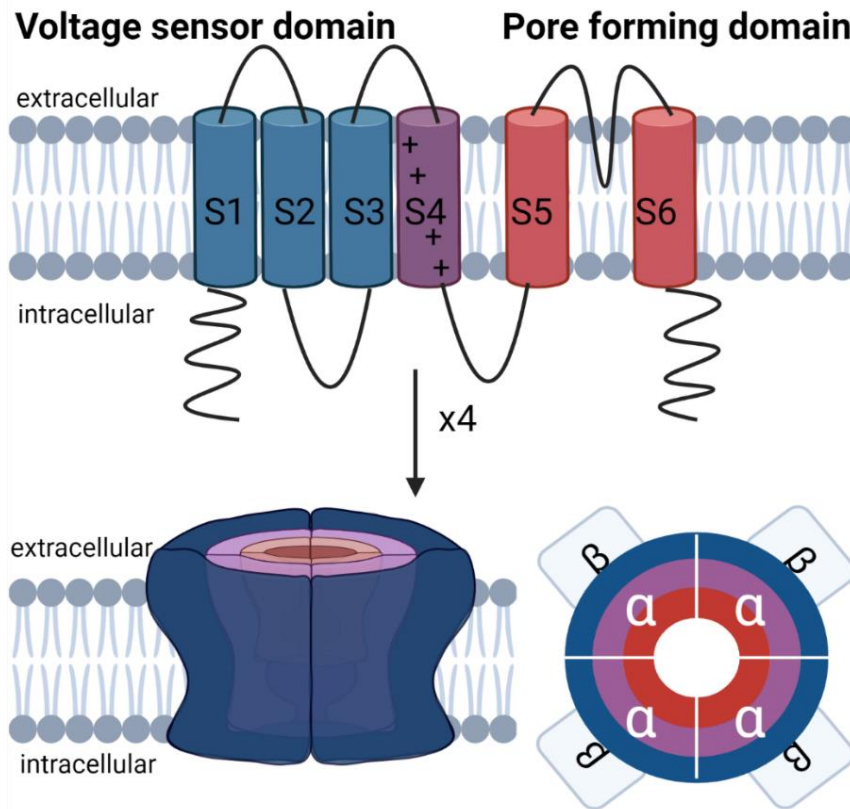


Figure 1.18 Schematic of K_v channel domains. K_v monomer shown within the cell membrane (left) and arrangement of K_v channel tetramers, both within the cell membrane (right) and as a map of α - and β -subunits (centre). Created with Biorender.com.

(O'Grady and Lee, 2005). The six transmembrane segments form a voltage sensor domain (VSD), containing 4 segments, and a 2-segment pore domain (Figure 1.18).

In addition to the 40 homotetrameric K_v channels, α -subunits can heteromultimerize within subfamilies, resulting in a broad range of potential channels, each with varying biophysical and pharmacological properties (O'Grady and Lee, 2005). Further variation is achieved through the binding of β -subunits, such as $K_v\beta 1-3$ proteins which bind to the intracellular domain of α -subunits belonging to the mammalian *Shaker*-family, also known as K_v1 . Post-translational modification of K_v channels also affects channel gating and function; modifications include ubiquitination, sumoylation, palmitoylation and phosphorylation. When open, K_v channels at the plasma membrane allow an efflux of K^+ , which can either cause membrane repolarisation or hyperpolarisation. Channelopathies associated with K_v mutations include epilepsy and cardiac arrhythmias.

1.3.1.2. K_{Ca} channels

The calcium-activated K^+ (K_{Ca}) channels also form tetramers and share similarity with the K_v channels (Kshatri et al., 2018). Large-conductance (BK_{Ca}) calcium-activated K^+ channels, consist of an α -subunit containing 7 transmembrane domains, and are activated by both membrane depolarization and intracellular Ca^{2+} . While BK_{Ca} channels contain an extra transmembrane domain, named S0, their structure is comparable to K_v channels; the S1-4 segments make up the VSD with S5 & S6 enabling pore formation (Figure 1.19). The α -subunit intracellular C-terminus contains two domains responsible for Ca^{2+} detection and regulating the K^+ flow through the channel pore. However, S0 and the extracellular N-terminus are distinctive to BK_{Ca} channels and allow for the binding of a variable β -subunit encoded by one of 4 genes, KCNMB1-4. The β -subunit modulates the ion channel and expression is cell-specific, providing better activation of the voltage sensor and reducing the amount of Ca^{2+} required for channel opening.

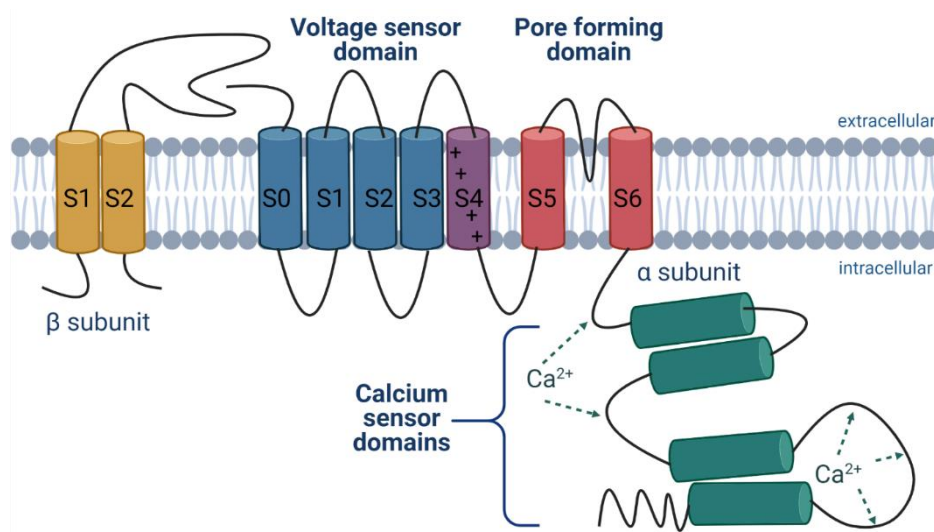


Figure 1.19 Schematic of monomeric BK_{Ca} channel domains within the cell membrane, showing both α - and β - subunits. There are four human genes encoding BK_{Ca} β - subunits, which regulate BK_{Ca} channel activity. Created with Biorender.com.

Small- (SK_{Ca}) or intermediate-conductance (IK_{Ca}) calcium-activated K^+ channels are only activated by intracellular Ca^{2+} and have 6 transmembrane domains, sharing a structure similar to K_v channels, as shown in Figure 1.18 (Kshatri et al., 2018). This is due to the variation in segment 4 of the VSD, which contains fewer positively charged residues thus rendering them insensitive to transmembrane voltage. This Ca^{2+} -dependent activation is mediated by

calmodulin which is continually bound to the C-terminal domain and acts as the calcium sensor for SK_{Ca} and IK_{Ca} channels. There are three SK_{Ca} channels; K_{Ca}2.1, K_{Ca}2.2 and K_{Ca}2.3. These are all found within the nervous system, although K_{Ca}2.3 is also present in vascular endothelium and a splice variant of K_{Ca}2.3 expressed on hepatocytes mediates their metabolic stress responses. SK_{Ca} channels regulate the frequency of neuronal firing and are responsible for cardiac action potential repolarization.

The single IK_{Ca} channel, K_{Ca}3.1, only shares around 40% homology with the SK_{Ca} channels, and therefore belongs in its own subfamily (Kshatri et al., 2018). The conductance of K_{Ca}3.1 is approximately 4 times that of SK_{Ca} channels. K_{Ca}3.1 channels are primarily expressed on immune system cells and epithelia. K_{Ca}3.1, along with K_{Ca}2.3, mediates the hyperpolarization response in vascular endothelium, inducing smooth muscle relaxation and vasodilation, through the reduction of Ca²⁺ influx through L-type Ca²⁺ channels. In lymphocytes and microglia, K_{Ca}3.1 regulates calcium signalling and activation of B or T cells (Chiang et al., 2017; Kshatri et al., 2018). They are responsible for the regulation of electrolyte and water movement within secretory lung epithelia, the gastrointestinal tract, and salivary glands. These channels also assist with cell volume regulation in red blood cells.

1.3.2. Ca²⁺

Calcium ion homeostasis is tightly regulated. Cells have a permanent store of Ca²⁺ within the endoplasmic reticulum (ER), which is maintained continuously by sarco/endoplasmic reticular Ca²⁺ ATPase pumps (Clapham, 2007; Hogan et al., 2010; Yoast et al., 2020; Zamponi et al., 2015). Calcium channels therefore control the intracellular calcium concentration, required for calcium signalling pathways. These channels also transmit signals across the neuromuscular junction enabling muscle contraction.

1.3.2.1. Calcium Signalling

Calcium signalling has vital roles in many cellular pathways (Clapham, 2007). For example, changes in cytoplasmic Ca²⁺ levels occur throughout the cell cycle process, with many phases being Ca²⁺ dependent including G₁ entry, and progression into S phase, along with the

transition of G₂ into M phase. Numerous transcription factors also require Ca²⁺ mediated activation, such as cyclic AMP response element-binding protein (CREB), nuclear factor- κ B (NF- κ B) and the four of the five nuclear factor of activated T-cells (NFAT1-4) proteins. Additionally, many enzymes are activated by Ca²⁺ binding, such as calmodulin, its dependent protein kinases and protein phosphatase, calcineurin (Clapham, 2007; Hogan et al., 2010). Calcium signalling is particularly important for both B and T cell activation and survival during immune responses (Clapham, 2007; Hogan et al., 2010). Ligand interaction with the B cell receptor, such as antigen binding, causes Ca²⁺ influx via potassium channel mediated membrane hyperpolarisation, regulating B cell activity through activation of the calcineurin and NFAT pathway (Figure 1.20). This leads to the production of NFAT-mediated immune response genes. A similar mechanism occurs in T cells, where ligand binding to the T cell receptor triggers the same mechanism, encouraging T cell proliferation via NFAT-mediated IL-2 production.

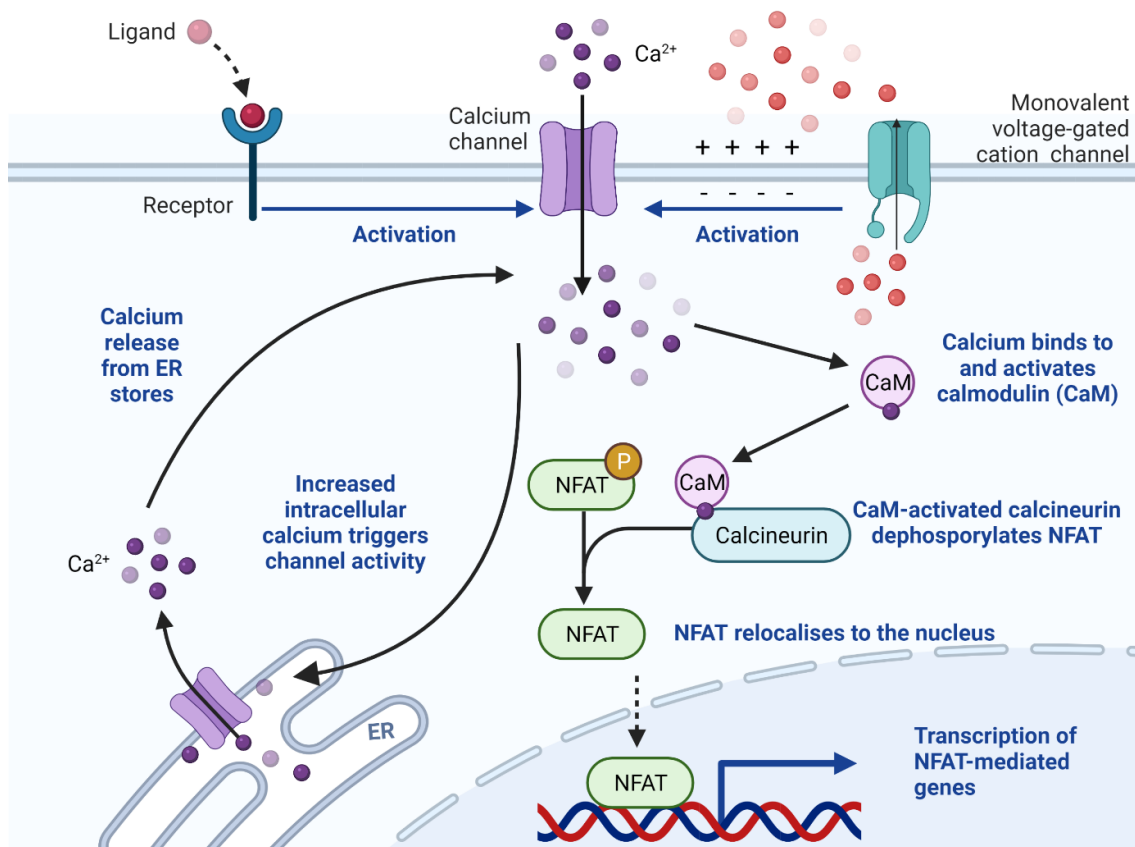


Figure 1.20 Schematic showing calcium signalling of NFAT pathway. Initial activation of a calcium-influx channel can occur via various mechanisms, shown are ligand binding, as with BCR-mediated activation and membrane hyperpolarisation, caused by monovalent cation efflux. Created with Biorender.com.

1.3.2.2. Ca_v channels

Voltage-gated calcium (Ca_v) channels control calcium influx at the cell membrane (Zamponi et al, 2015). This important regulation initiates various cellular responses, such as action potential firing and apoptosis. By increasing intracellular Ca^{2+} levels, Ca_v channels enable the activation of calcium-dependent enzymes inducing the calcium signalling pathway; leading to several processes depending on cell type, including muscle contraction, hormone release and gene transcription (Lin et al., 2014; Zamponi et al, 2015; Rossier, 2016).

The channels are characterised into two groups based on voltage activation (Zamponi et al, 2015). Low-voltage gated, or T-type current, channels consist of three channels, known as $\text{Ca}_v3.1$, $\text{Ca}_v3.2$ and $\text{Ca}_v3.3$. High-voltage gated channels are further grouped into L-, N-, P-, Q- and R-type currents. L-type channels only consist of the Ca_v1 subfamily, while Ca_v2 includes the other four types.

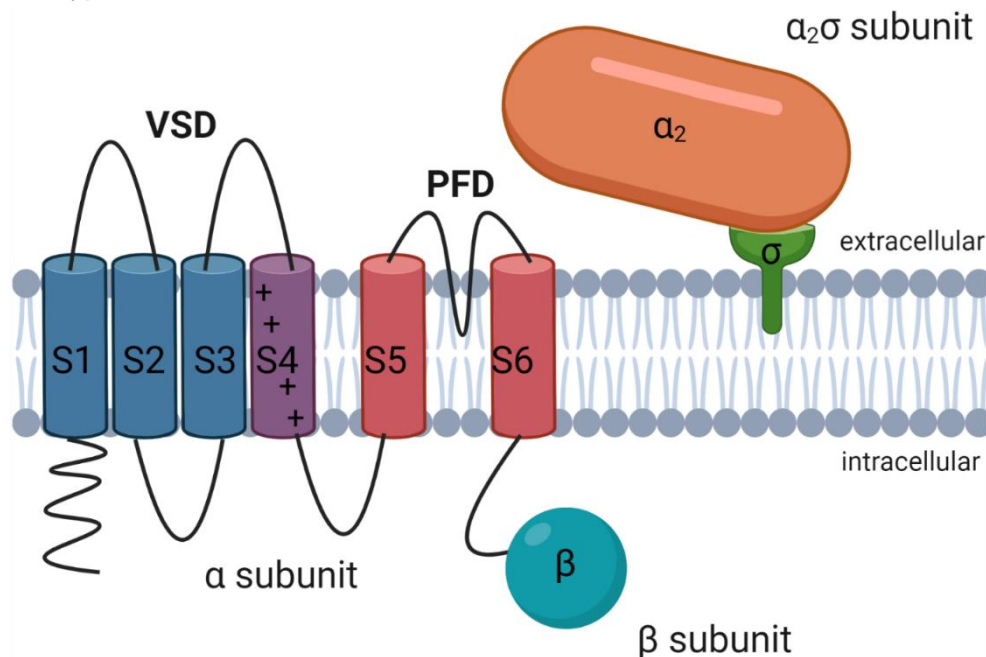


Figure 1.21 Schematic of Ca_v channel domains within the cell membrane, showing α - $\alpha_2\sigma$ - and β -subunits. Segments 1-4 within the α -subunit encompass the voltage-sensing domain, while the pore-forming domain consists of segments 5 and 6. Created with Biorender.com.

As with K_v channels, Ca_v channels contain six transmembrane segments which comprise the voltage sensitive and calcium-selective transmembrane pore of the α subunit (Zamponi et al, 2015). However, in addition to the β subunit, Ca_v channels can contain $\alpha_2\sigma$ subunits, which modify current density of the channels and assist with trafficking the protein complex to the cell membrane (Figure 1.21).

Due to their activation during hyperpolarisation states, T-type channels are vital for neuronal firing and have also been implicated in the release of neurotransmitters in the spinal cord (Zamponi et al, 2015). Activation of T-type channels also leads to gene expression activation, via the NFAT pathway in cartilage tissue and the CREB pathway in heart muscle cells. Each of the three channels have specific functions; $Ca_v3.1$ plays an important role in the sleep-wake cycle, while $Ca_v3.2$ and $Ca_v3.3$ both function within cerebral arteries. $Ca_v3.2$ is required for arterial relaxation in the cerebrum and $Ca_v3.3$ works in combination with $Ca_v1.2$ to allow smooth muscle contraction when expressed in cerebral arteries (Harraz et a., 2015).

L-type channels have a variety of functions and expression varies within cell type. $Ca_v1.1$ is required during contraction in skeletal muscle (Zamponi et al, 2015). $Ca_v1.2$ and $Ca_v1.3$ are expressed in the heart, brain, and endocrine systems. In the heart $Ca_v1.2$ is responsible for action potential firing, while pace making requires $Ca_v1.3$ expression. Both are responsible for the secretion of hormones, specifically insulin through $Ca_v1.2$ activity and adrenaline by $Ca_v1.3$. $Ca_v1.4$ is expressed in the retina, where it is required for neurotransmitter release.

$Ca_v2.1$ channel activity causes both P- and Q-type currents, β subunits enable variation between the two current types (Zamponi et al, 2015). $Ca_v2.2$ and $Ca_v2.3$ are responsible for N- and R-type currents, respectively. Ca_v2 channels support both neurotransmitter and hormone release, and like T-type channels trigger gene transcription via both the CREB and NFAT pathways (Zamponi et al, 2015). $Ca_v2.1$ and $Ca_v2.2$ channels interact with BK_{Ca} channels, providing the calcium influx required for their activation, leading to regulation of neuronal excitability due to the alteration of potassium efflux (Zamponi et al, 2015). BK_{Ca} interaction with another voltage-gated calcium channel has also been shown by Gackière et al. (2013).

1.3.2.3. CRAC channels

Calcium release activated Ca^{2+} (CRAC) channels play a role in the store-operated calcium entry (SOCE) pathway (Yoast et al., 2020). CRAC channels are the main effector for increasing the levels of cytoplasmic Ca^{2+} in many cell types, although most studies focus on their

involvement in the immune system. When required, the release of Ca^{2+} from the ER is initiated by inositol 1,4,5-triphosphate (IP_3). Decrease of Ca^{2+} within the ER causes stromal interaction protein 1 (STIM1) to form multimers and relocate from the ER membrane to the cellular membrane (Figure 20). Due to STIM1 interactions, Orai proteins form hexamers and assemble into a CRAC channel pore. Upon activation the channel then allows calcium influx, further increasing the Ca^{2+} concentration within the cytoplasm (Hogan et al., 2010; Dellis et al, 2011). As with Ca_v channels, the increase in cytoplasmic Ca^{2+} enables the activation of calcium-dependent enzymes, which switch on several cellular processes, including the NFAT pathway. While there are three known Orai proteins, Orai1 is the predominant component of CRAC channel pores and regulation of CRAC channel activity occurs via either Orai2 or Orai3, forming heteromers with Orai1 within the pore (Hogan et al., 2010; Dellis et al, 2011).

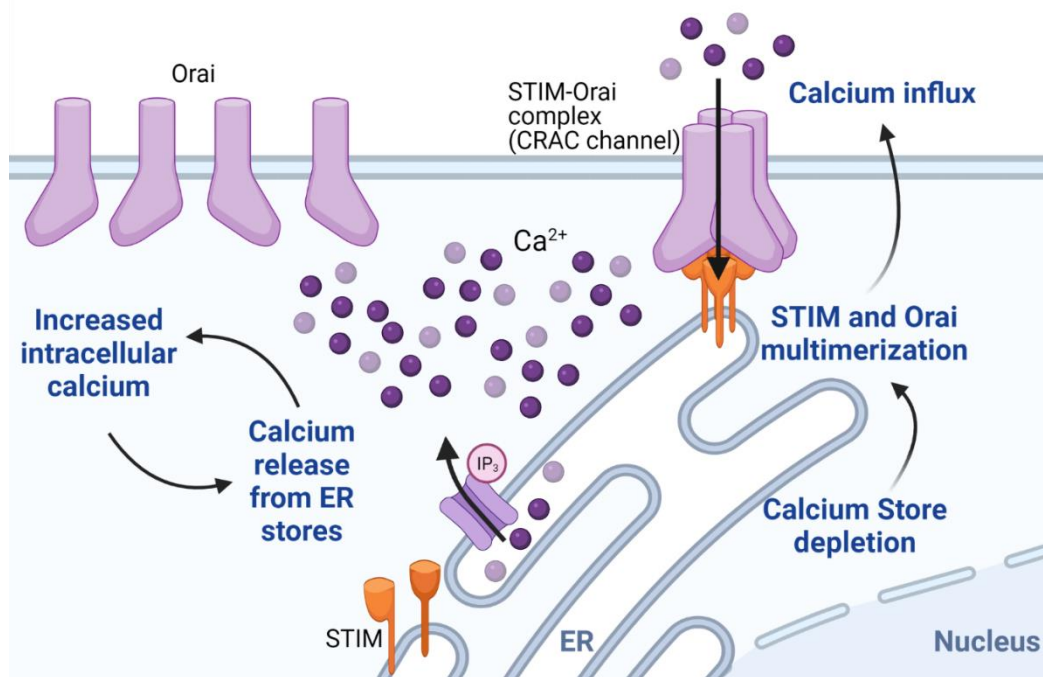


Figure 1.22 Schematic of SOCE pathway. Upon binding of inositol 1,4,5-triphosphate, calcium channels within the ER membrane open and allow calcium to enter the cytoplasm. This triggers CRAC channel formation, allowing influx of calcium and further increasing in cytoplasmic calcium levels. Created with BioRender.com.

1.3.3. Other channels

1.3.3.1. Na⁺ channels

Sodium channels are responsible for rapid depolarising impulses used to transmit messages quickly over large distances, particularly for movement and perception (de Lera Ruiz and

Kraus, 2015). Therefore, they are present in the nervous system of both vertebrates and invertebrates. Additionally, sodium channels are found in vertebrate muscle cells, such as mammalian myocardial cells where they are the most abundant ion channel.

The largest group, voltage-gated sodium channels (Na_v) channels, are responsible for the induction of electrical impulses in excitable membranes (de Lera Ruiz and Kraus, 2015). Members of this family are classified by their sensitivity to the neurotoxin, and ion channel inhibitor, tetrodotoxin. Several Na_v channels are found in neurons including tetrodotoxin sensitive, $\text{Na}_v1.3$, 1.5 and 1.7, and tetrodotoxin resistant, $\text{Na}_v1.8$ and 1.9 channels (Kennedy et al., 2013; de Lera Ruiz and Kraus, 2015). Electrical impulses occur within neurons when Na_v channels are opened due to depolarisation, allowing Na^+ ions to enter the cell, further increasing the depolarisation and Na^+ influx in a positive feedback loop. At this point, Na_v channels are inactivated due to their instability in the open conformation and K_v channels open (de Lera Ruiz and Kraus, 2015).

1.3.3.2. Other Cations

While the previously described channels are selective for specific ions, some channel families are less selective enabling transport of various cations (Brown et al., 2019). Hyperpolarization-activated cyclic nucleotide-gated (HCN) channels are selective only for monovalent cations, and therefore transport either K^+ or Na^+ ions. These channels regulate pace in both cardiac and nervous systems.

Other cation channels are permissive to multiple ions, such as two-pore channels (TPCs); these channels are unique due to the existence of two transmembrane pores within the fully formed channel which are located on organelle membranes (Grimm et al., 2017). The family consist of two members in humans; TPC1 is only permissive to Na^+ , whereas TPC2 allows the transport of both Na^+ and Ca^{2+} . These channels regulate endolysosomal trafficking and thus manipulation of TPCs can affect a number of metabolic and lysosomal storage processes (Grimm et al., 2017; Brown et al., 2019).

Furthermore, transient receptor potential (TRP) channels tend to permit most monoatomic cations, allowing transport of Ca^{2+} , Mg^{2+} in addition to K^+ and Na^+ . This diverse group of channels mostly play sensory roles in various processes, such as the TRP melastatin cation channel 8 (TRPM8) which detects the presence of menthol, or cold temperatures, in humans (Brown et al., 2019).

1.3.3.3. Anion channels

Most anionic channels, sometimes referred to as chloride channels, primarily transport chloride as it is the most abundant biophysical anion (Alexander et al., 2011; Zhang et al., 2012; Strange et al., 2019). The cystic fibrosis transmembrane conductance regulator (CFTR) channel is probably the most notable chloride channel, due to mutations within this channel causing cystic fibrosis (Alexander et al., 2011; Zhang et al., 2012). There are over 1600 mutations known to occur within the CFTR gene, with a single point mutation known to be present in over 90% of patients with cystic fibrosis. The disease is characterized by aberrant ion homeostasis due to total loss or dysfunction of the CFTR channel and its activity. Due to its role in a lethal channelopathy, CFTR has been extensively studied. Expression mostly occurs on epithelial cells within airway and gut linings along with exocrine gland epithelia. While the ligand-gated channel is mediated by cyclic AMP binding, the toxins of several bacterial pathogens also hyperactivate the channel on gut epithelia, causing Cl^- efflux (Zhang et al., 2012).

However, channels such as the volume-regulated anion channel (VRAC) are selective for multiple types of anions (Alexander et al., 2011; Strange et al., 2019). In addition to chloride and other halides, VRAC permits the efflux of thiocyanate (SCN^-) and nitrate (NO_3^-). As its name suggests, the VRAC channel is responsible for regulating cell volume and is triggered by cellular swelling, although ATP is also required for channel activity. In addition to volume regulation, VRAC also contributes to cell cycle control and cellular shrinkage during apoptosis. The channel is encoded by five members of the LRRC8 gene family, and thus is sometimes referred to as the LRRC8 channel, to avoid confusion with other volume-regulated channels.

Of the five genes, LRRC8A expression is required in all LRRC8 channels in combination with another LRRC8 protein for functional channel activity, homomeric LRRC8A channels can permit a small anionic efflux (Strange et al., 2019).

The two anion channels described vary in structure (Figure 1.23). The full CFTR channel is thought to consist of two repeated motifs, encompassing both a membrane spanning and nucleotide binding domain (NBD), connected by a regulatory (R) domain (Zhang et al., 2012). Channel activity is regulated by ATP-NBD binding or phosphorylation of the R domain. The LRRC8A monomers consist of four regions, extracellular, transmembrane, intracellular, and leucine-rich repeat (LRR) regions (Strange et al., 2019). In the hexameric channel, the LRR regions protrude out into the cytoplasm, away from the channel pore, which is formed by the N-terminal coil, transmembrane segments 1 and 2, extracellular loop 1 helix 1 (EL1H1) and intracellular loop 1 helices (IL1H) 1 and 3 (annotated in Figure 1.23).

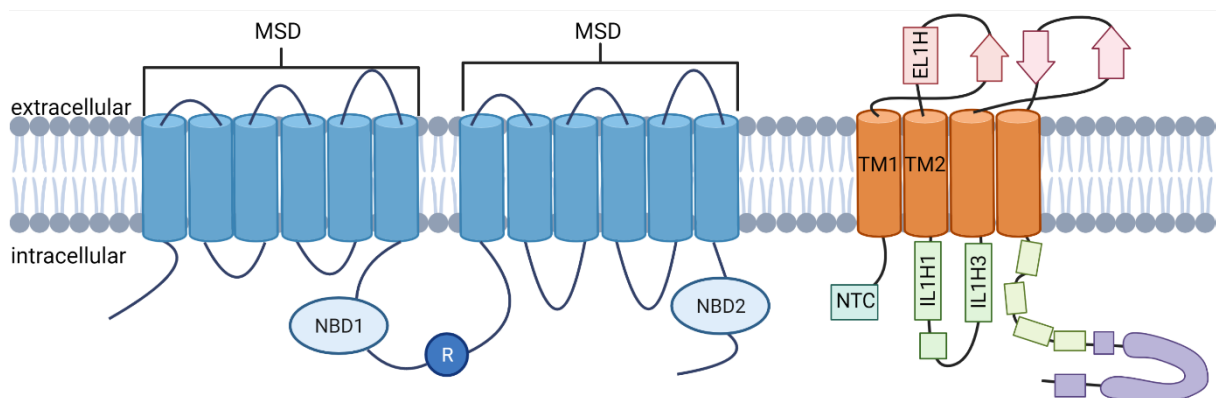


Figure 1.23 Schematic of CFTR channel (left) and LRRC8A monomer (right). While the whole CFTR channel is shown, the VRAC monomer dimerises to form the VRAC channel, the labelled domains within the VRAC monomer form the channel pore. Created with BioRender.com.

1.3.3.4. Viral ion channels

Many viruses encode their own ion channels, known as viroporins (Scott and Griffin, 2015). A summary is shown in Figure 1.24. Most consist of around 100 amino acids, which enable small DNA viruses to encode proteins with viroporin activity. For example, oncoprotein E5 encoded by human papillomavirus type 16 (HPV16) forms a proton channel, which can be inhibited by rimantadine. Moreover, the viroporin activity of JC polyomavirus (JCPyV) agnoprotein enables entry of extracellular Ca^{2+} , when localised at the host plasma membrane (Suzuki et al., 2010).

However, the presence of viroporins was originally discovered in RNA viruses, with many single stranded RNA viruses enabling proton (H^+) passage through viroporin activity (Scott and Griffin, 2015). Probably the most widely studied is M2 of influenza A virus (IAV), which enables viral entry into the host cell (To and Torres, 2019; Scott and Griffin, 2015). Conservation of a similar proton channel is also present in both influenza B (IBV) and influenza C (ICV) viruses. IBV also encodes another proton channel of unknown function. Severe acute respiratory syndrome coronavirus (SARS-CoV) encodes three viroporins, all specific for monovalent cations. While the SARS-CoV E viroporin is known to facilitate virion production and the K^+ -selective 3a viroporin enables viral spread, the function of the 8a viroporin is yet to be determined (Castaño-Rodríguez et al., 2018). The Vpu protein of human immunodeficiency virus (HIV) is permissive to K^+ and Na^+ , and its viroporin activity is required during virion formation (González, 2015).

Conservation of viroporins is also seen within distinct viral families, such as the 6K viroporin which is conserved within *Togaviridae*, and the *Flaviviridae*-specific p7 viroporin (Scott and Griffin, 2015). Both viroporins assist with particle production (Melton et al., 2002; Steinmann et al., 2007). The 6K viroporin is permissive to monovalent cations in three family members: Semliki Forest virus, Sindbis virus and Ross River virus. However, p7 viroporin selectivity

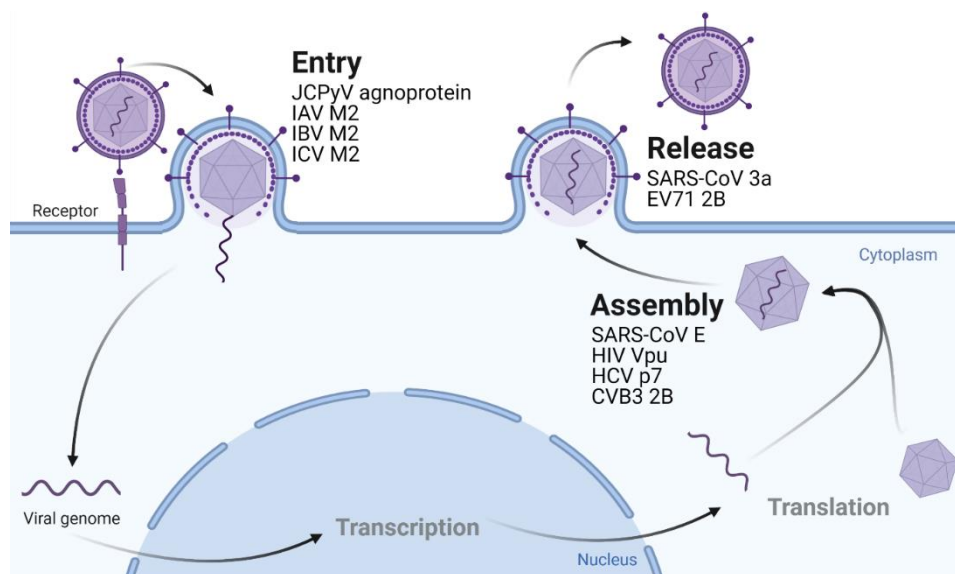


Figure 1.24 Schematic of viral lifecycle showing stages at which various viroporins are utilised by each virus. The M2 viroporin, conserved across IAV, IBV and ICV, assists with viral entry. SARS-CoV encodes two viroporins with separate known functions; E facilitates viral assembly while 3a is required for viral egress. Created with BioRender.com.

changes between *Flaviviridae*; Hepatitis C virus (HCV) allows transfer of protons, yet classical swine fever virus is selective for calcium ions (Steinmann et al., 2007; Gladue et al., 2018). Interestingly, viroporin conservation does not necessarily lead to a retention of function (Scott and Griffin, 2015); poliovirus, coxsackievirus B3 (CVB3), and enterovirus 71 (EV71) all encode the *Picornaviridae* specific 2B viroporin; yet the viroporin is anion permissive and enables viral spread in EV71, whereas 2B is a divalent cation selective viroporin enabling virion production and cell lysis within both poliovirus and CVB3 replication cycles (Scott and Griffin, 2015; Li et al., 2019).

1.4. Viral dependence on host ion channels

Ion channels control ion flux across membranes in all cells, as such they regulate ion homeostasis, which can act as signalling pathways controlling cellular physiology. This network of regulatory channels has led to discoveries of viral dependence on hijacked host cell ion channels assisting in various stages of their respective replication cycles (Hover et al., 2017; Charlton et al., 2020).

To date, most research has investigated the requirement of cation channels in viral life cycles, however BK polyomavirus (BKPyV) and Chikungunya virus (CHIKV) also require chloride channels during their replication cycles (Müller et al., 2019; Panou et al., 2020). In contrast to BKPyV, Merkel cell polyomavirus (MCPyV) and Simian virus 40 both require cation channels to successfully enter a host cell. This includes K_v and TPC2 channels for both, whereas T-type channels are also required by MCPyV (Dobson et al., 2020).

TPC2 is also required by Ebola virus, Middle Eastern respiratory syndrome coronavirus (MERS) and SARS-CoV 2, with MERS additionally utilizing TPC1 (Das et al., 2020; Gunaratne et al., 2018; Ou et al., 2020). The targeting of TPC channels by a wide variety of viruses is most likely due to endolysosomal trafficking regulation, a system which multiple viral families utilize to gain entry to a host cell. While the requirement of TPC2 implicates either Na^+ or Ca^{2+} flow dependence, other viruses specifically require Ca^{2+} channels, such as the *Flaviviridae* members Dengue virus (DENV) and Japanese encephalitis virus, which both require Ca_v channels during replication (Wang et al., 2017; Dionicio et al., 2018).

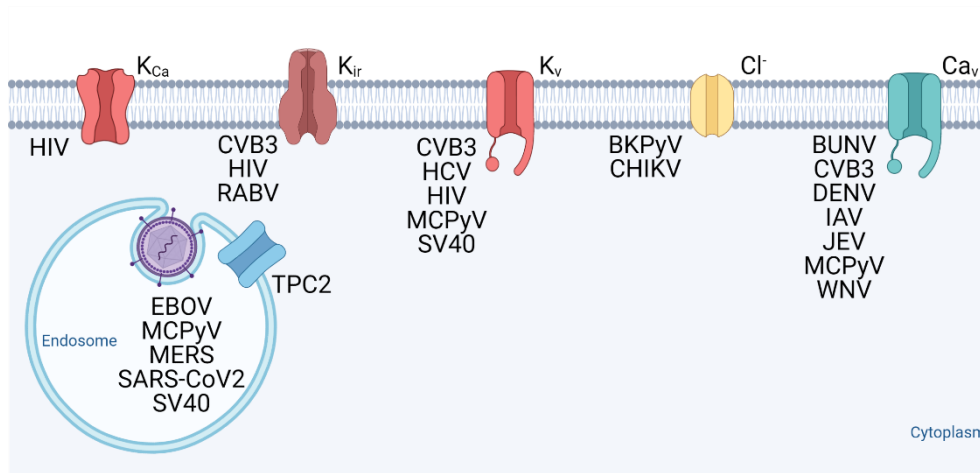


Figure 1.25 Schematic displaying various host ion channel families required during viral replication, along with respective viruses. Many viruses utilise potassium channels during replication, however other cation and chloride channels are also manipulated. Some viruses, such as HIV, require multiple host channels. Created with BioRender.com.

In addition to its Ca_v1.2-dependency, IAV entry is dependent on an undetermined K⁺ channel (Stauffer et al., 2014). CVB3, DENV, HCV, HIV, Bunyamwera orthobunyavirus (BUNV) and Hazara orthonairovirus replications are also dependent upon the activity of a variety of K⁺ channels (Charlton et al., 2020). Channel families required by several replication cycles are shown in Figure 1.25.

In addition to channel-dependency during replication, some channels have been linked to disease symptoms during viral infection. This includes the upregulation of chloride channels after exposure to the MCPyV small tumour antigen, which facilitates motility and migration; these activities would assist in MCPyV-associated tumorigenesis (Stakaitytė et al., 2018). CVB3-induced expression of K_v7.1 can lead arrhythmias and sudden cardiac death during viral infection (Peischard et al., 2019).

1.2.1. Host ion channel modification by *Herpesviridae*

HSV-1 infection affects the expression of several ion channels and their localisation, including the internalization of Na_v channels during lytic replication, as shown in Figure 1.26 (Charlton et al., 2020). However, rescue of channel activity occurs in latently infected neurones, with further Na_v channel internalisation and abolishment of channel activity coinciding with reactivation of HSV-1 lytic replication.

During HSV-1 infection, intracellular chloride concentration is increased, most likely to assist with viral entry (Zheng et al., 2014). However, treatment with chloride channel inhibitors tamoxifen or 5-nitro-2-(3-phenyl-propylamino) benzoic acid (NPPB) prevent the increased influx of chloride ions, reducing the levels of chloride ions to that of uninfected cells (Zheng et al., 2014). Additionally, the intracellular calcium concentration is increased during early stages of HSV-1 lytic replication, this increase is dependent upon chloride channel activity. This hints at the interplay between ion channels in both normal host activity and during the replicative cycle of infecting viruses.

Recently, Ding et al (2021) investigated the effect of Ca_v channel inhibitors on HSV-2, finding that Ca^{2+} influx caused by Ca_v3 channels were required during the later stages of HSV-2 lytic replication, and that Ca_v3 inhibition was sufficient to prevent HSV-2 replication. Furthermore, Zhang et al (2017) found that HSV-1 downregulates $Ca_v3.2$ channels and subsequent activity during early phases of replication in a murine neuroblastoma cell line. Downregulation is caused by a reduction in $Ca_v3.2$ protein levels, yet HSV-1 induces $Ca_v3.2$ mRNA expression (Zhang et al, 2017).

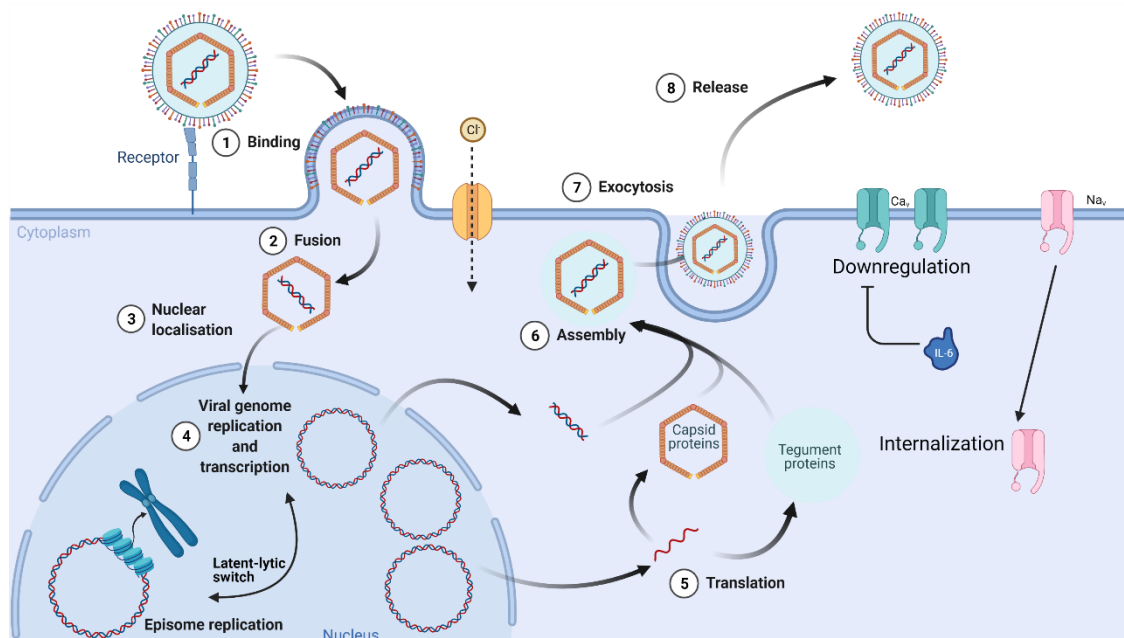


Figure 1.26 Schematic displaying host ion channel families affected during HSV-1 replication. Increased chloride channel activity occurs early during HSV-1 infection, voltage-gated sodium channels are internalised and voltage-gated calcium channels are downregulated at protein level during HSV-1 lytic replication. However, IL-6 production rescues voltage-gated calcium downregulation. Created with BioRender.com.

While acyclovir has been used to help reduce pain of post-herpetic neuralgia (PHN), both as a treatment during VZV lytic replication to reduce the risk of developing PHN and as a treatment during episodes of PHN, the drug has no effect on the host factors causing PHN and viral genes or proteins are not readily observed during PHN (Kennedy et al., 2013). When factoring in observed HSV-1 acyclovir resistance and the lower efficacy of acyclovir on VZV, there is already a heightened risk that this treatment will not have long-term efficacy. Both lidocaine, used as a local numbing agent and carbamazepine, an anticonvulsant used to treat epilepsy, are clinically approved and are also Na⁺ channel blockers and could be taken for pain relief during symptoms of PHN (de Lera Ruiz and Kraus, 2015). They have been shown to have some effect on Na_v channels thought to cause the neuropathic pain experienced during PHN (Markman and Dworkin, 2006).

Within a rat model Na_v1.3 and Na_v1.8 were upregulated during VZV infection (Garry et al., 2005). However in a human tissue culture model Kennedy et al. (2013), found upregulation of Na_v1.6 and Na_v1.7 occurred, but this was limited to viral strains which caused PHN. The effects of Na_v upregulation can be prevented with the sodium channel blockers, lidocaine and carbamazepine, which have been shown to alleviate PHN symptoms (Garry et al., 2005; Kennedy et al., 2013). Additionally, tetrodotoxin (TTX) a potent inhibitor of Na_v1.3, Na_v1.6 and Na_v1.7 activity extracted from pufferfish, is currently in clinical trials as an analgesic (Goldlust et al., 2021). Rat studies assessing TTX as a PHN therapeutic suggest oral administration had fewer side effects and enabled a higher dose in comparison to intramuscular injection (Hong et al., 2018).

During HCMV infection, a variety of potassium channels are known to be dysregulated. HCMV was found to downregulate Na_v channels and upregulate K⁺ delayed rectifier channels during the early stages of viral infection and replication, indicating immediate early or delayed early viral proteins are responsible for the dysregulation of these ion channels. At present the role of these channels in the HCMV lifecycle is unknown (Oberstein and Shenk, 2017).

Downregulation of Na_v channels directly contrasts with the upregulation seen during VZV infection, probably due to the cell-specific nature of ion channel expression and the variation

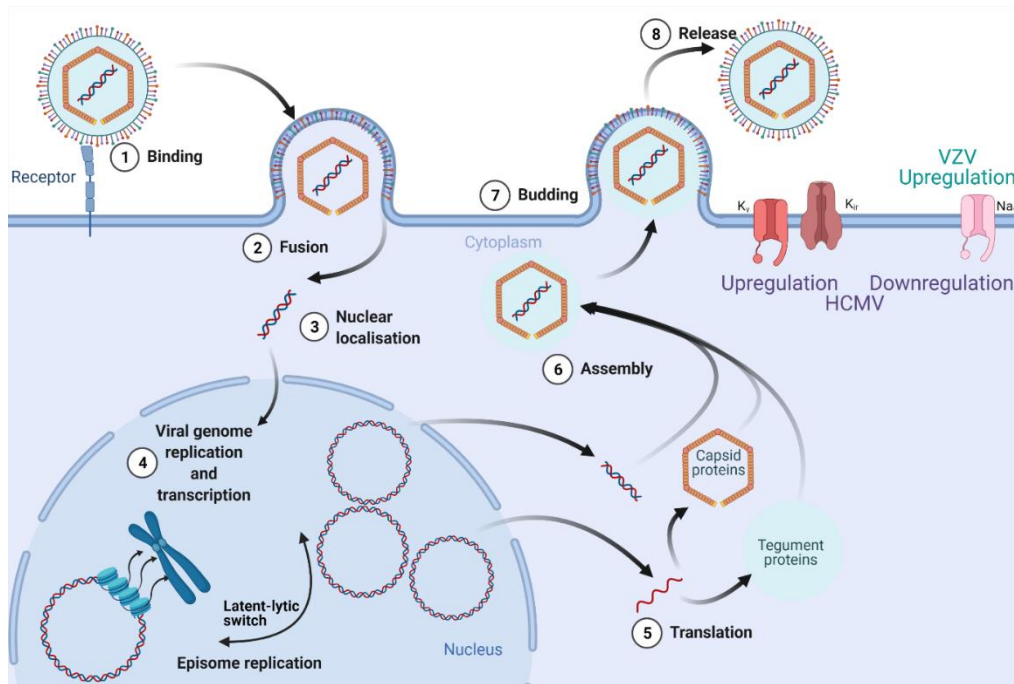


Figure 1.27 Schematic of channel dysregulation seen during VZV or HCMV replication cycles. Various potassium channels are upregulated during HCMV lytic replication, including both voltage-gated and inward-rectifying channels. While voltage-gated sodium channels are downregulated during HCMV lytic replication, VZV lytic replication causes upregulation of channels from this sub-family. Created with BioRender.com.

in cellular tropism between VZV and HCMV (Alexander et al., 2011; Grinde, 2013). Na_v channels are also internalized by HSV-1, which would reduce channel activity, indicating this reduction in Na_v channel activity is not limited to *Betaherpesvirinae*. Comparison of the ion channel modification during both VZV and HCMV lytic replication is shown in Figure 1.27.

The EBV-encoded oncogene latent membrane protein 1 (LMP-1) increases Ca²⁺ influx, affecting the intracellular calcium concentration through the upregulation of Orai1 expression (Figure 1.28) (Dellis et al., 2011; Shannon-Lowe and Rickinson, 2019). However, STIM1 expression is not upregulated by LMP-1. Cells infected with viral mutants lacking LMP-1 protein expression have a decreased Ca²⁺ concentration within the cytoplasm at rest. As Ca²⁺ signalling is important for B cell survival, and EBV can immortalise cells, the effect of LMP-1 on Ca²⁺ concentration could be a contributory factor in EBV-induced oncogenesis. Orai1 itself plays a role in the metastasis of breast cancers, further promoting the idea that the interactions of LMP-1 and Orai1 contribute to tumorigenesis (Dellis et al., 2011).

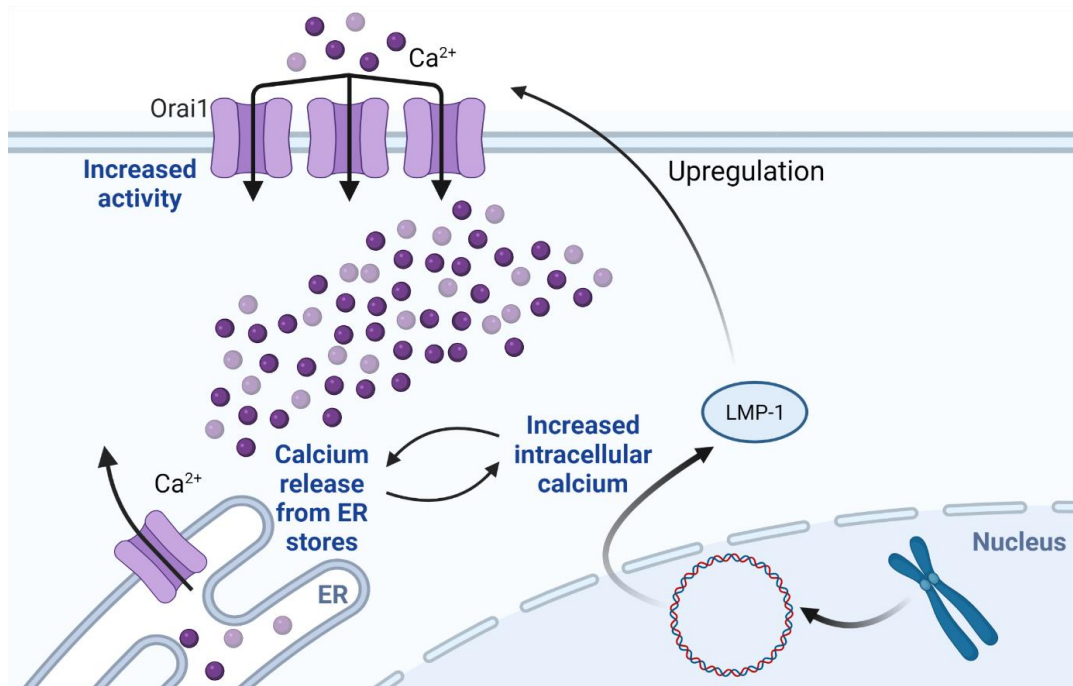


Figure 1.28 Schematic displaying effect of LMP-1 on Orai1 during EBV latency. LMP-1 is expressed during EBV latency, this protein upregulates Orai1 leading to CRAC channel formation and increased cytoplasmic calcium levels. Created with BioRender.com.

1.5. Ion channel inhibitors

General inhibitors consist of salts, such as KCl which inhibit K⁺ channels by dysregulating the external K⁺ concentration, or ionic mimics, such as tetraethylammonium chloride (TEA) which mimic the K⁺ ion thus blocking K⁺ channels (Mathie et al., 2020; Walsh, 2020; Wulff and Zhorov, 2008; Zamponi et al., 2015). There are many small molecule ion channel inhibitors known to restrict activity of a single channel, or a group of similar channels.

However, many known ion channel inhibitors are peptides which have been purified or derived from the venom of different species (Bajaj and Han, 2019). While many venomous animals have not yet had their venom fully investigated for potential ion channel inhibitors, the list of venom-derived cation channel inhibitors is vast.

Around 100 toxins purified from the venom of scorpions, spiders, snakes, and sea anemones have been shown to target cation channels, either specifically or with varied efficacy within subfamilies (Bajaj and Han, 2019; Mathie et al., 2020; Walsh, 2020; Wulff and Zhorov 2008; Zamponi et al., 2015). Some of these toxins have been utilised in the development of designer peptides created specifically to inhibit a particular ion channel, the most common target has been K_v1.3 due to its role in immunomodulation. In addition to its effect on K_v1.3; charybdotoxin

(CTX), purified from the deathstalker scorpion venom, has also been shown to inhibit both BK_{Ca} and IK_{Ca} channels. SK_{Ca} channels are unaffected by CTX, however the bee-venom derived apamin successfully inhibits all three SK_{Ca} channels.

As mentioned, TTX inhibits fast-acting Na_v channels (Bajaj and Han, 2019; de Lera Ruiz and Kraus, 2015;). Tetrodotoxin can be purified from a variety of natural sources including pufferfish; however, the toxin is produced by bacteria such as *Vibrio*, *Pseudomonas*, and *Pseudoalteromonas* species while symbiotically infecting the animals using TTX in their venom.

Ca_v inhibitors include nifedipine, nifedipine hydrochloride, nimodipine, nitrendipine, and verapamil hydrochloride mostly affect L-type currents (Wu et al., 2020; Zamponi et al., 2015). However, both L-type and T-type channels are inhibited by nifedipine hydrochloride and verapamil hydrochloride while SKF-96365 prevents T-type and TRP channels.

There are a number of Cl^- channel inhibitors, ranging from broad-acting such as 5-Nitro-2-(3-phenylpropylamino) benzoic acid (NPPB) to specific such as benzbromarone which targets the CFTR channel (Zhang et al., 2012; Zheng et al., 2014). While CFTR channel inhibitors would not be useful in the treatment of cystic fibrosis (Zhang et al., 2012), several CFTR activators, potentiators and correctors have been developed to increase ligand availability, channel gating and correctly localised functional expression, respectively. All these modulations increase channel activity and thus treat the channel dysfunction which causes cystic fibrosis (Zhang et al., 2012).

1.5.1. Ion channel inhibitors as therapeutics

Around 20% of all drugs currently approved by the FDA in the United States are ion channel modulators (Bajaj and Han, 2019; Charlton et al., 2020; Mathie et al., 2020; Walsh, 2020; Wulff and Zhorov, 2008; Zamponi et al., 2015; Zhang et al., 2012). These drugs have a variety of different targets and uses. Ion channel inhibitors have been used in various treatments, and some have been shown to have more than one therapeutic function.

Ca_v inhibitors, such as verapamil hydrochloride have been used to arrest the cell cycle, thus enabling cytostatic drug treatments on cancer cells (Wu et al., 2020; Zamponi et al., 2015). Verapamil has also been shown to prolong survival in lung cancer patients and reduces breast cancer proliferation in mouse studies. Additionally, nifedipine has been used to reduce lung cancer mitogenesis caused by endothelin 1 (Zhang et al., 2008).

Quinine, a naturally occurring product from the bark of *Cinchona* species, has long been used as an anti-malarial agent (D'Alessandro et al., 2020). Although quinine extraction from the tree bark originally occurred in 1820, the bark in powdered form had been used as a healing therapeutic for centuries. Its stereoisomer quinidine, and synthetic derivatives such as chloroquine, have also been used for malaria treatments. All three drugs reduce K⁺ and Na⁺ channel activity and have shown to treat both lupus and rheumatoid arthritis in clinical trials. Quinine can also be used as a muscle relaxant, whereas quinidine is used as an antiarrhythmic, and chloroquine studies have suggested it could be used in anti-cancer treatments.

While most research has focused on cation channel inhibitors, as the channels have been studied more extensively than anion channels, chloride channel modulators specific for the CFTR channel are in clinical trials to reduce cystic fibrosis symptoms and CFTR inhibitors are specifically being investigated as a treatment for diarrhoeas induced by enterotoxins, such as toxin release due to infection with *Vibrio cholerae* (Zhang et al., 2012). Tamoxifen, an anticancer drug mostly used during breast cancer treatment, is also a chloride channel inhibitor (Zheng et al., 2014).

1.5.2. Ion channel inhibitors as antivirals

Antimalarial drugs based upon the K⁺ channel inhibitor quinine have been studied for their potential antiviral properties since 1946, when quinine was first investigated in relation to influenza virus infection in mice (D'Alessandro et al., 2020). More recent studies into the effect of the synthetic derivative chloroquine prevented replication of two IAV strains, H1N1 and H3N2, in vitro. Clinical trials investigating the effect of chloroquine on DENV infection showed

while treatment was found to reduce pain symptoms, there was no difference in the duration of disease in patients (Borges et al., 2013).

Investigation into the urgent requirement of treatments for the novel coronavirus SARS-CoV 2 led to discoveries of FDA-approved calcium channel blockers successfully inhibiting viral infection of epithelial lung cells; the study utilised various drugs used in cardiovascular treatments in cell culture (Zhang et al., 2020). Furthermore, one of the therapies used, amlodipine, was linked to increased survival in hypertension patients infected with SARS-CoV 2. Calcium channel inhibitors have also been confirmed to prevent infection of numerous viruses in cell culture studies, including IAV (Intakhab Alam et al, 2016).

Targeting viroporins instead of host channels has given rise to several antiviral treatments; amantadine and its derivatives have been shown to effectively inhibit IAV replication by targeting the M2 viroporin (Scott and Griffin, 2015). Furthermore, this class of drugs can be utilised to inhibit the HCV p7 and DENV M viroporins. However, due to the error rate of various viral polymerases, resistance mutations are inevitable and have been reported against amantadine and its derivatives in both IAV and HCV infections (Hurt et al, 2006; Foster et al., 2011). Additional compounds also target the HCV p7 viroporin, with amilorides also affecting SARS-CoV E, HIV Vpu and DENV M viroporin functions (Scott and Griffin, 2015).

1.6. Thesis aim

The aim of this thesis is to continue investigations into understanding regulatory mechanisms of the KSHV lytic replication cycle and the latent-lytic switch to determine novel opportunities for KSHV treatments and uncover whether host ion channel modulation is a potential avenue for KSHV therapeutics, given the vast array of research within viral manipulation of host ion channels.

Chapter three aimed to identify whether a potassium channel is required during the lytic phase of the KSHV lifecycle. Research led to the identification of $K_v1.3$ as a potassium channel essential for efficient KSHV lytic replication. Furthermore, the viral protein responsible for $K_v1.3$ upregulation was identified and subsequent increase in $K_v1.3$ channel activity was shown to cause hyperpolarisation of the cell membrane.

Following on from the hyperpolarisation mechanism, chapter four investigates how calcium movement within the cell can affect lytic KSHV replication. Increased $K_v1.3$ activity mediated a hyperpolarised cell state, which led to calcium influx, regulated by $Ca_v3.2$ channels. Increased intracellular calcium levels was shown to cause the relocalisation of NFAT1 to the nucleus, leading to transcriptional activation of NFAT-regulated genes.

Finally, chapter five investigated the conservation of this mechanism within HSV1 and HCMV. While the hyperpolarisation-mediated calcium influx occurred in cells infected with either virus, the potassium channel responsible for hyperpolarisation was not conserved. The specific potassium channels required by each virus were discovered whereas $Ca_v3.2$ -mediated calcium influx requirements were shown to be conserved.

To summarise, this research shows that KSHV, along with HSV-1 and HCMV, requires a hyperpolarisation-mediated calcium influx during lytic viral replication. This mechanism can be targeted via host ion channel inhibitors at various stages to prevent lytic replication.

Chapter 2: Materials and Methods

2 Materials and Methods

2.1. Materials

2.1.1. Cell lines

TREx BCBL1-Rta are a suspension B cell line latently infected with KSHV. This latent infection can be reactivated into lytic replication using a tetracycline-based antibiotic. The adherent cells used were A549; a human lung adenocarcinoma cell line, U87; a primary glioblastoma cell line, human foreskin fibroblasts (HFF), and human embryonic kidney expressing the SV40 T antigen (HEK-293T) cell line. HFF, U87 and TREx BCBL1-Rta cell lines were kind gifts from J. Sinclair (University of Cambridge), J. Ladbury (University of Leeds), and J. Jung (University of Southern California), respectively. A549 and HEK-293T cell lines were obtained from the Health Protection Agency Culture Collection.

2.1.2. Antibodies

All primary antibodies used during Western blotting and confocal microscopy (IF), along with their working concentrations and suppliers, are listed in Table 2.1 below.

Target (clone)	Host Species	Concentration	Supplier
GAPDH (60004-1)	Mouse	1:5000	Proteintech
ORF57 (207.6)	Mouse	1:1000 (1:100 for IF)	Santa Cruz
ORF59	Mouse	1:1000	Britt Glaunsinger; University of California, Berkeley (gift)
c-Myc (9E10)	Mouse	1:500	Sigma-Aldrich
K _v 1.3	Rabbit	1:200	Sigma-Aldrich
Lamin B (ab16048)	Rabbit	1:5000	Abcam
ORF65	Mouse	1:500	SJ Gao; University of Pittsburgh (gift)
NFAT1	Rabbit	1:500 (1:100 for IF)	Abcam

Table 2.1 Primary antibodies used

Secondary antibodies used are listed in Table 2.2. HRP-conjugated antibodies were used in Western blotting experiments, Alexa Fluor-conjugated antibodies were used for confocal microscopy.

Antibody	Concentration	Company
Goat anti-mouse HRP	1:5000	Dako
Goat anti-rabbit HRP	1:5000	Dako
Alexa Fluor 488 anti-rabbit	1:500	ThermoFisher
Alexa Fluor 568 anti-mouse	1:500	ThermoFisher

Table 2.2 Secondary antibodies used

2.1.3. Oligonucleotides

Oligonucleotide primers used in qRT-PCR, were obtained from Integrated DNA Technologies.

Tables of the human (Table 2.3) and viral (Table 2.4) primers used are below.

	Forward	Reverse
GAPDH	TGTCAGTGGTGGACCTGAC	GTGGTCGTTGAGGGCAATG
K_v1.3	CGGTGTCTTGACCATCGCATTG	AAGAGGAGAGGTGCTGGCAACT
K_v1.3 promoter	AACAACCTAGAGCGCTGCAAA	GCGGGGAAATAAGAGGAAAA
K_v3.3	TTGGCTCAGGAGGAGGTGATTG	GGACATGGCAGGCTGGTCAATG
K_v3.4	CCATGTACTGCAAGTCTGAGGAG	CCTCATCAGACAGCACTGCGTT
K_v9.3	ACTTCGGTCTCTAGGTGCCACA	TGAGGCTGGATGTGTGGTCATC
K_v10.2	GTGGAGAAGATGTTTTCGGTGGC	CAGCATCTCATGGTATCGGTTGG
K_v11.1	CATCTGCGTCATGCTCATTGGC	TCTGGTGGAAGCGGATGAACTC
K_{Ca}3.1	CATTCCTGACCATCGGCTATGG	GCCTTGTTAAACTCCAGCTTCCG
Ca_v3.1	TTCACCGCAGTCTTTCTGGCTG	TGACGGAGATGAGCACCAACAG
Ca_v3.2	GGAACATCTCCACCAAGGCACA	TCCATCCTTGGATGACAGCACG
Ca_v3.3	GTGTCCAACCTACATCTTCACGGC	GACAAGAAAGCCATCCAGCACG
IL-6	CATCCCATAGCCCAGAGCATC	GGGTCAGGGGTGGTTATTGC
NFAT1	GATAGTGGGCAACACCAAAGTCC	TCTCGCCTTTCCGCAGCTCAAT
NFAT2	CACCAAAGTCCTGGAGATCCCA	TTCTTCCTCCCGATGTCCGTCT
ANGPT2	ATTCAGCGACGTGAGGATGGCA	GCACATAGCGTTGCTGATTAGTC
COX2	CGGTGAAACTCTGGCTAGACAG	GCAAACCGTAGATGCTCAGGGA
CSF2	GGAGCATGTGAATGCCATCCAG	CTGGAGGTCAAACATTTCTGAGAT
FGF2	AGCGGCTGTACTGCAAAAACGG	CCTTTGATAGACACAACCTCCTCTC
IFNγ	GAGTGTGGAGACCATCAAGGAAG	TGCTTTGCGTTGGACATTCAAGTC
RCAN1	ATACCCAGGCCTCATCACT	CCAGGGAGTCACCCATAGGA
TNFα	GCTGCACTTTGGAGTGATCG	GTGTGCCAGACACCCTATCT

Table 2.3 Human primer sequences used during qRT-PCR analysis

ORF50 (KSHV)	CGCAATGCGTTACGTTGTTG	GCCCGGACTGTTGAATGG
ORF57 (KSHV)	GCCATAATCAAGCGTACTGG	GCAGACAAATATTGCGGTGT
UL69 (HCMV)	TCGGTGGGATGAATTTGGTC	CATGATAGCGTACTGTCCCTTC
US6 (HSV-1)	ATCACGGTAGCCCGGCCGTGTGACA	CATACCGGAACGCACCACACAA
UL48 (HSV-1)	CCGGGTCCGGGATTTACC	CTCGAAGTCGGCCATATCCA

Table 2.4 Viral primer sequences used during qRT-PCR analysis

2.1.4. Compounds

Pre-treatments of each compound listed in Table 5 were given 45 min prior to induction of reactivation, except for ShK-Dap²² (24 hours) and A23187 (treated and reactivated simultaneously).

<u>Compound (abbr.)</u>	<u>Solvent used</u>	<u>Supplier</u>
(2R/S)-6-PNG (PNG)	DMSO	Bio-Techne
4-Aminopyridine (4AP)	H ₂ O	Sigma-Aldrich
Blood Depressing Substance I (BDS I)	DMSO	Bio-Techne
Calcium ionophore A23187 (A23187)	DMSO ≤50 mg/ml (+ heat)	Sigma-Aldrich
Charybdotoxin (CTX)	DMSO	Sigma-Aldrich
Cyclosporin A (CsA)	DMSO	Fluorochem Limited
Flunarizine (Flun.)	DMSO	Alfa Aesar
Margatoxin (MgTX)	PBS + 0.1% BSA	Sigma-Aldrich
Mithramycin A	DMSO	Insight Biotechnology
Mibefradil (Mib)	DMSO	Cambridge Bioscience
Nifedipine (Nif)	DMSO	Sigma-Aldrich
Quinine hydrochloride dihydrate (Qn)	H ₂ O	Sigma-Aldrich
Pimozide (Pim)	DMSO	Cambridge Bioscience
Potassium chloride (KCl)	H ₂ O	ThermoFisher
ShK-Dap ²² (ShK)	DMSO	Bio-Techne
SKF-96365 (SKF)	DMSO	Sigma-Aldrich
Tetraethylammonium chloride (TEA)	H ₂ O	Sigma-Aldrich
TRAM-34 (TRAM)	DMSO ≤2 mg/ml	Sigma-Aldrich

Table 2.5 Drug compounds with solvents and suppliers used

2.1. Methods

2.2.1. Cell culture

All cell culture media and selection antibiotics were obtained from ThermoFisher Scientific unless otherwise stated. The adherent cell lines (A549, U87, HFF and HEK-293T) were all grown in DMEM media with 10% heat inactivated foetal bovine serum (FBS) and 1% penicillin-streptomycin. Adherent cells were passaged by 5 min of treatment with trypsin (0.05% V/V in PBS) to enable disassociation from the flask. TREx BCBL1-Rta, were grown in RPMI-1640 media containing 10% heat inactivated FBS, 1% penicillin-streptomycin and 100 µg/ml hygromycin B. All cells were incubated at 37°C in 5% CO₂ and pelleted by centrifugation at 1500 rpm for 5 min.

TREx BCBL1-Rta were treated with 2µg/ml doxycycline hyclate (Dox) (Sigma-Aldrich) to induce reactivation of the lytic KSHV cycle. Due to autofluorescence of Dox 2mM sodium butyrate was used to induce reactivation during flow cytometry experiments.

2.2.2. Cell Proliferation Assay (MTS)

Cellular metabolic activity was determined using a non-radioactive CellTiter 96 AQueous One Solution Cell Proliferation Assay (MTS) (Promega), according to the manufacturer's manual. 20,000 cells TREx BCBL1-RTA or 10,000 HFF cells were seeded in duplicate in a flat 96-well culture plate (Corning). Each compound was tested at various concentrations and for the same incubation period as required for reactivation experiments; thus BaCl₂⁻, KCl⁻, Qn⁻, TEA⁻ and ShK-Dap²²-treated TREx BCBL1-Rta were incubated for 48 hours while the other compounds in Table 5 were incubated for 24 hours. Compound treated-HFFs were incubated for 7 days. Following compound incubation, CellTiter 96 AQueous One Solution Reagent (Promega) was added and cells were incubated for 1 hour in a humidified incubator in 5% CO₂ at 37 °C. Absorbance was measured at 490 nm using a Powerwave XS2 plate reader (BioTek). Background control consisted of culture medium, without cells, and the signal from this was subtracted to all other absorbance values.

2.2.3. Plasmid preparation

TRC Lentiviral Human KCNA3 shRNA set (5 individual clones) were obtained as glycerol stocks from Dharmacon. pEGFP-N1 was obtained from Clontech, pRTA-EGFP was a kind gift from Gary Hayward (Johns Hopkins University) and pEGFP-ORF57 was created by a previous lab member, James Boyne. All plasmids were prepared using QIAGEN Plasmid Midiprep Kits (Qiagen) according to the protocol provided by the manufacturer.

2.2.4. Transfection

Transfections were performed using Lipofectamine™ 2000 (ThermoFisher), according to the manufacturer's instructions. A total of 2 µg of plasmid DNA and 4 µL Lipofectamine™ 2000 were added to separate aliquots of 100 µl Opti-MEM® (Life Technologies™) and incubated for 10 min at room temperature. The Lipofectamine™ 2000 solution was then mixed with the DNA solution and incubated for 15 min at room temperature before the transfection media was added dropwise onto cells. 1×10^6 A549 or U87 cells were seeded into each well of a 6-well plate prior to transfection, to achieve approximately 80% confluency at the time of transfection. Cells were harvested 24 hours after transfection.

5×10^5 HEK-293T cells were seeded into each well of a 12-well plate prior to transfection, to achieve approximately 70% confluency at the time of transfection. 0.65µg of both psPAX2 vector and pVSV.G vector (both gifts from Dr. Edwin Chen, University of Leeds), and 1.2 µg of each lentiviral vector separately. The cells were incubated at 37°C for approximately 6 hours and the media replaced with complete DMEM, followed by incubation at 37°C. 48 hours post-transfection, the cells were harvested and spun at 1200 rpm for 3 min to pellet cells. The media from shRNA lentiviral production, via transfection, was then filtered using 0.45µm filter to allow the virus-containing supernatant to be used to infect 500,000 TREx BCBL1-Rta cells per well in a 6-well plate containing a final concentration of 8µg/ml polybrene to assist lentiviral infection. Viral particles were incubated with the TREx BCBL1-Rta cells for 6 hours, before being replaced by fresh RPMI media.

2.2.5. Patch Clamping

Coverslips were washed with 70% Ethanol, followed by a PBS wash. Poly-L-lysine was then added for 1 min. Two additional PBS washes occurred before 5×10^4 cells were seeded in 2 ml media. Cellular solutions are listed in Table 7.

Extracellular Solution			Intracellular Solution		
140mM NaCl	2mM MgCl ₂	10mM glucose	140mM KCl	2mM MgCl ₂	10mM glucose
5mM KCl	2mM CaCl ₂	10mM HEPES- NaOH, pH7.2	5mM EGTA	1mM CaCl ₂	10mM HEPES- KOH, pH7.2

Table 2.6 Solutions used during patch clamping experiments

Cell-coated coverslips were transferred into extracellular solution in a 3.5 mm Petri dish mounted on the stage of an Olympus CK40 inverted microscope. Patch pipettes (5-8 M Ω) were filled with intracellular solution. Series resistance was monitored after breaking into the whole cell configuration and throughout. Each cell was subjected to a series of depolarizing steps from -100 to +60 mV in 10 mV increments for 100 ms to examine K⁺ currents. Voltage-clamp recordings were performed with the use of an Axopatch 200 A amplifier/Digidata 1200 interface controlled by Clampex 9.0 software and analysis was performed using the data analysis package Clampfit 9.0 (both Molecular Devices). Results are presented as means \pm SEM.

2.2.6. Confocal Microscopy

Coverslips were rinsed in 100% ethanol and place in 12-well dish. After air-drying, the coverslips were coated in poly-L-lysine for 5 min. The poly-L-lysine was removed, and coverslips were washed in 2 ml PBS and left to air dry for over 3 hours before adding TReX BCBL1-Rta cells to each well.

After 24 hours, the cells were washed in 2ml PBS before fixation with 2 ml PBS + 4% v/v formaldehyde for 15 mins at room temperature. The cells were washed in 2 ml PBS three times before being permeabilized in 2 ml PBS + 1% v/v Triton-X100 for 15 mins at room temperature. Coverslips were transferred to a humidity chamber and blocked using PBS + 1% w/v BSA for 1 hr at 37 °C. The blocking solution was removed, and coverslips were incubated in 100 μ l

primary antibody, diluted in PBS + 1% w/v BSA for 1 hr at 37 °C. Afterwards, coverslips were washed five times with PBS before being incubated with 100 µl Alexa Fluor secondary antibody (ThermoFisher), diluted 1:500 in PBS + 1% w/v BSA, for 1 hr at 37 °C. Coverslips were washed five times with PBS, mounted onto slides using Vectashield + DAPI (Vector Laboratories) and stored at 4 °C. Images were collected using a LSM880 Upright confocal microscope (Zeiss) and corresponding Zen software.

2.2.7. RNA extraction

During HSV-1 and HCMV experiments, samples were resuspended in Trizol and incubated at room temperature for 5 mins before 200 µl chloroform was added and tubes were mixed vigorously for 15 sec. After a further 3 min incubation at room temperature samples were spun at 12000 g for 15 mins at 4°C. 500 µl of the upper colourless phase was transferred to a fresh RNase-free tube, 1 µl of glycogen and 500 µl isopropanol was added and the samples were incubated at room temperature for 5 min before being spun at 12000 g for 10 min at 4°C. The supernatant was removed, and the RNA pellet was washed with 1ml 75% ethanol and briefly vortexed. The samples were spun at 7500 g for 5 min at 4°C before the supernatant was removed and the pellets were left to air dry for 5 min. During KSHV experiments, total RNA was extracted using the Monarch® Total RNA Miniprep Kit (New England Biolabs) using the manufacturer's protocol.

All RNA pellets were resuspended in 16 µl RNase-free water. 1.6 µl 10X DNase I Buffer and 1 µl rDNase I to the RNA and mixed gently before being incubated at 37°C for 30 min. Afterwards, 2 µl DNase Inactivation Reagent was added and the samples were incubated for 2 min at room temp, with occasional mixing. The RNA was spun at 10,000 g for 1.5 min and transferred to a fresh tube and stored at -80 °C.

2.2.8. Quantitative real-time polymerase chain reaction (qRT-PCR)

1 µg RNA was diluted in a total volume of 16 µl nuclease-free water, and 4 µl LunaScript RT SuperMix (5X) (New England Biolabs) was added to each sample. Reverse transcription was performed using the protocol provided by the manufacturer. cDNA was stored at -20 °C.

Samples were set up in Corbett tubes and a pre-chilled Corbett tube rack (Corbett Life Sciences). Each primer pair was added in duplicate to cDNA samples extracted at different times (biological replicates). The PCR master mix contained the following for each reaction: 10 µl GoTaq® qPCR Master Mix (Promega), 2 µl primer mix (5 µM of both forward and reverse primers), 3 µl nuclease-free water and 5 µl cDNA (10 ng final amount). The PCRs were performed using a Rotor-Gene™ 6000 Real-Time PCR machine (Qiagen™) using a 3-Step with Melt program. A PCR cycle parameter consisted of 95 °C for 10 min and then 35 cycles of: 95 °C for 15 s, 60 °C for 30 s, and 72 °C for 20 s. Quantitative analysis was then performed using the comparative CT method as previously described (Boyne and Whitehouse 2006).

2.2.9. Chromatin Immunoprecipitation

Chromatin was prepared from 2×10^6 latent or lytic (24 hours post-reactivation) TREx BCBL1-Rta using Pierce™ Chromatin Prep Module (ThermoFisher) following the protocol provided by the manufacturer. Chromatin immunoprecipitations were performed using the EZ ChIP kit (Sigma-Aldrich), following the manufacturer's protocol. Anti-myc (9E10, Sigma-Aldrich) was used at 2 µl. Both Sp1 (ab13370, Abcam) and rabbit IgG (Sigma-Aldrich) were used at 5 µl. Control antibodies and primers were provided within the kit and used as instructed, the K_v1.3 promoter primers are listed in Table 4. qRT-PCR reactions contained 5 µl purified DNA and was quantified as described above.

2.2.10. Subcellular Fractionation

Cell pellets were washed with 1ml PBS and spun at 500 g for 5 min at 4°C. The pellet was resuspended in 600 µl of PBS with 1% Triton (v/v) and lysed for 10 min on ice. 250 µl of the sample was saved for the whole cell fraction. The remaining 350 µl was spun at 720 g for 5 min at 4 °C, the cytoplasm-containing supernatant was transferred into a fresh tube and kept

on ice. The pelleted nuclei were washed in 1 ml of PBS and centrifuged at 720 g for 5 min at 4 °C, the supernatant was discarded and the pellet resuspended in 100 µl PBS with 1% Triton.

2.2.11. Western Blotting

Tris-glycine polyacrylamide running gels (Table 8) were overlaid with stacking gels (per 1 ml: 170µl acrylamide/bis acrylamide solution 37.5:1 (Severn Biotech Ltd), 130 µl 0.25M Tris-HCL (pH 6.8), 10 µl 10% (w/v) SDS, 670µl ddH₂O, 10 µl 10% ammonium persulfate, 2 µl TEMED).

Reagent	10%	12%	15%
ddH ₂ O	1.9 ml	1.8 ml	1.1 ml
Acrylamide/bisacrylamide (37.5:1)	1.7 ml	1.8 ml	2.6 ml
1 M Tris-HCl (pH 8.8)	1.3 ml	1.3 ml	1.3 ml
10% (w/v) SDS	50 µl	50 µl	50 µl
10% (w/v) ammonium persulfate	50 µl	50 µl	50 µl
TEMED	2 µl	2 µl	2 µl

Table 2.7 Tris-glycine polyacrylamide running gel solutions

2x protein solubilizing buffer (50 mM Tris-HCl (pH 6.8), 2% (w/v) SDS, 20% (v/v) glycerol, 50 µg/ml Bromophenol Blue and 10 mM DTT) was added to protein lysates and the samples were denatured by heating at 95 °C for 5 min. Samples were loaded onto appropriate polyacrylamide gels, next to pre-stained protein ladder (Bio-Rad Laboratories, Inc.), as an indicator of molecular weight (kDa). Prior to sample loading, gels were immersed in Tris-glycine running buffer (0.25 M Tris-base, 192 mM glycine, 0.1% (w/v) SDS). Gels were run at 180 V for 45 min or until the solubilizing buffer reached the bottom to the gel. All SDS-PAGE was carried out using a Bio-Rad™ Mini-PROTEAN 3 cell (Bio-Rad Laboratories, Inc.), set up according to the manufacturer's instructions.

Proteins from SDS-PAGE gels were transferred onto Thermo Scientific™ Pierce™ Nitrocellulose membranes (Thermo Fisher), each SDS-PAGE gel and nitrocellulose membrane were soaked in transfer buffer (25 mM Tris- base, 190 mM glycine, 20% (v/v) methanol) and placed in a cassette in sequential order. Transfer from the gel to the membrane

took place at 25 V for 30 min, followed by incubation of the membrane in 5% TBS-Tween blocking buffer (500 mM NaCl, 20 mM Tris, 0.1% (v/v) Tween-20, 5% non-fat dried milk (Marvel) at room temperature for 1 hour. The membrane was then incubated in the corresponding primary antibody (listed in Table 7) diluted in 5% TBS-Tween blocking buffer overnight at 4°C. Membranes were washed 3x for 5 min in 1x TBS-tween buffer (20 mM Tris, 0.1% Tween-20, 150 mM NaCl), and incubated for 1 hour at room temperature in the appropriate polyclonal goat secondary horseradish peroxidase (HRP) conjugated antibody (Dako), diluted to 1:5000. The membranes were then washed 3x for 5 min in 1x TBS-Tween buffer. Protein bands were visualized by enhanced chemiluminescence using EZ-ECL enhancer solutions A and B kit (Geneflow™) (1:1 ratio) and imaged using a G-Box (Syngene). All incubations and washes were performed with agitation.

2.2.12. Flow Cytometry

(Bis-(1,3-Dibutylbarbituric Acid) Trimethine Oxonol (DiBAC₄(3)) and Fura Red (both ThermoFisher) were added to cells at 1 μM final concentration in DMEM or RPMI media. Cells were incubated at 37°C with Fura Red for 30 min, or DiBAC₄(3) for 5 min before being washed in PBS and analysed on a CytoFLEX Flow Cytometer (Beckman).

2.2.13. Statistical analysis

Statistical significance of data was determined by performing Student's t-test. Significance values correspond to P-values of ≤0.05, ≤0.01, ≤0.001, and ≤0.0001.

**Chapter 3: Investigating the role of host K⁺ channels in the KSHV
lytic replication cycle**

3 Investigating the role of host K⁺ channels during KSHV lytic replication

3.1. Introduction

Potassium ion (K⁺) channels are the largest family of ion channels, with around 80 genes relating to K⁺ channels encoded within the human genome (O'Grady and Lee, 2005). Channels from within this superfamily play various roles in viral replication cycles, such as MCPyV and Simian virus 40, which both require specific K_v channels during host cell entry, while an undetermined K⁺ channel is required for IAV entry (Stauffer et al., 2014). HIV interacts with several K⁺ channels, including K_v2.1, K_v1.3, K_v11.1, and K_{2P}3.1 specifically, along with an undetermined BK_{Ca} and two K_{ir} channels (Hover et al., 2017; Charlton et al., 2020). HCV also interacts with K_v2.1, which are usually expressed within the liver (Mankouri et al., 2009). Along with other cation channels, rabies virus infection leads to the reduced activity of K_{ir} within neurons, thus affecting action potential firing (Iwata et al., 1999). While research into potassium channel dependency within *Bunyavirales* has shown BUNV requires a K_{2P} channel, the specific potassium channels required by both Schmallenberg virus and Hazara virus are yet undetermined (Hover et al., 2016). Therefore, manipulation of the host cell channelome is utilised by multiple viruses in addition to the activity of virally-encoded viroporins.

The roles of both Ca_v and Na_v channels have been studied during both HSV-1 and HSV-2 lytic replication (Ding et al., 2021; Zhang et al., 2019), and HCMV upregulates several K⁺ channels (Oberstein and Shenk, 2017). However, no role for any host ion channels have been reported in the KSHV lytic replication cycle to date. As K⁺ channels are the most abundant family of ion channels, we began our investigation by assessing the effect of potassium inhibitors in KSHV reactivation. This chapter describes KSHV-mediated upregulation of K_v1.3, which increases channel activity and leads to membrane hyperpolarisation, essential for KSHV lytic replication.

3.2. General K⁺ inhibition affects KSHV lytic replication

To determine whether any K⁺ channels were essential for KSHV lytic replication a range of general K⁺ channel inhibitors were screened. Initially, TREx BCBL1-Rta were treated with different concentrations of broad-spectrum K⁺ channel blockers (O'Grady and Lee, 2005; Wulff and Zhorov, 2008); potassium chloride (KCl), tetraethylammonium (TEA) and quinine (Qn), in an MTS assay to determine non-toxic levels appropriate for 48-hour treatment (Figure 3.1). KCl causes imbalances in the ion concentration, due to an increase in the levels of extracellular K⁺ ions, along with extracellular levels of Cl⁻. Qn affects both K⁺ and Na⁺ voltage-gated channels and TEA mimics the K⁺ ion, thus acting as a broad-spectrum K⁺ channel inhibitor. As around 70% of TREx BCBL1-Rta survived with treatments of 25 mM, 200 μ M or 50 mM of KCl, Qn or TEA respectively (Figure 3.1), these concentrations were used in further experiments.

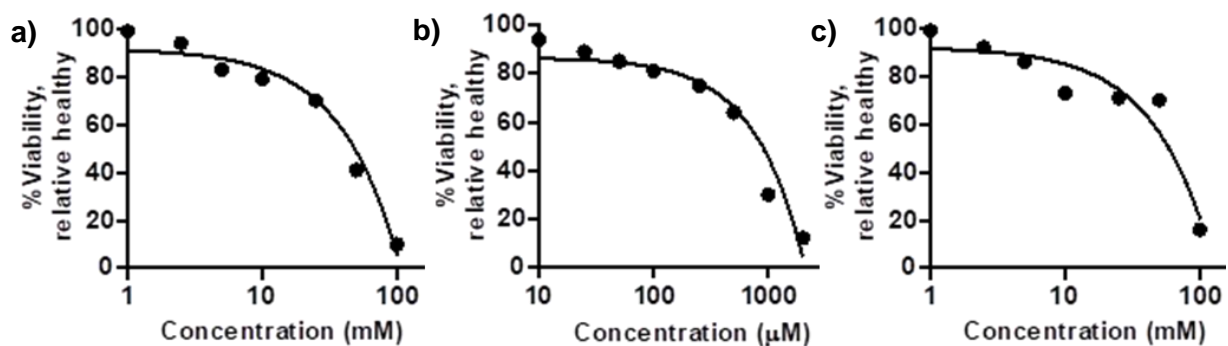


Figure 3.1 Cell viability of TREx BCBL1-Rta in the presence of KCl (a), Qn (b) or TEA (c). TREx BCBL1-Rta cells were treated with varying concentrations of KCl, Qn or TEA for 48 hours before cell survival was assessed via MTS assay. Results are presented on an XY-graph using a log-scale.

The selected inhibitors were then used to assess whether KSHV reactivation and lytic replication could be prevented by blocking K⁺ channels; all were successful in reducing the levels of the early ORF57, delayed early ORF59, and late ORF65 protein levels in TREx BCBL1-Rta cells (Figure 3.2). Whereas, Myc-Rta levels were still evident, indicating Rta production had been successful and that the K⁺ inhibitors did not affect reactivation of the virus. Together, these results suggest that K⁺ channels are required for efficient KSHV lytic replication.

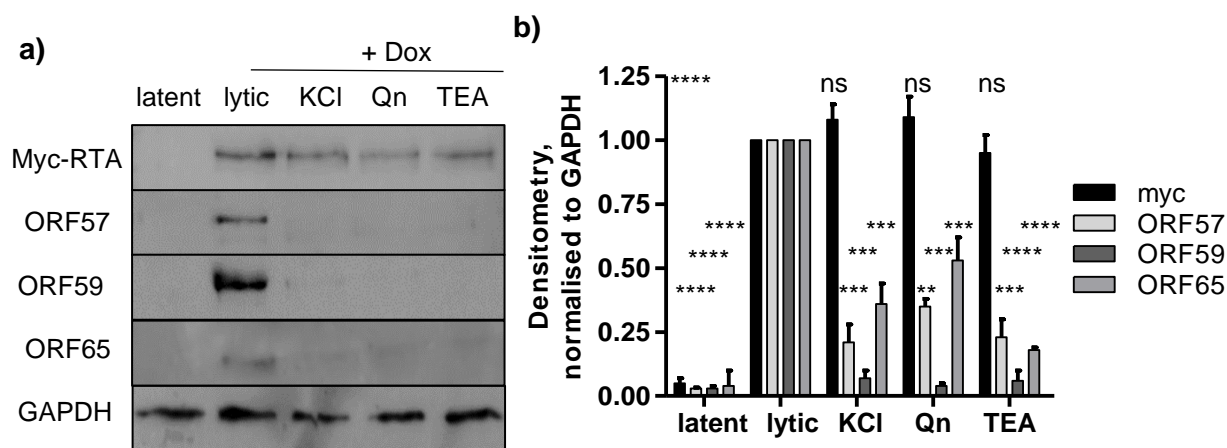


Figure 3.2 Effect of general potassium inhibitors on KSHV lytic replication. TReX BCBL1-Rta cells were treated with DMSO or non-cytotoxic concentrations of each K^+ inhibitor prior to reactivation with Dox. Cells were then harvested at 48 hours post-induction and Western blotting performed to assess lytic protein production. KCl, Qn and TEA pre-treatments were all able to prevent Dox treatment reactivating the lytic phase of the KSHV replication cycle (a). Densitometry for each protein were normalised to GAPDH levels (b). Asterisks correspond to P-values of ≤ 0.05 (*), ≤ 0.01 (**), ≤ 0.001 (***), and ≤ 0.0001 (****), respectively; ns denotes a P-value of > 0.05 .

3.3. K_v activity is required for KSHV lytic replication

Given that general K^+ blockers, particularly Qn, a voltage-gated channel inhibitor, could prevent KSHV lytic replication in TReX BCBL1-Rta cells, 4-114 Aminopyridine (4AP), a K_v1 -selective voltage-gated K^+ channel inhibitor (O'Grady and Lee, 2005; Wulff and Zhorov, 2008), was used further pinpoint a potential family of K^+ channels required for KSHV lytic replication. Concentrations of up to 1mM 4AP showed more than 70% cell viability in an MTS assay (Appendix, supplementary figure 1), therefore a suitable dose-dependent pre-treatment experiment was performed. Results in Figure 3.3 show a reduction in ORF57 protein levels upon increasing concentrations of 4AP, prior to reactivation. These results suggest a K_v1 channel is required during the KSHV lytic replication cycle.

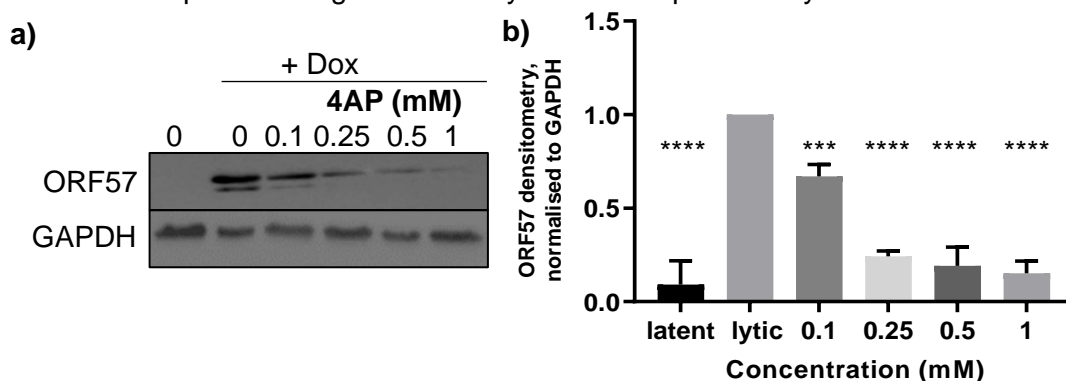


Figure 3.3 Effect of K_v inhibitor, 4AP, on KSHV lytic replication. Western blotting shows ORF57 protein levels were reduced in a dose dependent manner by 4AP pre-treatment (a). Densitometry for ORF57 levels were normalised to GAPDH levels (b). Asterisks correspond to P-values of ≤ 0.05 (*), ≤ 0.01 (**), ≤ 0.001 (***), and ≤ 0.0001 (****), respectively; ns denotes a P-value of > 0.05 .

3.4. K_v1.3 is required for KSHV lytic replication

The *Shaker*-family (K_v1) is a large family of K⁺ channels, which are specifically expressed in different cell types (O'Grady and Lee, 2005). Review of the literature suggests that one K_v channel, K_v1.3, is specifically expressed in B cells (Wulff et al., 2004, Wulff and Zhorov, 2008). Therefore, margatoxin (MgTX) and ShK-Dap²² (ShK), specific inhibitors of the K_v1.3 channel (Kalman et al., 1998, Bajaj and Han, 2019), were used to assess the role of K_v1.3 in KSHV lytic replication. Concentrations of up to 100nM MgTX showed cell viability of around 80%, whereas ShK was non-toxic in picomolar concentrations (Appendix, supplementary figure 2). Results in Figure 3.4 show that both MgTX and ShK reduce the level of ORF57 protein production in a dose-dependent manner, suggesting K_v1.3 is specifically required during the

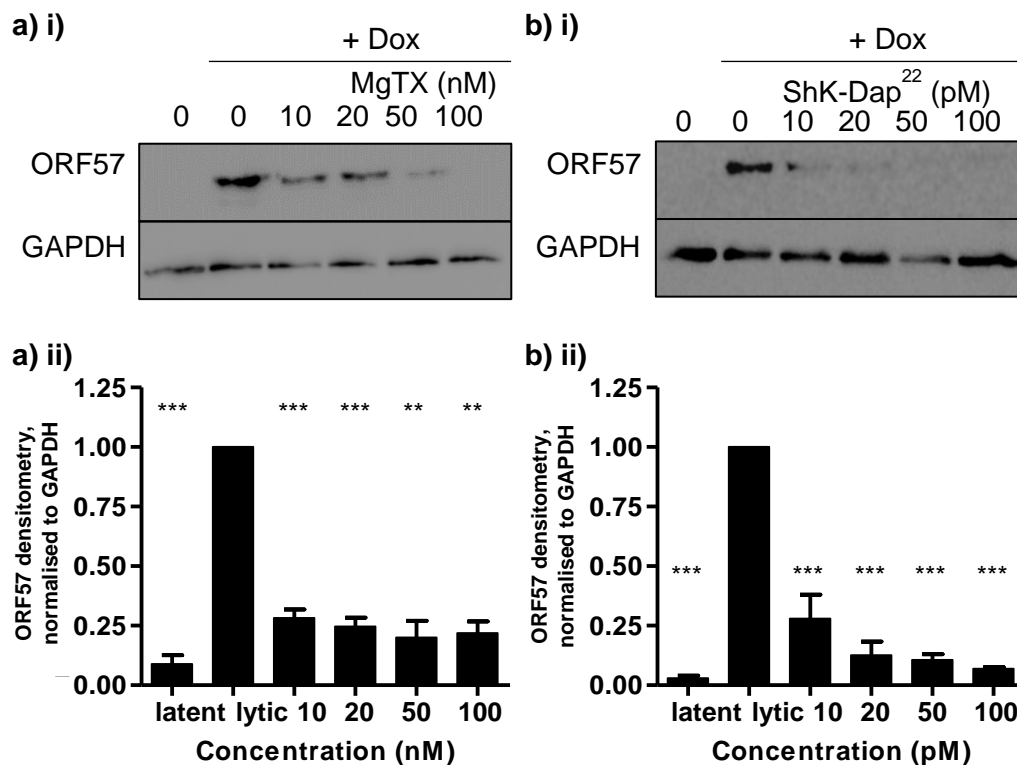


Figure 3.4 Effect of K_v1.3 inhibitors on KSHV lytic replication. MgTX inhibits ORF57 protein expression in a dose dependent manner (a). ShK-Dap²² inhibits ORF57 protein expression in a dose dependent manner, shown via Western blot (b). Densitometries for ORF57 levels were normalised to GAPDH levels (ii). Asterisks correspond to P-values of ≤0.05 (*), ≤0.01 (**), ≤0.001 (***), and ≤0.0001 (****), respectively; ns denotes a P-value of > 0.05.

KSHV replicative cycle.

To confirm the observed inhibition of KSHV lytic replication was K_v1.3 specific, similar experiments were performed with non-cytotoxic concentrations (previously assessed by MTS assay, Appendix, supplementary figure 3) of TRAM, an inhibitor of K_{Ca}3.1, a Ca²⁺-activated K⁺

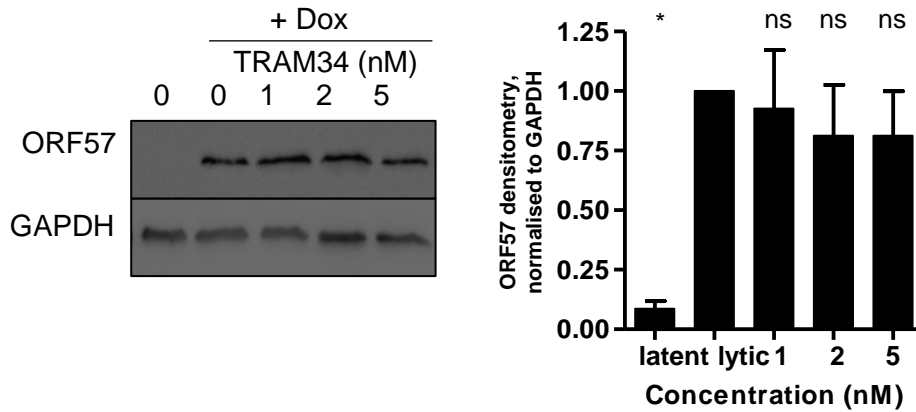


Figure 3.5 Effect of $K_{Ca}3.1$ inhibitor, TRAM-34, on KSHV lytic replication. TRAM-34 had no effect on ORF57 protein levels, shown via Western blot (a). Densitometries for ORF57 levels were normalised to GAPDH levels (b). Asterisks correspond to P-values of ≤ 0.05 (*), ≤ 0.01 (**), ≤ 0.001 (***), and ≤ 0.0001 (****), respectively; ns denotes a P-value of > 0.05 .

channel present in lymphocytes, including TREx BCBL1-Rta (Wulff et al., 2004, Wulff and Zhorov, 2008). Notably, there has been some indication of compensation between the two channels (Chiang et al, 2017). However, ORF57 protein production was unaffected after 24 hours in the presence of a dose-dependent increase in TRAM-34 levels (Figure 3.5), showing that KSHV lytic replication cycle was not reliant on $K_{Ca}3.1$ channel activity.

3.5. $K_v1.3$ expression is induced during KSHV lytic replication

As $K_v1.3$ blockade was sufficient to prevent KSHV lytic replication, $K_v1.3$ gene expression was analysed during infection. mRNA levels of $K_v1.3$ were assessed using qRT-PCR comparing latent and lytically reactivated cells. Results show that while $K_v1.3$ is expressed in latently infected TREx BCBL1-Rta cells, $K_v1.3$ expression is dramatically increased 24 hours after KSHV reactivation (Figure 3.6a). In contrast, no change in $K_{Ca}3.1$ expression was observed. To confirm the increase in $K_v1.3$ expression, protein levels were also assessed using immunoblotting, comparing latent and lytically reactivated cell lysates. $K_v1.3$ protein levels

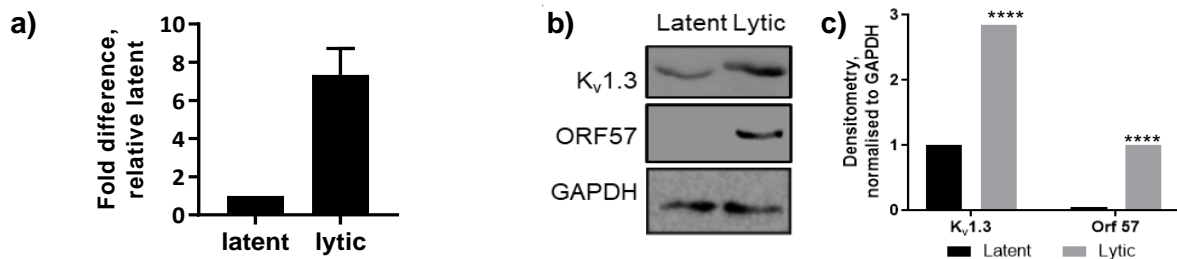


Figure 3.6 $K_v1.3$ expression in TREx BCBL1-Rta cells. RNA levels of $K_v1.3$ and $K_{Ca}3.1$ in both latently and lytically KSHV-infected TREx BCBL1-Rta cells (a). Protein levels of $K_v1.3$ and ORF57 in both latently and lytically KSHV-infected TREx BCBL1-Rta cells, shown via Western blot (b). Densitometries for each protein were normalised to GAPDH levels (c). Asterisks correspond to P-values of ≤ 0.05 (*), ≤ 0.01 (**), ≤ 0.001 (***), and ≤ 0.0001 (****), respectively; ns denotes a P-value of > 0.05 .

were present in latently infected TREx BCBL1-Rta cells, however the levels of K_v1.3 were significantly increased at 24 hours post KSHV reactivation (Figure 3.6b). Efficient reactivation of KSHV lytic replication was confirmed by the presence of ORF57 protein. Together the results show a significant increase in K_v1.3 expression in lytically infected cells, 24 hours post-reactivation, suggesting that KSHV induces K_v1.3 levels during lytic replication.

3.6. KSHV Rta protein induces K_v1.3 expression

Upregulation of K_v1.3 is seen rapidly after KSHV reactivation, therefore viral protein expression is likely to be activating this increase. To confirm this, transient expression of the two major immediate early transcription factors was performed to determine if they altered endogenous K_v1.3 expression in A549 and U87 cell lines. Both cell lines have endogenous K_v1.3 expression and are more readily transfectable than TREx BCBL1-Rta cells. Results showed GFP-Rta upregulated K_v1.3 mRNA levels in both A549 and U87 cells, in contrast to GFP-ORF57. IL-6, a host gene known to be upregulated by Rta (Deng et al., 2002), was used as a positive control (Figure 3.7a). To confirm the role of GFP-Rta in K_v1.3 induction, a similar experiment was repeated using a dose-dependent increase in GFP-Rta levels. Results showed a clear dose-dependent increase in K_v1.3 levels relative to the amount of GFP-Rta (Figure 3.7b).

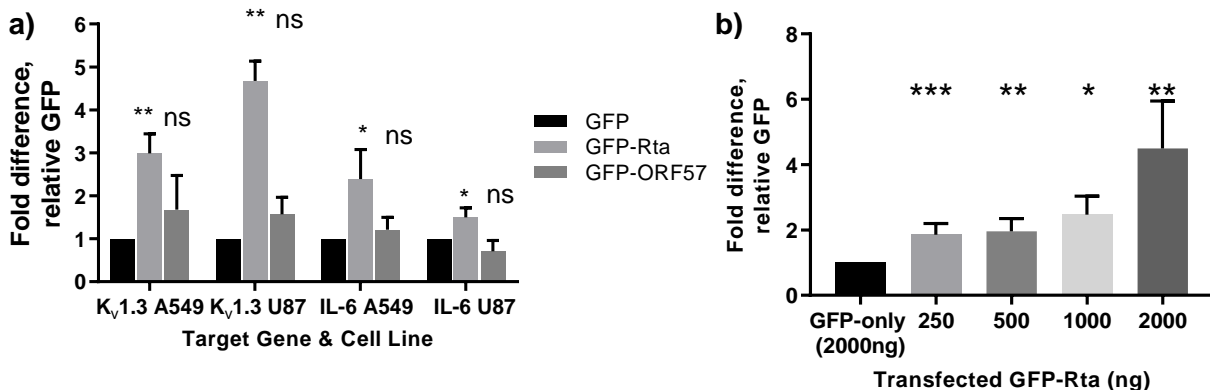


Figure 3.7 Expression levels of K_v1.3 after transfection of GFP-viral constructs. K_v1.3 & IL-6 expression in A549 and U87 cell lines transfected with either GFP, GFP-Rta or GFP-ORF57 (a). K_v1.3 expression in U87 cell lines transfected with varying doses of GFP-Rta (supplemented with GFP, to 2 μ g total DNA transfection) (b). Asterisks correspond to P-values of ≤ 0.05 (*), ≤ 0.01 (**), ≤ 0.001 (***), and ≤ 0.0001 (****), respectively; ns denotes a P-value of > 0.05 .

KSHV Rta functions as a transcriptional activator by direct and indirect activation mechanisms. K_v1.3 has previously been shown to be regulated by Specificity Protein 1 (Sp1) (Jang et al., 2015). Interestingly, Rta utilises Sp1 to activate a range of viral and host cell promoters. Therefore, additional transfection experiments were performed to determine whether Rta-

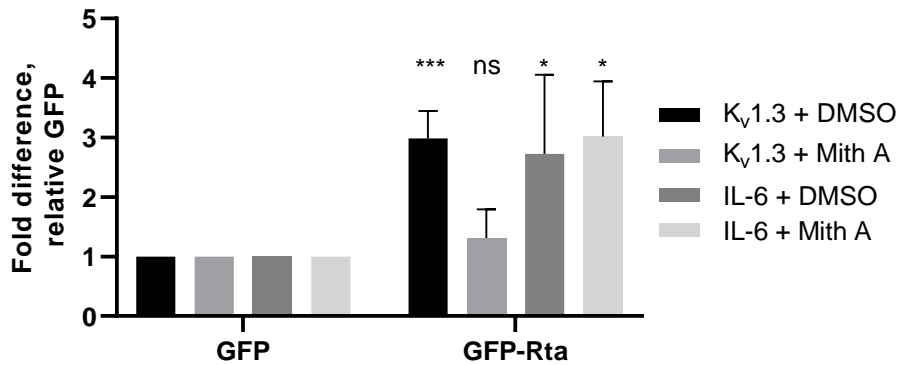


Figure 3.8 K_v1.3 and IL-6 expression in transfected U87 cells, pre-treated with Mith A or DMSO. Asterisks correspond to P-values of ≤ 0.05 (*), ≤ 0.01 (**), ≤ 0.001 (***), and ≤ 0.0001 (****), respectively; ns denotes a P-value of > 0.05 .

mediated K_v1.3 upregulation was dependent upon Sp1. Results show that non-cytotoxic levels of Mithramycin A (Mith A) (Appendix, supplementary figure 4), an Sp1 inhibitor (Liu et al., 2019), prevented Rta-induced upregulation of K_v1.3 in U87 cells, however Rta-mediated IL-6 upregulation was unaffected (Figure 3.8). This suggests that KSHV Rta upregulation of K_v1.3 expression may involve an Sp1-mediated indirect mechanism.

To confirm that KSHV Rta protein associated with the K_v1.3 gene promoter, ChIP assays were performed. Results using specific antibodies showed that myc (for Rta) and Sp1 precipitated the K_v1.3 promoter, showing that Rta and Sp1 proteins both associated to K_v1.3 promoter during KSHV lytic replication (Figure 3.9). Rabbit IgG was used as a negative control antibody. This suggests that Rta binding is required to induce K_v1.3 expression. Additionally, Sp1 binding was significantly increased in lytically infected TREx BCBL1-Rta cells supporting a potential indirect mechanism.

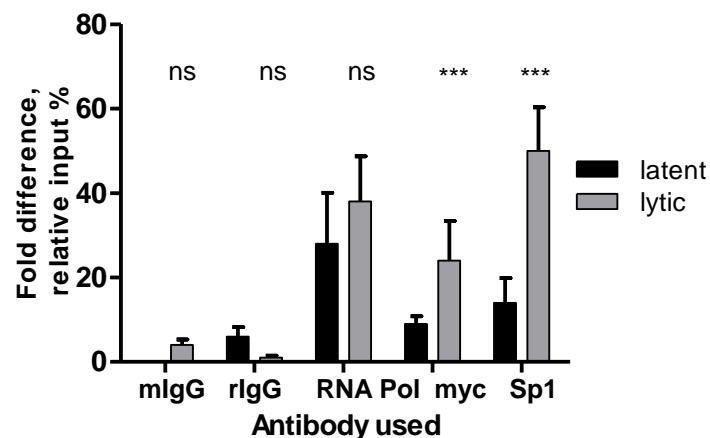


Figure 3.9 ChIP analysis of proteins binding the K_v1.3 promoter region in latent and lytically infected cells. RNA polymerase, myc and Sp1 all bound to the K_v1.3 promoter, with increased binding of both myc and Sp1 occurring within lytically infected TREx BCBL1-Rta cells. Asterisks correspond to P-values of ≤ 0.05 (*), ≤ 0.01 (**), ≤ 0.001 (***), and ≤ 0.0001 (****), respectively; ns denotes a P-value of > 0.05 .

3.7. $K_v1.3$ activity is increased during KSHV lytic replication

As an increase in $K_v1.3$ protein levels was observed, $K_v1.3$ activity was subsequently measured using whole cell patch-clamp recordings in TREx BCBL1-Rta cells, comparing latent and lytic replication cycles. Results showed a voltage-gated outward K^+ current in latent TREx BCBL1-Rta cells, which is significantly enhanced during KSHV lytic replication (Figure 3.10). To confirm the outward current was specific to $K_v1.3$, cells were pre-treated with ShK-Dap²² or control DMSO prior to patch clamp experiments. TREx BCBL1-Rta cells pre-treated with ShK showed significantly reduced voltage-gated outward K^+ current density during both latent and KSHV lytic replication, confirming the current density seen in DMSO-treated cells was due to $K_v1.3$ activity and that $K_v1.3$ activity is increased in lytically-replicating TREx BCBL1-Rta cells. Overall, this indicates cells undergoing KSHV lytic replication have increased $K_v1.3$ expression which enhances $K_v1.3$ activity.

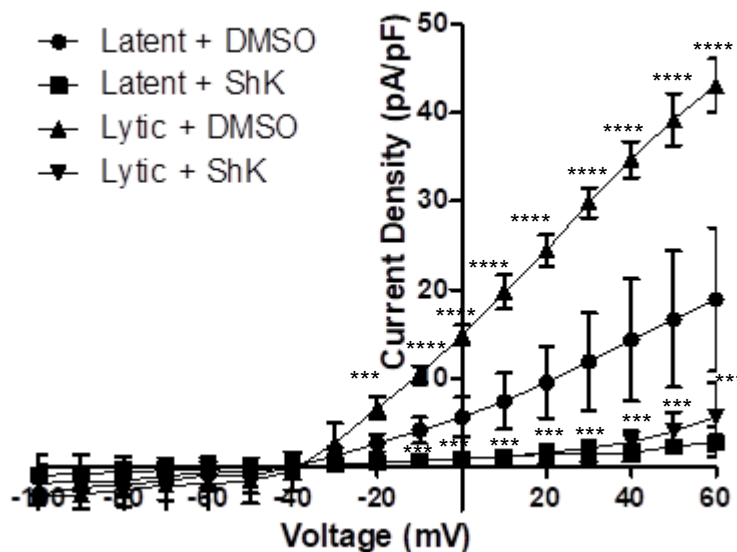


Figure 3.10 $K_v1.3$ channel activity as seen via patch clamping in TREx BCBL1-Rta cells. Both latent and lytic TREx BCBL1-Rta cells were pre-treated with ShK-Dap²² or DMSO for channel activity experiments. Asterisks correspond to P-values of ≤ 0.05 (*), ≤ 0.01 (**), ≤ 0.001 (***), and ≤ 0.0001 (****), respectively.

3.8. KSHV lytic replication causes cell membrane hyperpolarisation

Patch clamping experiments showed a voltage-gated outward K^+ current due to KSHV-mediated upregulation of $K_v1.3$ activity. An outward K^+ current removes K^+ ions from the cell, which would lead to a hyperpolarised cell membrane. To confirm that KSHV lytically-replicating cells were hyperpolarised, DiBAC₄(3) was used in flow cytometry experiments (Krasznai et al., 1995). DiBAC₄(3) is a membrane-permeable fluorescent dye which readily enters depolarised

cells, therefore exhibiting a greater mean fluorescence, due to the greater concentration in depolarised cells. However, in hyperpolarised cells DiBAC₄(3) concentration is reduced and thus cells display a lower fluorescence intensity.

Prior to experiments with lytically infected cells, an appropriate concentration of DiBAC₄(3) was

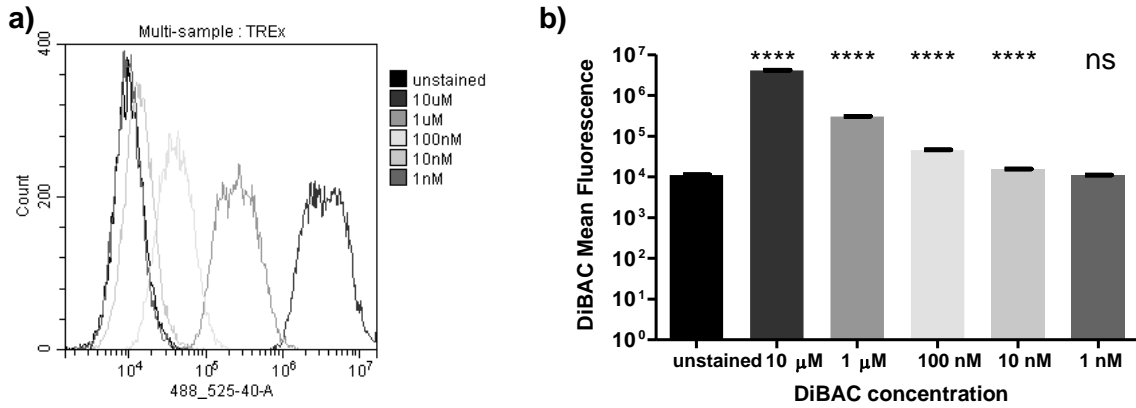


Figure 3.11 Mean fluorescence caused by serial dilutions of DiBAC₄(3). Presented as raw histograms (a) and bar chart with statistical analysis (b) Asterisks correspond to P-values of ≤0.05 (*), ≤0.01 (**), ≤0.001 (***), and ≤0.0001 (****), respectively; ns denotes a P-value of > 0.05.

determined. While any concentration above 10 nM showed a statistically significant increase in mean fluorescence (Figure 3.11), the mean fluorescence histogram generated by concentrations less than 100nM showed overlap with the unstained mean fluorescence histogram (Figure 3.11a). Visualising a decrease in signal due to hyperpolarisation would have been more challenging under these conditions, therefore a final concentration of 1 μM DiBAC₄(3) was chosen for experimental purposes.

To assess whether a hyperpolarised state is observed in KSHV-lytically replicating cells, DiBAC₄(3) mean fluorescence was measured at regular intervals post reactivation. A reduction in fluorescence in KSHV lytic samples was observed confirming a hyperpolarised state is

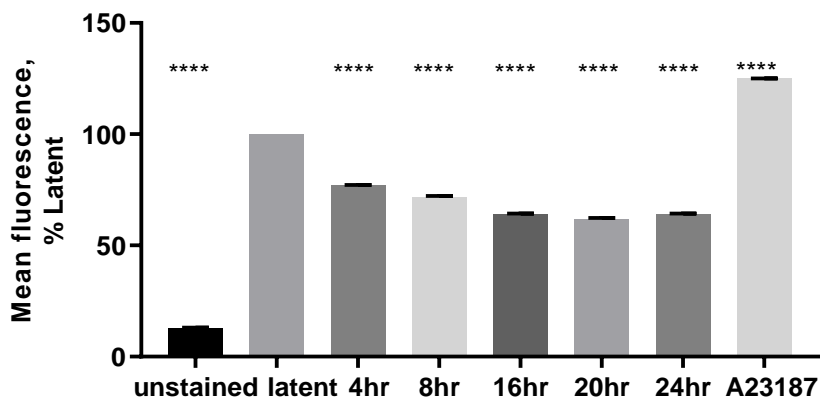


Figure 3.12 DiBAC₄(3) mean fluorescence of TReX BCBL1-Rta cells, as measured by flow cytometry. DiBAC₄(3) mean fluorescence, over a reactivation time-course in TReX BCBL1-Rta cells, displayed as a percentage, relative to latent. Asterisks correspond to P-values of ≤0.0001 (****).

induced by KSHV lytic replication. This hyperpolarised state was seen throughout the first 24 hours of KSHV lytic replication (Figure 3.12). The hyperpolarised state was most apparent after 16 hours post-reactivation, coinciding with the increased activity of $K_v1.3$ seen during patch clamping experiments. A23187, a calcium ionophore (Abbott et al., 1979), was used to cause depolarisation within cells as a positive control.

3.9. $K_v1.3$ is essential for KSHV lytic replication

To definitively demonstrate that $K_v1.3$ is required for KSHV lytic replication, targeted lentivirus $K_v1.3$ shRNA-mediated depletion was performed. Two weeks after lentiviral transduction, two separate cell lines showed reduced levels of $K_v1.3$ mRNA compared to a scramble control (Figure 3.13a). Further analysis of $\Delta K_v1.3a$ (now termed $\Delta K_v1.3$) showed that $K_v1.3$ protein level was also reduced by 90% when compared to the scramble control (Figure 3.13b).

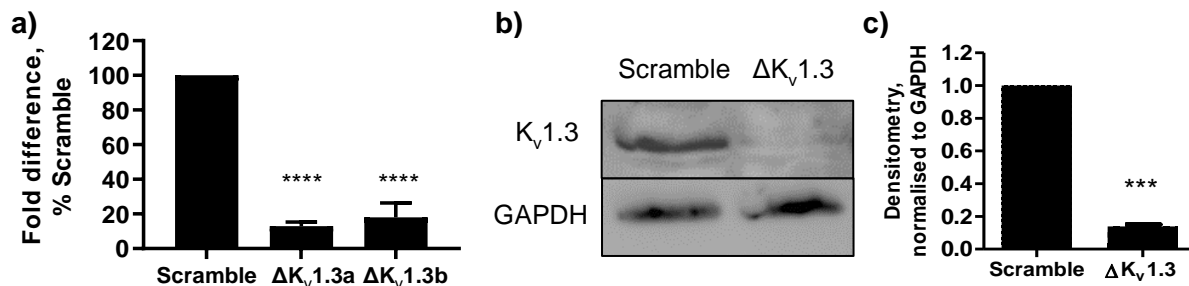


Figure 3.13 RNA and protein levels of $K_v1.3$ in knockdown cell lines, compared to the control scramble cell line. $K_v1.3$ RNA expression in scramble and knockdown cell lines (a). $K_v1.3$ protein levels in the scramble cell line and a $K_v1.3$ knockdown cell line (b). Asterisks correspond to P-values of ≤ 0.05 (*), ≤ 0.01 (**), ≤ 0.001 (***), and ≤ 0.0001 (****), respectively; ns denotes a P-value of > 0.05 .

3.10. Channel activity in $K_v1.3$ knockdown is decreased

To examine the effect of $K_v1.3$ depletion during KSHV lytic replication, voltage gated outward channel activity was measured compared to the scramble control. The scramble cell line exhibited similar activity to wild-type TREx BCBL1-Rta cells, with significantly heightened activity during KSHV lytic replication when compared to latently infected scramble cells (Figure 3.14). In contrast, $K_v1.3$ depletion resulted in reduced voltage-gated channel activity during both latent and lytic replication, with no significant difference in activity between the two states. Similarly, the current density of both latent and lytic $\Delta K_v1.3$ cells tested showed no significant difference to that of latently infected scramble cells.

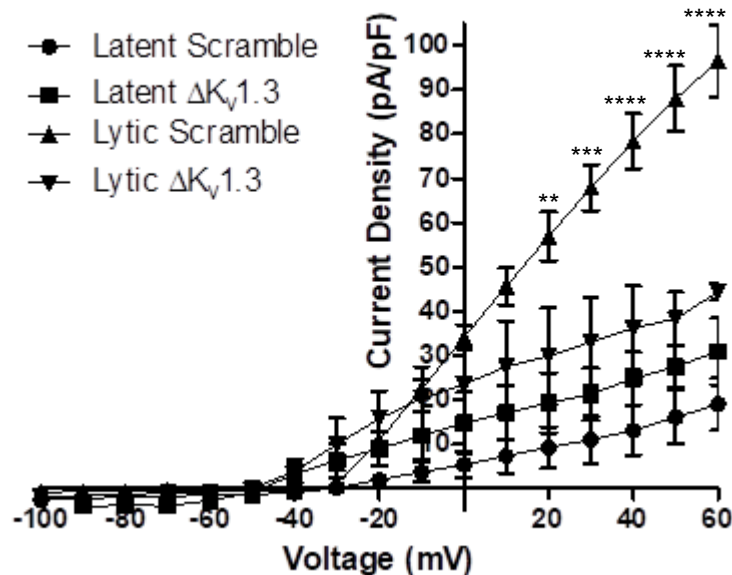


Figure 3.14 $K_v1.3$ channel activity and hyperpolarisation as seen via patch clamping. Patch clamping experiments showing current density in scramble and $\Delta K_v1.3$ cell lines undergoing either latent or KSHV lytic replication. Asterisks correspond to P-values of ≤ 0.05 (*), ≤ 0.01 (**), ≤ 0.001 (***), and ≤ 0.0001 (****), respectively.

To further confirm the activity of $K_v1.3$ resulted in the hyperpolarization observed in lytically infected TReX BCBL1-Rta cells, DiBAC₄(3) fluorescence was assessed via flow cytometry.

The scramble cell line showed a similar pattern of hyperpolarization as TReX BCBL1-Rta, however $\Delta K_v1.3$ cells showed no significant difference, when compared to the untreated control throughout the time-course of Dox treatment (Figure 3.15). However, both cell lines were significantly depolarized by A23187. Together this confirms that $K_v1.3$ activity is required for KSHV-mediated hyperpolarisation during KSHV lytic replication.

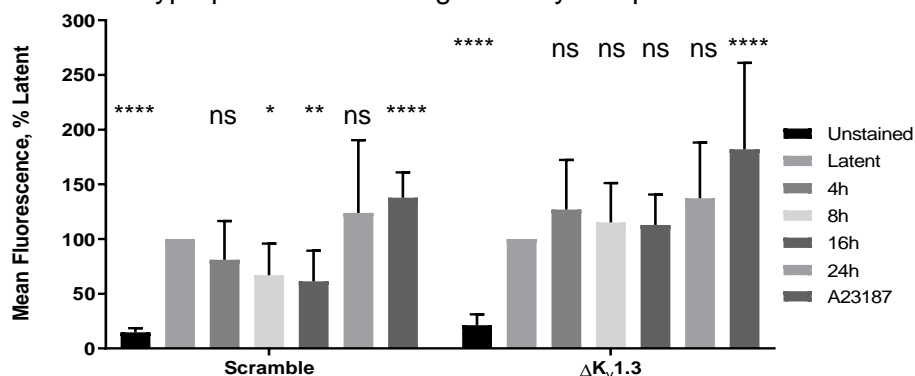


Figure 3.15 DiBAC₄(3) mean fluorescence, measured via flow cytometry. DiBAC₄(3) mean fluorescence, over a reactivation time-course in scramble and $\Delta K_v1.3$ cell lines, displayed as a percentage, relative to latently infected TReX BCBL1-Rta cells. Asterisks correspond to P-values of ≤ 0.05 (*), ≤ 0.01 (**), ≤ 0.001 (***), and ≤ 0.0001 (****), respectively; ns denotes a P-value of > 0.05 .

3.11. $K_v1.3$ knockdown inhibits KSHV lytic replication

To assess what effect $K_v1.3$ depletion has on KSHV lytic replication, both the scramble and $\Delta K_v1.3$ cell lines were reactivated, and lytic replication quantified using ORF57 expression as a marker. The scramble control reactivated similar to wild type levels, successfully expressing

ORF57 RNA, whereas $K_v1.3$ depletion resulted in significantly reduced levels of lytic replication, with $K_v1.3$ depletion reducing ORF57 RNA levels by 90% (Figure 3.16a). Additionally, protein levels were assessed using immunoblotting. ORF57, ORF59 and ORF65 were all markedly reduced in the $K_v1.3$ knockdown cell line by between 80 and 95% when compared to the scramble control (Figure 3.16c). To further assess the impact of $K_v1.3$ depletion on infectious virion production, a re-infection assay was performed; there supernatant was harvested from TREx-BCBL1-Rta cells 72 hours post-reactivation and used to infect naïve 293T cells. RNA levels of ORF57 within infected 293T cells were assessed after 24 hours, results in Figure 3.16b show a 90% reduction in ORF57 RNA from 293T cells infected with virion-containing media harvested from the $\Delta K_v1.3$ cell line compared to the scramble control. Together these results suggest that $K_v1.3$ is essential for KSHV lytic replication, as viral gene expression and infectious virion production is significantly reduced.

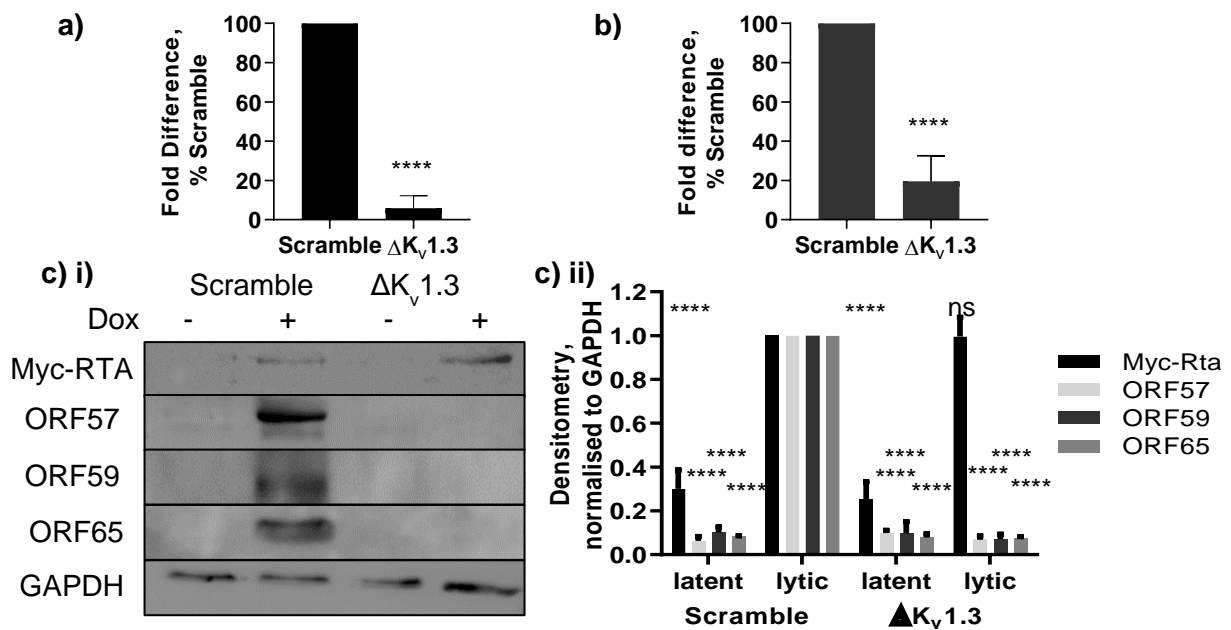


Figure 3.16 Viral gene expression in scramble and $\Delta K_v1.3$ cell lines. ORF57 RNA levels, in latent cells and 24 hours after reactivation (a), in 293T cells 24 hours after infection with virion containing media from either scramble or $\Delta K_v1.3$ cell lines (b), both measured via qRT-PCR. Viral protein levels in latent cells and 48 hours after reactivation, measured by immunoblotting (c i)) Densitometries were normalised to GAPDH levels (c ii)). Asterisks correspond to P-values of ≤ 0.05 (*), ≤ 0.01 (**), ≤ 0.001 (***), and ≤ 0.0001 (****), respectively; ns denotes a P-value of > 0.05 .

3.12. Discussion

As K_v upregulation has been associated with tumorigenesis in a variety of carcinomas (Chiang et al., 2017; Jang et al., 2011; Jang et al., 2015; O'Grady and Lee, 2005), the KSHV-mediated upregulation of $K_v1.3$ could contribute to the oncogenic nature of the virus by enhancing lytic replication. Further investigation into the potential role of $K_v1.3$ in KSHV lytic replication infections could assist in elucidating why KSHV requires $K_v1.3$ expression. Results show that $K_v1.3$ expression is upregulated in an Rta-dependent manner. However, confirmation of Rta-Sp1- $K_v1.3$ promoter binding would be useful either by proximity ligation assay or assessing the protein-protein interactions of Sp1 and Rta. Preliminary investigation into the Rta binding sites within the human genome did not indicate a classical Rta response element within the $K_v1.3$ promoter, suggesting an indirect activation mechanism, where Sp1 binds directly to the promoter with Rta binding to Sp1. Sp1- $K_v1.3$ promoter binding has previously been shown by Jang et al (2015). Therefore, preventing $K_v1.3$ upregulation by inhibiting the Rta-mediated Sp1- $K_v1.3$ promoter binding presents a potential therapeutic target, as shown by Sp1 inhibition via Mith A.

$K_v1.3$ is highly expressed in lymphocytes and many cellular functions depend on $K_v1.3$ -mediated currents including activation, differentiation, proliferation, and cellular homeostasis (Wulff et al., 2004, Wulff and Zhorov, 2008). T cell receptor binding induces $K_v1.3$ -mediated membrane hyperpolarisation, activating the NFAT-calcium signalling pathway and thus production of cytokines required during the immune response. This mechanism is sustained by $K_{Ca}3.1$ channels, which are also activated due to the increased intracellular calcium levels. $K_v1.3$ expression varies within T cell subtypes, with effector memory T (T_{EM}) cells favouring $K_v1.3$. Furthermore, T_{EM} cells depends on $K_v1.3$ activity for triggering the NFAT-calcium signalling cascade, this discovery has hindered the use of $K_v1.3$ blockers as alternatives to traditional immunosuppressants such as calcineurin inhibitor, cyclosporin. However, it does present an opportunity to utilise $K_v1.3$ blockers to treat autoimmune diseases as T_{EM} cells which contribute to autoimmune pathogenesis.

While $K_v1.3$ activity in B cells has not been studied to the same extent as T cell research (Wulff et al., 2004, Wulff and Zhorov, 2008). As with T_{EM} cells, class-switched B cells rely upon $K_v1.3$ channel activity during activation. Given TREx BCBL1-Rta cells are of B cell lineage, the identification of $K_v1.3$ upregulation as a downstream effect of KSHV reactivation and its requirement to enhance lytic replication could lead to the initiation of the calcium signalling cascade. This pathway is highly important for B cell function and triggering calcium influx via calcium ionophore treatment in cells, latently infected with KSHV, has been shown to reactivate KSHV lytic replication (Chang et al., 2000).

The role of $K_v1.3$ as a regulator of membrane voltage and cellular volume, both of which have been implicated as requirements for cell cycle phase transitions, has long been established (Jang et al., 2011). This is theorised to occur via $K_v1.3$ -mediated K^+ efflux, causing membrane hyperpolarisation required prior to S phase initiation. This hyperpolarisation increases the requirement for a voltage-stabilising calcium influx, which initiates depolarisation and enables G_2/M progression. By triggering entry into S phase via $K_v1.3$ -mediated hyperpolarisation, the host cell would become a more favourable environment for KSHV lytic replication as episomes would become readily accessible for host cell machinery to replicate copies of the DNA genome while the cell is undergoing suitable conditions for DNA synthesis. Investigations into cell cycle progression during KSHV lytic replication are currently ongoing.

While many potassium channels are active in TREx BCBL1-Rta cells, expression of $K_v1.3$ is upregulated during the first 24 hours of viral lytic replication. This suggests that $K_v1.3$ is an ideal target for assessing the effect of ion channel inhibition during KSHV reactivation. Furthermore, viral replication is halted by K^+ channel blockade, showing promise for both further investigation into the role of $K_v1.3$ during the KSHV lytic replicative cycle, and the wider implications of utilising ion channel inhibitors as a pan-herpes treatment. A bonus is evidence suggesting $K_v1.3$ is not vital for cellular survival although preventing expression of the ion channel does hinder KSHV lytic replication, this could be advantageous in targeted therapeutics.

Several ion channel inhibitors specifically target $K_v1.3$, these inhibitors can either comprise small organic molecules such as quinine and 4AP or peptides purified from venom (Bajaj and Han, 2019; Chiang et al., 2017; Jang et al., 2011, Jang et al, 2015; O'Grady and Lee, 2005; Wulff et al.2004, Wulff and Zhorov, 2008). These venom-derived peptides are highly stable and resist denaturation due to the disulphide bridges formed within the molecules (Bajaj and Han, 2019). As with margatoxin, most are derived from scorpion venom, such as agitoxins, kaliotoxin, maurotoxin and noxiustoxin yet many inhibitors have been derived from ShK, a peptide originally isolated from the sea anemone *Stichodactyla helianthus*. Given the abundance of natural sources for $K_v1.3$ -inhibition a safe, effective therapeutic based on these compounds is a promising target for prevention of KSHV lytic replication and thus KSHV-associated malignancies.

Hyperpolarisation, caused by K^+ efflux due to increased $K_v1.3$ channel activity, could lead to Ca^{2+} influx, as shown in Figure 3.17; increases in intracellular calcium levels have already been shown to be sufficient to induce KSHV reactivation (Chang et al., 2000). Within this mechanism two targets for therapeutics present themselves, utilising compounds which are either already approved treatments or currently undergoing clinical trials.

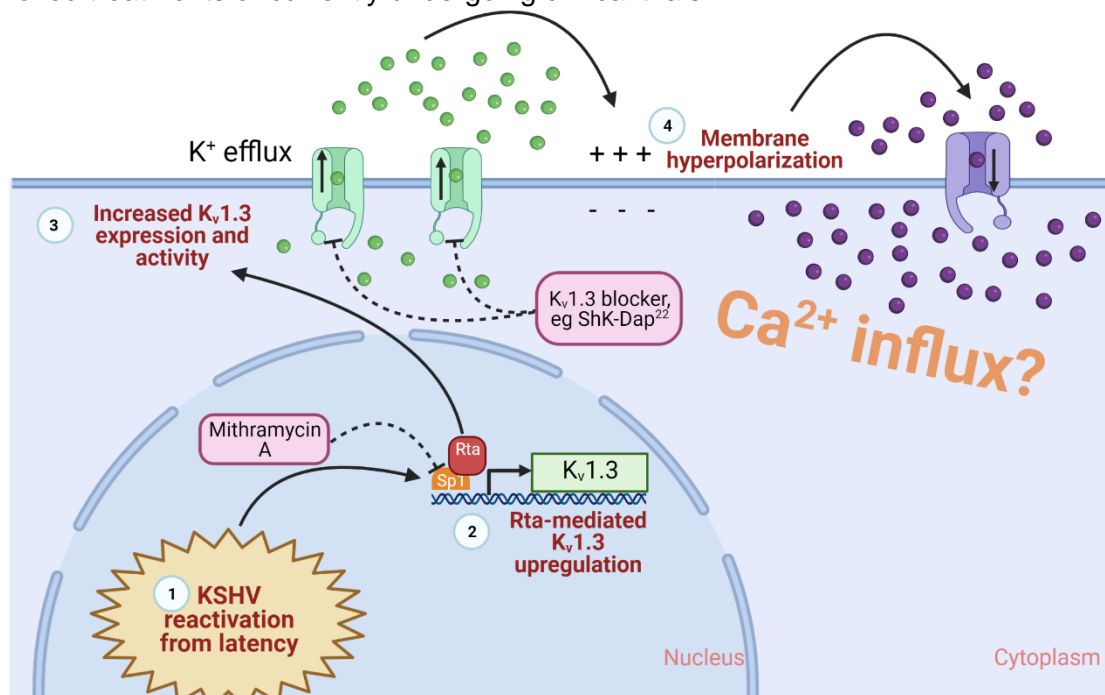


Figure 3.17 Schematic of Rta-mediated, $K_v1.3$ dependent hyperpolarisation mechanism. Therapeutic interventions are also shown, along with the hypothetical continuation of the mechanism. Upon KSHV reactivation, $K_v1.3$ is upregulated via Rta and Sp1, leading to increased activity and hyperpolarisation. This is hypothesised to trigger calcium influx. Created with Biorender.com.

Chapter 4

Investigating the role of hyperpolarisation-induced calcium influx in KSHV lytic replication

4 Investigating the role of hyperpolarisation-induced calcium influx in KSHV lytic replication

4.1. Introduction

In the previous chapter, results showed that a KSHV-mediated hyperpolarisation mechanism occurs, which is caused by KSHV Rta-mediated upregulation of $K_v1.3$ expression and subsequent channel activity, leading to potassium efflux. To characterise the implications of the KSHV-mediated hyperpolarisation mechanism, the potential effects of calcium influx on KSHV lytic replication was assessed. This consisted of an initial confirmation of calcium influx during KSHV lytic replication, followed by the effects of various calcium channel inhibitors on different stages of lytic replication, concluding with the effects of increased intracellular calcium, triggering the calcineurin-NFAT pathway.

Notably, Ca^{2+} ionophores, such as ionomycin have been shown to induce Rta-mediated activation (Chang et al., 2000), which is sufficient to trigger the latent to lytic switch and reactivate viral replication (Gradoville et al., 2000). Thapsigargin, which blocks the sequestration of intracellular calcium, also showed similar effects on Rta expression (Zoetewij et al., 2001). Together, these studies strongly suggest calcium signalling plays a vital role in initiating and enhancing the KSHV lytic cycle. Supporting this hypothesis is the fact that, ethylene glycol-bis (β -aminoethyl ether)-N,N,N',N'-tetraacetic acid (EGTA), a chelator of Ca^{2+} , prevented both ionomycin and thapsigargin mediated KSHV reactivation. Further evidence of the importance of Ca^{2+} signalling is also emphasised by blocking calcineurin signalling, either through calcineurin inhibitors or a VIVIT peptide, which prevents the calcium-dependent reactivation of KSHV. This further suggests that calcium signalling, and specifically the calcineurin-NFAT pathway is vital for KSHV lytic replication. While they are not ion channel inhibitors, both tacrolimus and cyclosporin (CsA) are already in clinical use as immunosuppressants (Colombo et al., 2014); these drugs target the Ca^{2+} -dependent calcineurin, thus inhibiting its function as a phosphatase. Further investigation into calcium movement during KSHV lytic replication could lead to a therapy based on calcium blockade or calcineurin targeting.

4.2. Calcium ionophores can override $K_v1.3$ depletion to activate KSHV lytic replication

In chapter 3, it was suggested that KSHV-mediated hyperpolarisation could initiate a Ca^{2+} influx to enhance KSHV lytic replication. To test this hypothesis experiments were performed to assess whether a calcium ionophore could override $K_v1.3$ depletion to initiate KSHV lytic replication. To this end, A23187 was added to scramble and $K_v1.3$ depleted cells in a dose-dependent manner at non-cytotoxic levels (previously assessed by MTS assay, Appendix, supplementary figure 5). As previously shown, the control scramble cell line successfully expressed ORF57 protein after Dox treatment, indicative of an efficient reactivation (Figure 4.1a). In contrast, the $\Delta K_v1.3$ cell line only expressed ORF57 protein in the presence of calcium ionophore, A23187, suggesting a positive effect of calcium influx on lytic replication (Figure 4.1b).

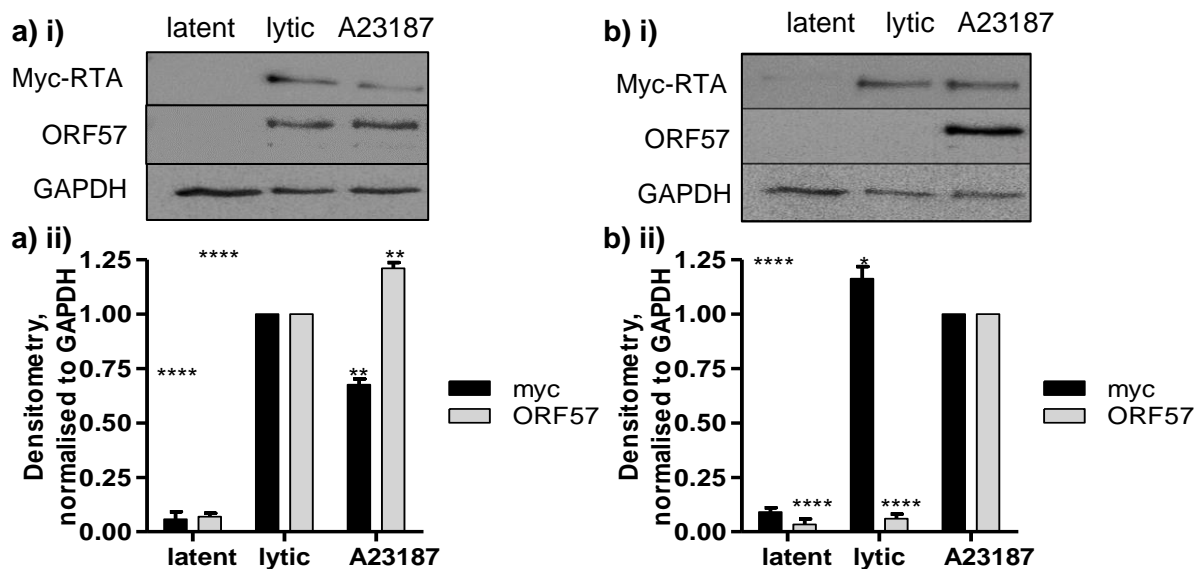


Figure 4.1 Effect of A23187 on KSHV lytic replication in scramble and $\Delta K_v1.3$ cell lines. Scramble (a) and $\Delta K_v1.3$ (b) cell lines were treated with DMSO, Dox or Dox and 50 μ M A23187 for 24 hours. Myc and ORF57 protein levels were assessed via Western blotting, densitometries for both myc and ORF57 levels were normalised to GAPDH levels (ii). Asterisks correspond to P-values of ≤ 0.05 (*), ≤ 0.01 (**), ≤ 0.001 (***), and ≤ 0.0001 (****), respectively; ns denotes a P-value of > 0.05 .

4.3. A calcium influx is induced during KSHV lytic replication

As calcium influx was sufficient to rescue KSHV lytic replication, in a $K_v1.3$ depleted cell line, TREx BCBL1-Rta cells were reactivated and treated with Fura RedTM, AM (Fura Red) to assess intracellular calcium levels throughout the first 24 hours of KSHV lytic reactivation. Fura Red is a fluorescent calcium indicator excited by visible light (Bailey and Macardle, 2006). Most experiments use Fura Red in addition to a green-fluorescent calcium indicator to determine

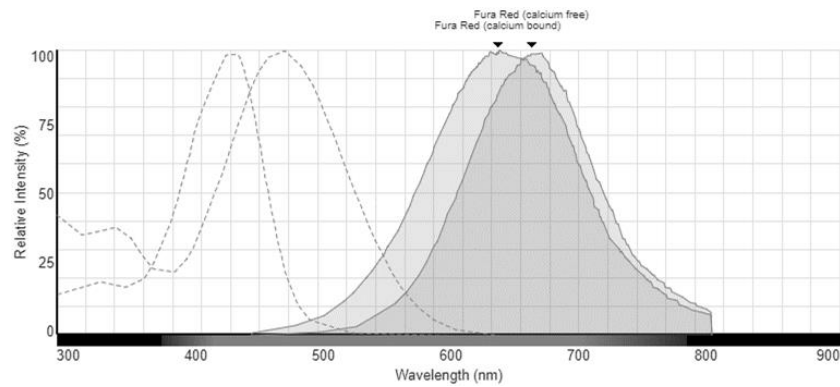


Figure 4.2 Emission and excitation spectra of calcium bound and calcium free Fura Red. Both the excitation and emission of Fura Red decrease when calcium is bound to the dye, thus enabling detection of bound and free Fura Red. Spectra were generated using the ThermoFisher Spectra Viewer.

ratiometric analysis of intracellular calcium levels via flow cytometry, yet Fura Red can be used alone as a ratiometric indicator, as the wavelengths of both the excitation and emission spectra are reduced when calcium binds to Fura Red (Figure 4.2) (Wendt et al., 2015).

To determine the calcium ratio during KSHV lytic replication, Fura Red was excited by lasers emitting wavelengths of either 405 nm or 561 nm. This allowed detection of unbound Fura Red

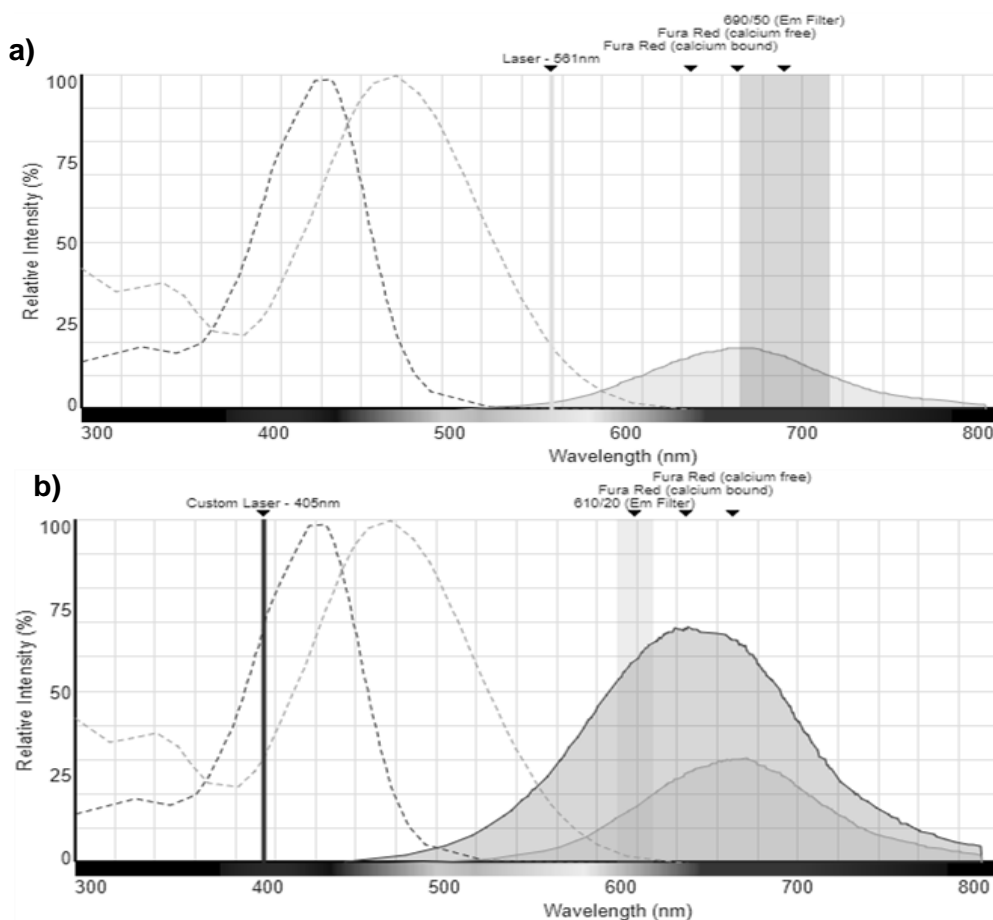


Figure 4.3 Emission and excitation spectra of calcium bound and calcium free Fura Red. Excitation lasers of 561nm (a) or 405nm (b) emission wavelengths and emission bandwidth filters are indicated. Utilising separate lasers for each Fura Red state allows ratiometric analysis of calcium concentrations. Spectra were generated using the ThermoFisher Spectra Viewer.

through a bandwidth filter of around 690 nm after excitation with the 591 nm laser, whereas calcium bound Fura Red was detected within a bandwidth of around 610 nm after excitation with the 405 nm laser. Figure 4.3 shows the spectra of both Fura Red states with each laser and its bandwidth filter. A concentration of 1 μM was used to confirm Fura Red had stained the treated cells; this would not cause over-staining thus altering the calcium ratio, or cell death due to the toxicity of both Fura Red and its solvent, DMSO.

To assess whether a calcium influx occurs during KSHV lytic replication, the calcium ratio was determined using Fura Red staining at regular intervals post reactivation. An increased calcium ratio was observed within lytically replicating TREx BCBL1-Rta cells (Figure 4.4a), indicating that intracellular calcium levels are increased during the initial 24 hours of KSHV lytic replication, compared to latently infected TREx BCBL1-Rta cells. This suggests a prolonged calcium influx. To specifically assess the role of $\text{K}_v1.3$ in inducing a calcium influx, the calcium ratio was compared in scramble and $\text{K}_v1.3$ depleted cells. An increased calcium influx was seen in the scramble lentiviral cell line, however depletion of $\text{K}_v1.3$ resulted in a lack of calcium influx upon reactivation, which suggests calcium influx during KSHV lytic replication is $\text{K}_v1.3$ dependent (Figure 4.4b). The calcium ionophore, A23187, was used as a positive control.

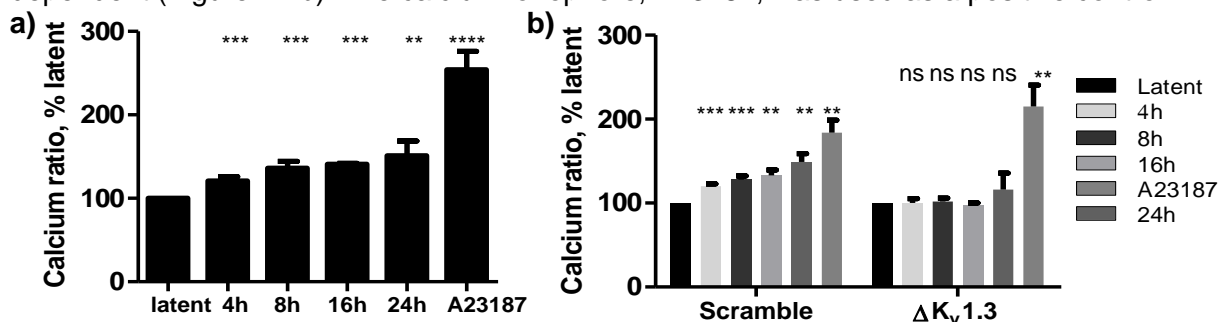


Figure 4.4 Calcium ratio in wild-type TREx BCBL1-Rta cells (a) and scramble or $\Delta\text{K}_v1.3$ cell lines (b), measured via flow cytometry. Cells were harvested at various time-points and incubated with Fura Red for 30 minutes at 37°C, before fluorescence was measured. Asterisks correspond to P-values of ≤ 0.05 (*), ≤ 0.01 (**), ≤ 0.001 (***), and ≤ 0.0001 (****), respectively; ns denotes a P-value of > 0.05 .

4.4. KSHV lytic replication is suppressed by Ca_v inhibition

As potassium efflux and hyperpolarisation cause a voltage shift, resulting in an increase in extracellular positive charge, the effect of voltage-gated calcium channel inhibitors was assessed to determine whether a specific Ca_v channel was responsible for the calcium influx necessary for KSHV lytic replication. Two general Ca_v blockers were assessed in an MTS

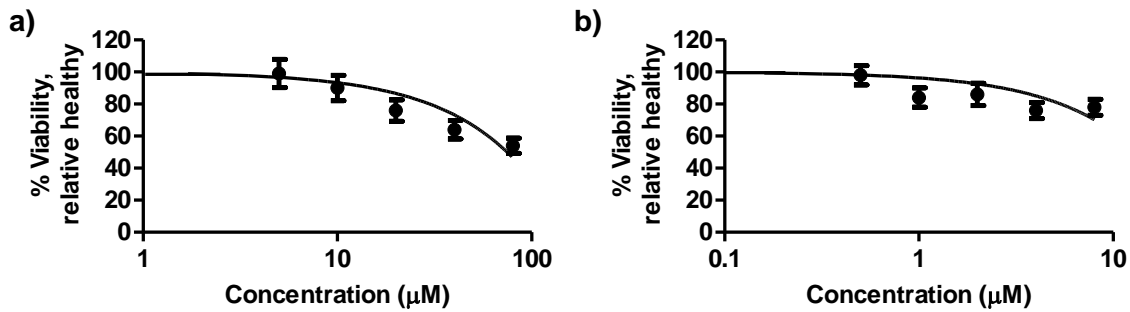


Figure 4.5 Cell viability of TREx BCBL1-Rta cells after 24-hour treatment with nifedipine or SKF. TREx BCBL1-Rta cells were treated with varying concentrations of nifedipine or SKF for 24 hours before cell survival was assessed via MTS assay. Results are presented on an X-Y graph using a log-scale.

assay to identify non-toxic concentration to be used in downstream assays. Nifedipine inhibits L-type (Ca_v1) channels and more than 50% of cells survived treatments of concentrations below 50 μ M (Figure 4.5a), whereas SKF-96365 blocks TRP and T-type (Ca_v3) calcium channels, cells were viable after 24 hours with concentrations between 1-10 μ M (Figure 4.5b). After suitable non-toxic concentrations were determined, both drugs were used in a dose-dependent pre-treatment reactivation assay, measuring ORF57 lytic protein production. SKF-96365 successfully inhibited KSHV lytic replication, however no effect of nifedipine treatment was observed (Figure 4.6), indicating either a TRP or T-type channel was required to generate a calcium influx during lytic KSHV replication.

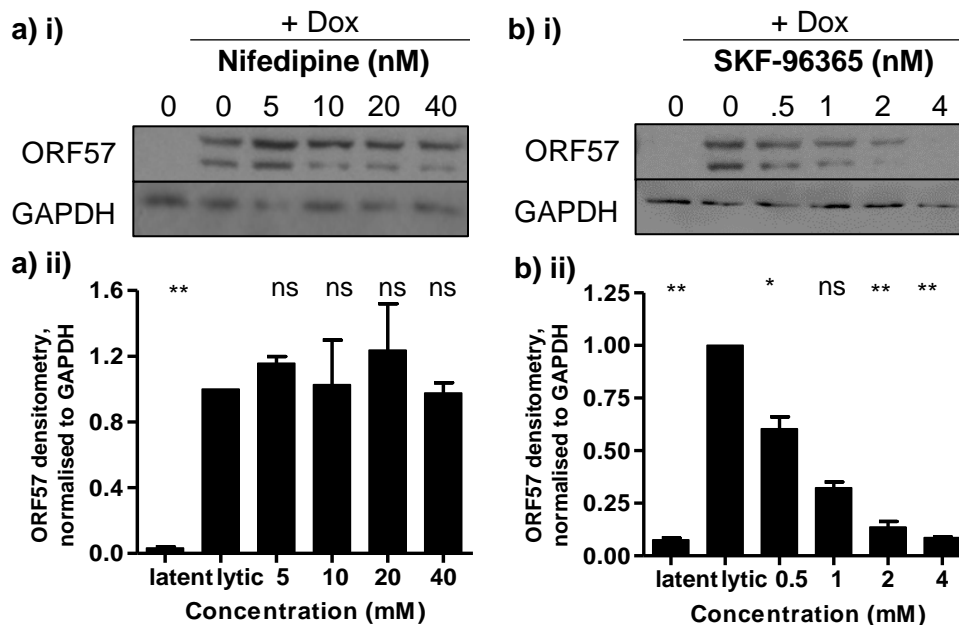


Figure 4.6 Dose-dependent effect of general voltage-gated calcium channel inhibitors, nifedipine (a) and SKF-96365 (b), on KSHV reactivation. Nifedipine has no effect on ORF57 protein expression (a). SKF-96365 inhibits ORF57 protein expression in a dose dependent manner, shown via Western blot (b). Densitometries for ORF57 levels were normalised to GAPDH levels (ii). Asterisks correspond to P-values of ≤ 0.05 (*), ≤ 0.01 (**), ≤ 0.001 (***), and ≤ 0.0001 (****), respectively; ns denotes a P-value of > 0.05 .

4.5. Ca_v3 inhibition is sufficient to suppress KSHV lytic replication

As the KSHV-mediated calcium influx was $K_v1.3$ dependent, a voltage-gated calcium channel was likely to be causing this influx. Given SKF-96365 inhibits Ca_v3 channels; investigations into Ca_v3 inhibition were performed. Three Ca_v3 inhibitors, flunarizine, mibefradil and pimozide, were used in MTS assays to determine appropriate concentrations prior to reactivation experiments. Although pimozide treatment had stable toxicity levels, both flunarizine and mibefradil caused significant reductions in cell viability (Figure 4.7).

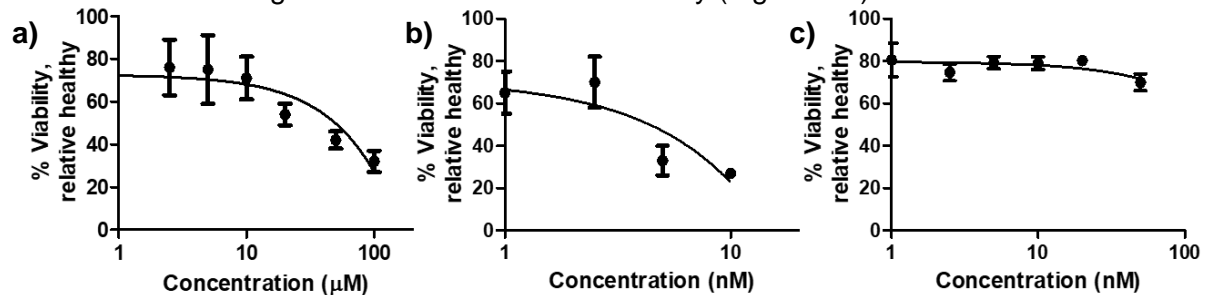


Figure 4.7 Cell viability of TReX BCBL1-Rta cells after 24-hour treatment with flunarizine (a), mibefradil (b) or pimozide (c). TReX BCBL1-Rta cells were treated with varying concentrations of flunarizine, mibefradil or pimozide for 48 hours before cell survival was assessed via MTS assay. Results are presented on an XY-graph using a log-scale.

For dose-dependent reactivation assays, 2 μM flunarizine was sufficient to significantly reduce KSHV lytic replication. Micromolar doses of mibefradil also inhibited KSHV replication, although pimozide treatment required a higher concentration to significantly inhibit ORF57 production and thus KSHV lytic replication (Figure 4.8). All three reduced ORF57 protein production, confirming a Ca_v3 channel is required during KSHV lytic replication.

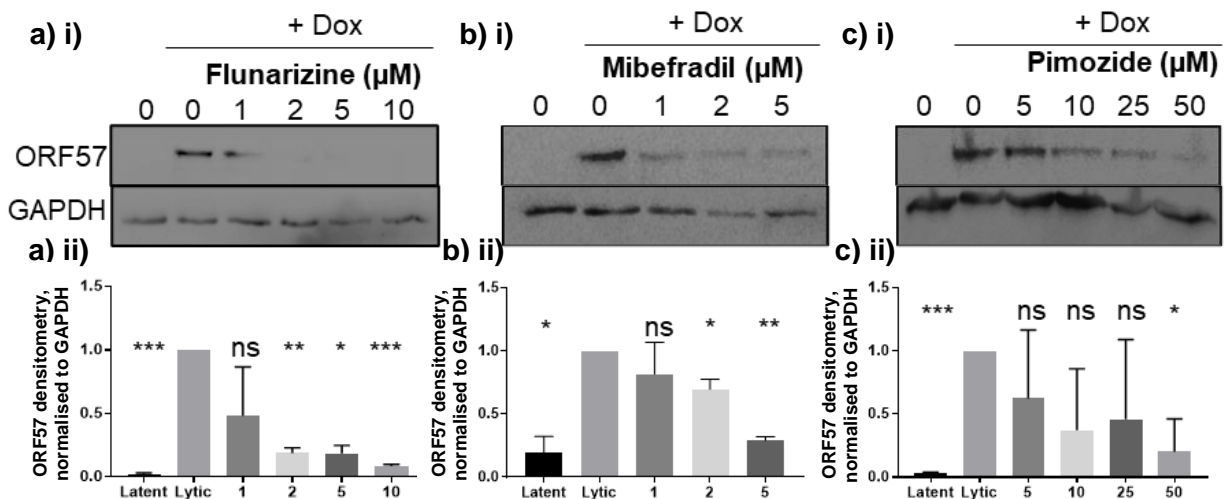


Figure 4.8 Dose-dependent effect of Ca_v3 inhibitors; flunarizine (a), mibefradil (b) and pimozide (c), on KSHV lytic replication. TReX BCBL1-Rta cells were treated with DMSO or non-cytotoxic concentrations of each Ca_v3 inhibitor prior to reactivation with Dox. Cells were then harvested at 24 hours postinduction and Western blotting performed to assess lytic protein production. All three Ca_v3 inhibitors reduced ORF57 protein production in a dose-dependent manner. Densitometries for ORF57 levels were normalised to GAPDH levels (ii). Asterisks correspond to P-values of ≤ 0.05 (*), ≤ 0.01 (**), ≤ 0.001 (***), and ≤ 0.0001 (****), respectively; ns denotes a P-value of > 0.05 .

4.6. Ca_v3 expression during KSHV lytic replication

Three Ca_v3 channels have been identified; $Ca_v3.1$, $Ca_v3.2$ and $Ca_v3.3$. To determine which channel was required by KSHV replication, it was first determined which Ca_v3 channel was expressed in TREx BCBL1-Rta cells, using human foetal brain (HFB) cDNA as a positive control. Results show that only $Ca_v3.2$ was expressed in TREx BCBL1-Rta cells (Figure 4.9a), neither $Ca_v3.1$ nor $Ca_v3.3$ primers amplified TREx BCBL1-Rta cDNA to detectable levels. Although $Ca_v3.2$ expression was significantly lower than the expression of any Ca_v3 channel within cDNA isolated from HFB. Interestingly, $Ca_v3.2$ RNA levels were also consistently increased during lytic replication (Figure 4.9b), suggesting a potential requirement for this channel during KSHV lytic replication.

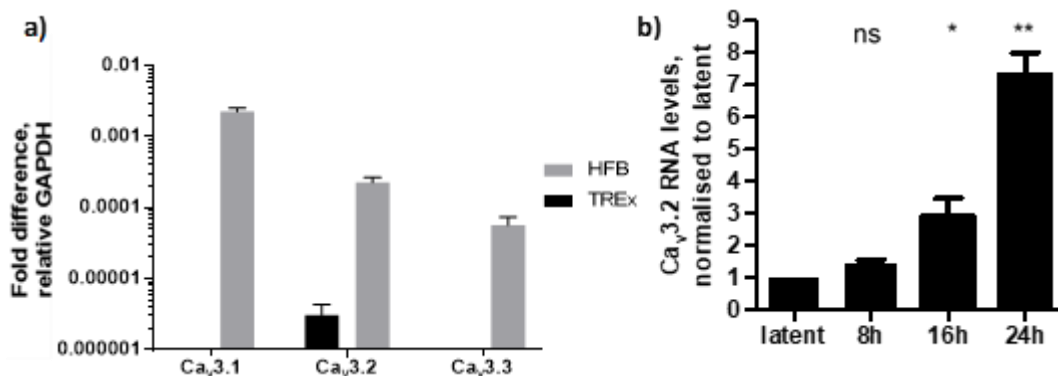


Figure 4.9 Ca_v3 expression in HFB and TREx BCBL1-Rta cells (a) and $Ca_v3.2$ expression in TREx BCBL1-Rta cells during a reactivation time-course (b). RNA was extracted from latent TREx BCBL1-Rta cells post-induction before being probed for Ca_v3 expression via qRT-PCR. $Ca_v3.2$ expression was also assessed over a reactivation time-course in TREx BCBL1-Rta cells. Asterisks correspond to P-values of ≤ 0.05 (*), ≤ 0.01 (**), ≤ 0.001 (***), and ≤ 0.0001 (****), respectively; ns denotes a P-value of > 0.05 .

4.7. $Ca_v3.2$ activity is required during KSHV lytic replication

To confirm that $Ca_v3.2$ was required during KSHV lytic replication, TREx BCBL1-Rta cells were treated with the specific $Ca_v3.2$ inhibitor, 2(R/S)-6-prenylningenin (PNG), prior to reactivation. PNG was highly toxic at micromolar concentrations causing over 50% cell death (Appendix, supplementary figure 6). Therefore, a dose-dependent experiment was performed using nanomolar concentrations. Additionally, to confirm $Ca_v3.2$ was the channel responsible for the $K_v1.3$ -mediated calcium influx observed during KSHV lytic replication, A23187 was used to override PNG treatment and allow calcium influx. Results showed that PNG reduced KSHV lytic replication in a dose-dependent manner (Figure 4.10), however, A23187 treatment was sufficient to rescue lytic replication in PNG pre-treated TREx BCBL1-Rta cells. This indicates that $Ca_v3.2$ is responsible for the $K_v1.3$ -mediated calcium influx during KSHV lytic replication.

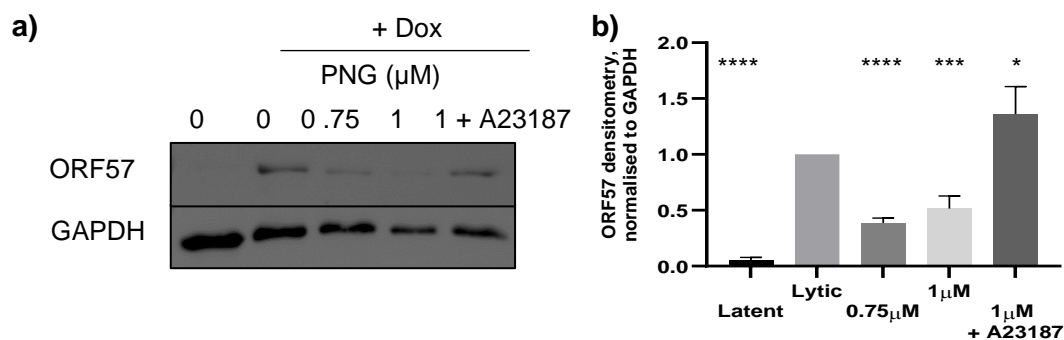


Figure 4.10 PNG and A23187 treatment in TREx BCBL1-Rta cells. TREx BCBL1-Rta cells were treated with DMSO or non-cytotoxic concentrations of PNG and A23187 prior to reactivation with Dox. Cells were then harvested at 24 hours post-induction and Western blotting performed to assess lytic protein production. Densitometries for ORF57 levels were normalised to GAPDH levels (ii). Asterisks correspond to P-values of ≤ 0.05 (*), ≤ 0.01 (**), ≤ 0.001 (***), and ≤ 0.0001 (****), respectively; ns denotes a P-value of > 0.05 .

4.8. Calcineurin-NFAT inhibition prevents KSHV lytic replication

To determine the role of Ca^{2+} influx in enhancing KSHV lytic replication, the role of calcium signalling was investigated. Intracellular calcium can bind to calmodulin, which activates calcineurin, this then dephosphorylates NFAT, allowing NFAT to relocate to the nucleus and function as a transcriptional activator. This mechanism can be prevented by cyclosporin A, which inhibits the phosphatase activity of calcineurin. Therefore, to determine whether the calcineurin-NFAT pathway was important in KSHV lytic replication, TREx BCBL1-Rta cells were treated with non-toxic levels of CsA (assessed by MTS assay, Appendix, supplementary figure 7) in a dose-dependent manner and ORF57 protein levels were assessed by immunoblotting (Figure 4.11). Results showed that CsA reduced KSHV lytic replication in a dose-dependent manner, suggesting NFAT dephosphorylation and nuclear translocation were required for KSHV lytic replication.

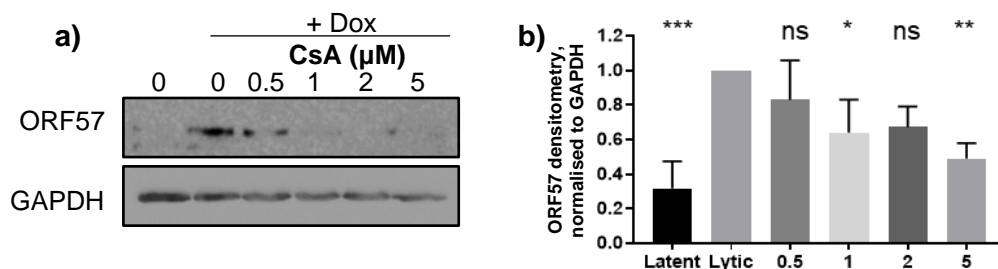


Figure 4.11 Dose-dependent effect of CsA on lytic KSHV replication. Western blotting shows ORF57 protein levels were reduced in a dose dependent manner by CsA pre-treatment. Densitometry of ORF57 levels were normalised to GAPDH (b). Asterisks correspond to P-values of ≤ 0.05 (*), ≤ 0.01 (**), ≤ 0.001 (***), and ≤ 0.0001 (****), respectively; ns denotes a P-value of > 0.05 .

4.9. NFAT1 is localized in the nucleus during KSHV lytic replication

To determine whether NFAT1 was activated by KSHV lytic replication, the subcellular localisation of NFAT1 was determined using subcellular fractionation. Results showed that NFAT1 was only present in the cytoplasmic fraction during latency, however, an increase in nuclear levels of NFAT1 was observed upon KSHV lytic replication (Figure 4.12). Total NFAT1 protein level did not appear to change, as indicated in the whole cell fraction of both latent and lytic samples.

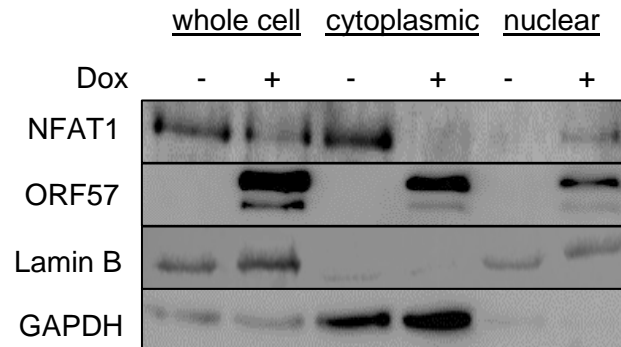


Figure 4.12 Subcellular fractionation of TReX BCBL1-Rta cells during latency and KSHV lytic replication.

Cytoplasmic and nuclear fractions were extracted from and compared to whole cell samples of TReX BCBL1-Rta protein lysate. NFAT1 localisation was assessed, while ORF57 was used as an indicator of lytic replication. Lamin B and GAPDH were used as nuclear and cytoplasmic markers, respectively.

Additionally, confocal microscopy was used to visualise and confirm the re-localisation of NFAT1 to the nucleus during KSHV lytic replication (Figure 4.13). During latency, NFAT1 predominantly appeared as a halo around the nucleus. However, upon reactivation, NFAT1 colocalised with DAPI and ORF57 within the nucleus of TReX BCBL1-Rta cells with reduced cytoplasmic presence. Notably, NFAT1 re-localisation could be prevented by a variety of drugs; K_v1.3 inhibitor, ShK; Ca_v3.2 inhibitor, PNG; and calcineurin inhibitor, CsA. For example, treatment with ShK showed a halo-like NFAT1 localisation pattern similar to the localisation seen in latent cells, with significantly reduced expression of ORF57 indicating effective inhibition of KSHV lytic replication. Although both PNG and CsA showed reduced ORF57 expression, the NFAT1 localisation appeared more disperse throughout the cell, unlike the distinct halos seen in latent cells. These results further support the role of K_v1.3-mediated hyperpolarisation inducing a calcium influx, which then activates the Ca²⁺ signalling cascade during KSHV lytic replication.

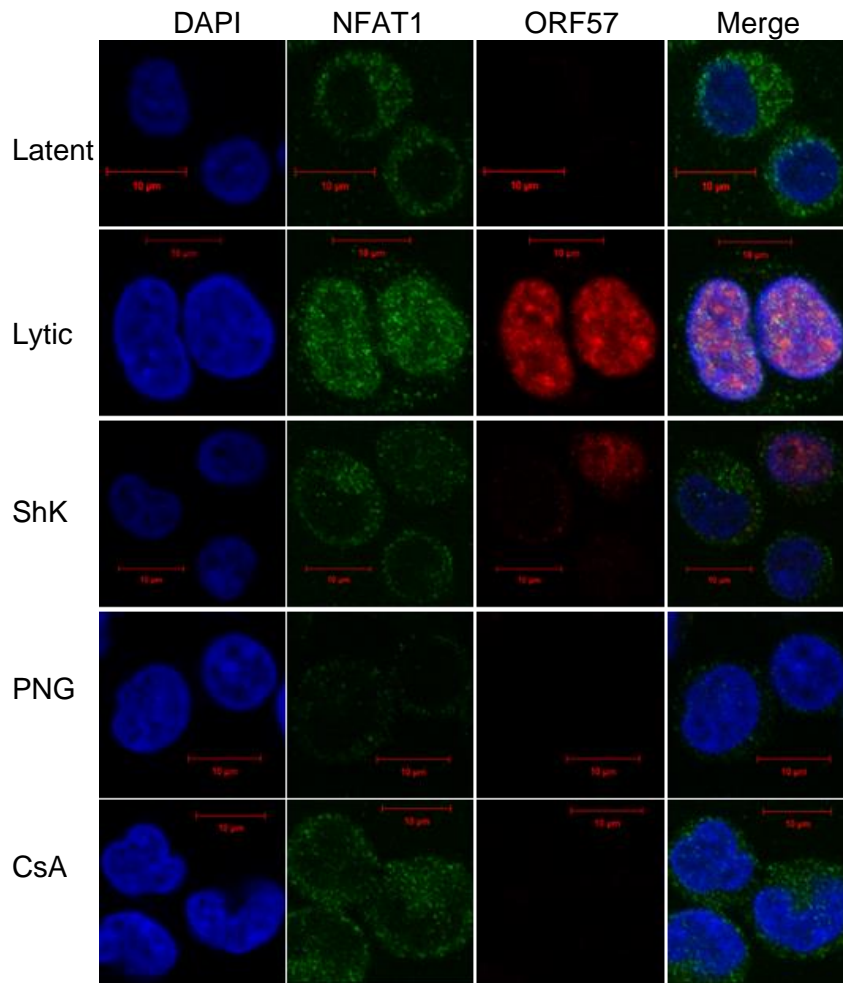


Figure 4.13 Confocal microscopy images showing the localisation of NFAT1 in TREx BCBL1-Rta cells during latent or KSHV lytic replication and after pre-treatment with a variety of drugs. TREx BCBL1-Rta cells latently infected with KSHV showed a halo of cytoplasmic NFAT1, this halo was also seen in TREx BCBL1-Rta cells pre-treated with ShK, PNG or CsA. TREx BCBL1-Rta cells undergoing lytic replication of KSHV showed co-localisation of DNA, NFAT1 and ORF57 viral protein.

4.10. NFAT-responsive gene expression is induced by KSHV lytic replication

To confirm whether the relocalisation of NFAT1 into the nucleus increased NFAT1 transcriptional activity during KSHV lytic replication, the expression of a selection of NFAT-responsive genes was assessed via qRT-PCR. Aligned with an increase in NFAT1 nuclear localisation, results show a clear increase in NFAT-responsive gene expression during KSHV lytic replication (Figure 4.14a). Of particular note was TNF α which is only responsive to NFAT1. In contrast, this increase in NFAT-responsive gene expression was dramatically reduced in the presence of K_v1.3 or Ca_v3.2 inhibitors ShK or PNG, respectively. This indicates that the nuclear localisation and subsequent increase in NFAT-mediated gene expression is due to a KSHV-induced calcium influx which results in NFAT1 nuclear localisation.

A similar result was also observed upon $K_v1.3$ depletion but not in the control scramble cell line (Figure 4.14b). This suggests that $K_v1.3$ -mediated hyperpolarisation is required to enable NFAT1 nuclear relocalisation and transcriptional activity seen during KSHV lytic replication.

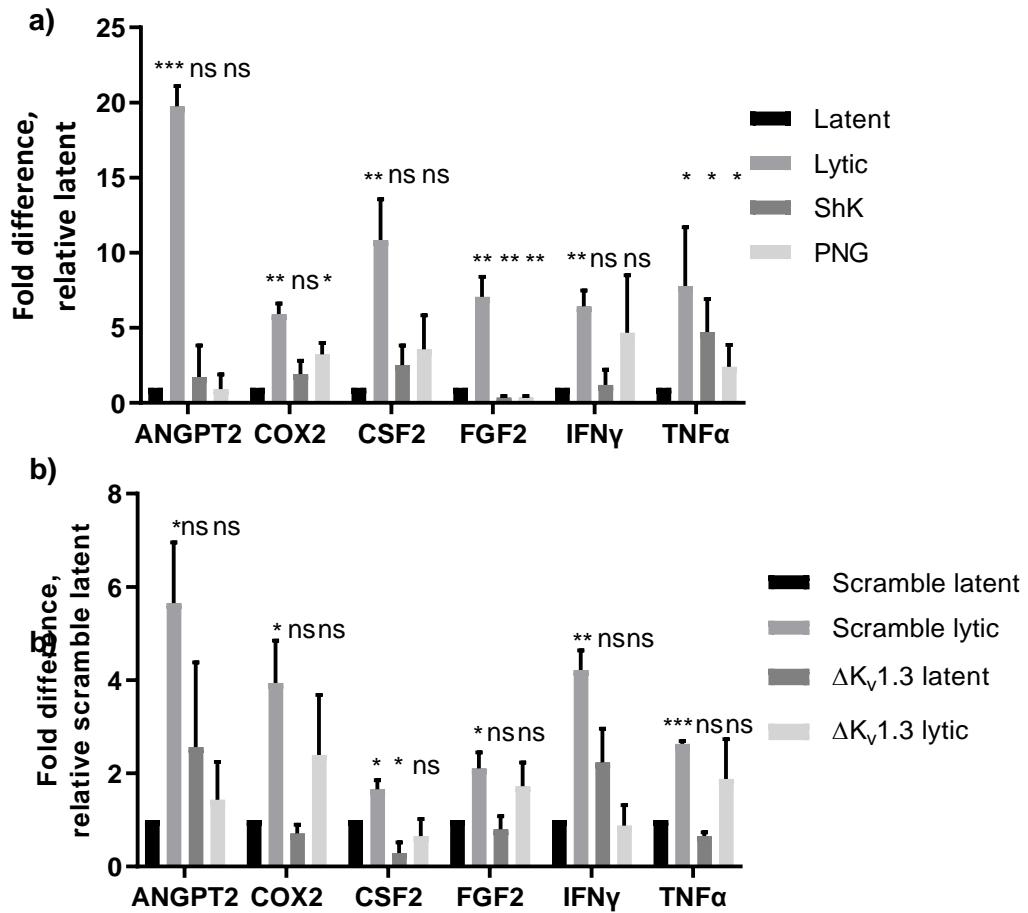


Figure 4.14 NFAT-mediated gene expression during latency and KSHV lytic replication in the presence and absence of ShK or PNG in TREx BCBL1-Rta cells (a) and in scramble and $\Delta K_v1.3$ cell lines (b). Cells were harvested 24 hours post-reactivation and RNA extracted. Asterisks correspond to P-values of ≤ 0.05 (*), ≤ 0.01 (**), ≤ 0.001 (***), and ≤ 0.0001 (****), respectively; ns denotes a P-value of > 0.05 .

4.11. Discussion

The activation of $K_v1.3$ initiates Ca^{2+} influx through a hyperpolarisation activated Ca^{2+} channel, $Ca_v3.2$. This influx induces the nuclear localisation of NFAT1 via calmodulin- calcineurin phosphatase activity and the induction of NFAT-driven gene expression. This mechanism is summarised in Figure 4.15, along with specific inhibitors acting at different stages. In addition to the effect of $K_v1.3$ inhibition or depletion on KSHV lytic replication shown in chapter 3, results within chapter 4 show several targets for KSHV therapeutics including an additional host ion channel and the calcineurin-NFAT pathway.

Attempts to knockdown $Ca_v3.2$ in TREx BCBL1-Rta cells to confirm $Ca_v3.2$ is required for KSHV lytic replication were unsuccessful, due to the channel being essential for cell survival. This was further indicated by the toxicity of PNG, as its IC_{50} is 991nM yet concentrations above 1 μ M halved cell viability. Interestingly, general Ca_v3 inhibitors, such as mibefradil, are already approved drugs and are in use as anti-hypertensives and during angina treatment, this presents additional opportunities for drug repurposing to prevent KSHV lytic replication and its subsequent malignancies. While flunarizine is not approved for use in the UK, investigations into its use as a treatment for migraines are ongoing (Karsan et al., 2018).

Calcium influx plays a vital role in KSHV reactivation (Chang et al., 2000, Zoetewij et al., 2001) and is the next step in the hyperpolarisation mechanism. This influx starts the calcium

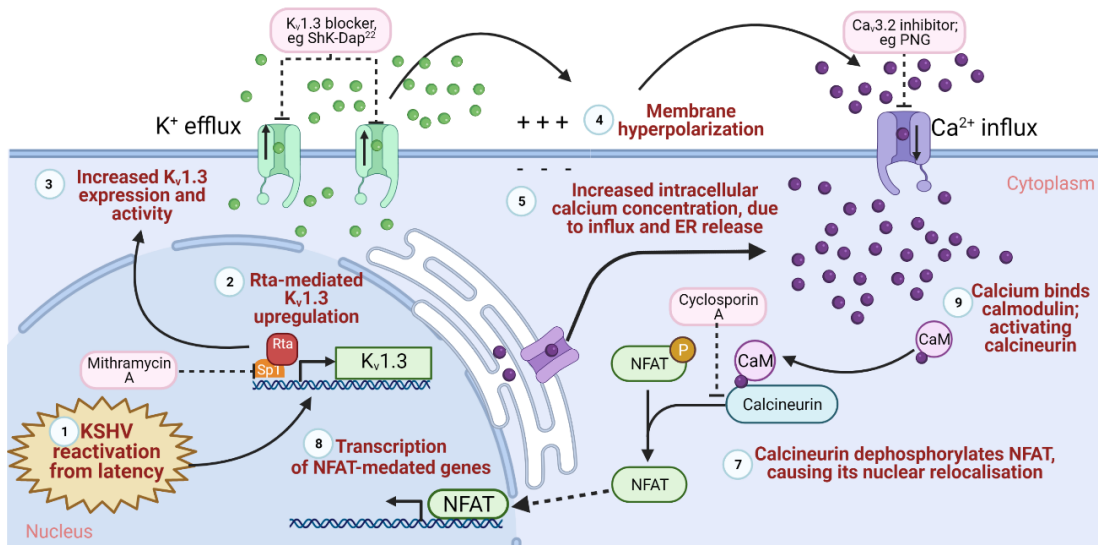


Figure 4.15 Schematic of hyperpolarisation-mediated calcium influx-dependent NFAT relocalisation mechanism, triggered by KSHV lytic replication, along with potential therapeutic targets. After Rta-mediated upregulation of $K_v1.3$ and its subsequent channel activity, $Ca_v3.2$ activity is triggered, leading to increased intracellular calcium which then causes NFAT1 nuclear localisation and transcriptional activation of NFAT1-mediated genes. Created with Biorender.com

signalling cascade, which has been shown to be important for KSHV lytic replication. Similarly, NFAT and calcineurin inhibitors, have recently been shown to prevent KSHV lytic replication (Zoetewij et al., 2001), thus hold promise as an antiviral treatment, given their current use as immunosuppressants (Colombo et al. 2014, Zoetewij et al., 2001)

There are two potential reasons for NFAT1 relocalisation during KSHV lytic replication; either nuclear NFAT1 modulates the host cell into a more suitable environment for KSHV lytic replication or nuclear NFAT1 is directly beneficial to lytic replication and thus upregulation of host NFAT-mediated genes is an off-target effect of KSHV lytic replication. Assessing potential NFAT1 transcriptional binding sites within the KSHV genome would be the next step in further clarifying this mechanism.

Interestingly, ANGPT2 has been implicated as a diagnostic marker for metastatic colon cancer, patients with ANGPT2 positive tumours have poorer prognosis (Jary et al., 2020). Notably, COX-2 has been shown to be upregulated in KSHV infection, with investigations showing an increased COX-2 expression linked to an increase in KSHV pathogenesis (Sharma-Walia et al., 2010). Furthermore, overexpression of COX-2 can lead to inflammation along with the promotion of both angiogenesis and tumour invasion, and this increased expression has been linked to reduced survival rates in bladder cancers along with carcinogenic functions within development of breast cancer (Agrawal et al., 2018). CSF2 shows a similar link between overexpression and poor prognosis (Xu et al., 2019) and FGF2 induces growth in breast cancer cells via MYC upregulation (Giulianelli et al., 2019). TNF α plays roles in promoting several hallmarks of cancer, including angiogenesis, metastasis, and proliferation (Balkwill, 2006). While IFN γ has long been shown to have antitumour effects, it can also enable immune evasion within tumours (Mojic et al., 2017). Overall, the upregulation of these NFAT1-responsive genes could contribute to KSHV-mediated oncogenesis.

As this hyperpolarisation mediated calcium influx mechanism is instrumental in enabling lytic replication, investigating whether it is conserved amongst other human herpesviruses could present various novel host targets for pan-herpes antivirals.

Chapter 5

Investigating the conservation of K⁺ channel mediated hyperpolarisation-induced calcium influx in HSV-1 and HCMV lytic replication cycles

5 Investigating the conservation of K⁺ channel mediated hyperpolarisation-induced calcium influx in HSV-1 and HCMV lytic replication cycles

5.1. Introduction

HSV-1, a member of the *Alphaherpesvirinae*, is usually acquired during childhood, spread through direct contact with an infected individual and can cause sporadic skin lesions (Birkmann and Zimmermann, 2016; Kennedy et al., 2015; Poole and James, 2018; Zheng et al., 2014). During HSV-1 lytic replication, intracellular chloride concentration is increased, which is thought to assist in early-stage HSV-1 replication, such as viral entry (Zheng et al., 2014). Tamoxifen or NPPB treatment prevents the increased influx of chloride ions, reducing the levels of chloride ions to that of uninfected cells and thus reducing HSV-1 infection (Kennedy et al., 2015). HCMV, the largest of the human *Herpesviridae*, belongs to the *Betaherpesvirinae* sub-family, HCMV infection is common worldwide, although asymptomatic in healthy individuals it is implicated in birth defects if lytic replication occurs during pregnancy (Bakhrarov et al., 1995; Griffiths et al., 2014; Hancock et al., 2021; Kapoor et al., 2012; Kostopoulou et al., 2017; Oberstein and Shenk, 2017). A variety of potassium channels are known to be upregulated during HCMV lytic replication (Oberstein and Shenk, 2017), whereas Na_v channel activity is undetectable (Bakhrarov et al., 1995). At present the role of these channels in the HCMV lifecycle is unknown.

While the hyperpolarisation-induced calcium influx mechanism and specific host ion channel-dependency shown in chapters 3 and 4 have not been investigated in HSV-1 or HCMV lytic replication, there is a precedent for host channel modulation by both viruses. Therefore, investigations into the conservation of this mechanism within *Herpesviridae* was performed utilizing K⁺ inhibitors and PNG during HSV-1 and HCMV lytic replication. Furthermore, flow cytometry experiments into membrane polarization and calcium movement were performed as previously described.

5.2. Both HSV-1 and HCMV successfully infect HFF cells

Given the cellular tropism of Alphaherpesvirinae and Betaherpesvirinae compared to Gammaherpesvirinae, a new cell line was required for HSV-1 and HCMV experiments. To determine whether HSV-1 could successfully infect and replicate in Human Foreskin Fibroblast (HFF) cells, a viral titre was performed. Results showed that serial dilutions of stock HSV-1 could infect HFFs, viral protein was detectable via immunoblotting at dilutions of 10^{-4} , 10^{-5} and 10^{-6} (Figure 5.1) This enabled further HSV-1 experiments to use a dilution of 10^{-5} .

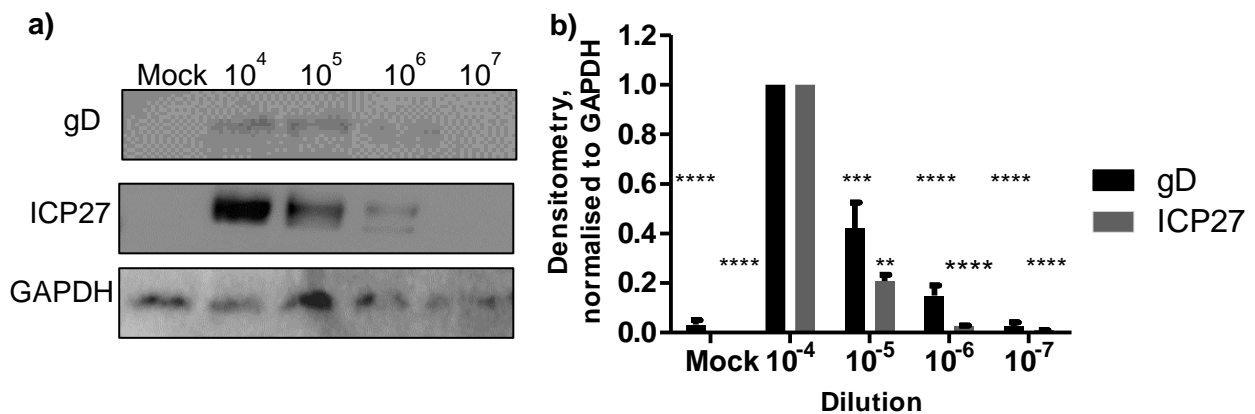


Figure 5.1 Viral proteins from HFFs infected with serial dilutions of HSV-1 stock (a). Densitometries for viral genes were normalised to GAPDH (b). Asterisks correspond to P-values of ≤ 0.05 (*), ≤ 0.01 (**), ≤ 0.001 (***), and ≤ 0.0001 (****), respectively; ns denotes a P-value of > 0.05 .

As the HCMV lytic replication cycle occurs over a longer duration, a time course for detection of UL69 mRNA was performed to determine both suitable experiment durations and stock dilution. The results showed that 7 days incubation time and a dilution of 10^{-4} were appropriate for further HCMV experiments (Figure 5.2).

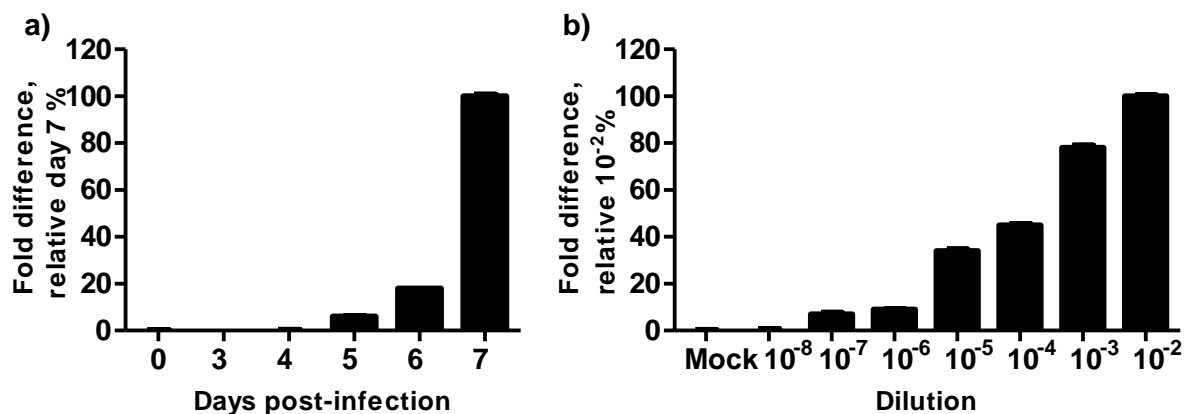


Figure 5.2 UL69 RNA levels in infected HFFs during a timecourse (a) and with varying serial dilutions (b). HFFs were infected with a 10^{-2} dilution of HCMV stock and harvested 3-7 days post-infection, serial dilutions of HCMV stock were harvested after 7 days.

5.3. K⁺ inhibitors reduce HSV-1 and HCMV lytic replication

Ion channel expression varies based on cell type, therefore initial investigations began with general inhibitors to confirm whether K⁺ channels were required by HSV-1 and HCMV lytic replication, before attempting to elucidate the specific channel. Non cytotoxic concentrations of a selection of K⁺ inhibitors (25 mM KCl, 200 μM Qn, or 50 mM TEA) all showed that both HSV-1 and HCMV are sensitive to potassium channel inhibitors. Due to the abundance of K_v channels, and the requirement of K_v1.3 in lytic KSHV replication, 4AP was used in addition to the more general K⁺ inhibitors. All three general inhibitors and 4AP reduced both HSV-1 and HCMV lytic gene mRNA expression (Figure 5.3a & b). This suggests both HSV-1 and HCMV are dependent upon a K_v channel for lytic replication, as seen during KSHV lytic replication. However, while 4AP caused a reduction in HCMV Pp65 protein levels, no effect was observed on HSV-1 gD protein levels, detected via Western blotting (Figure 5.3c & d).

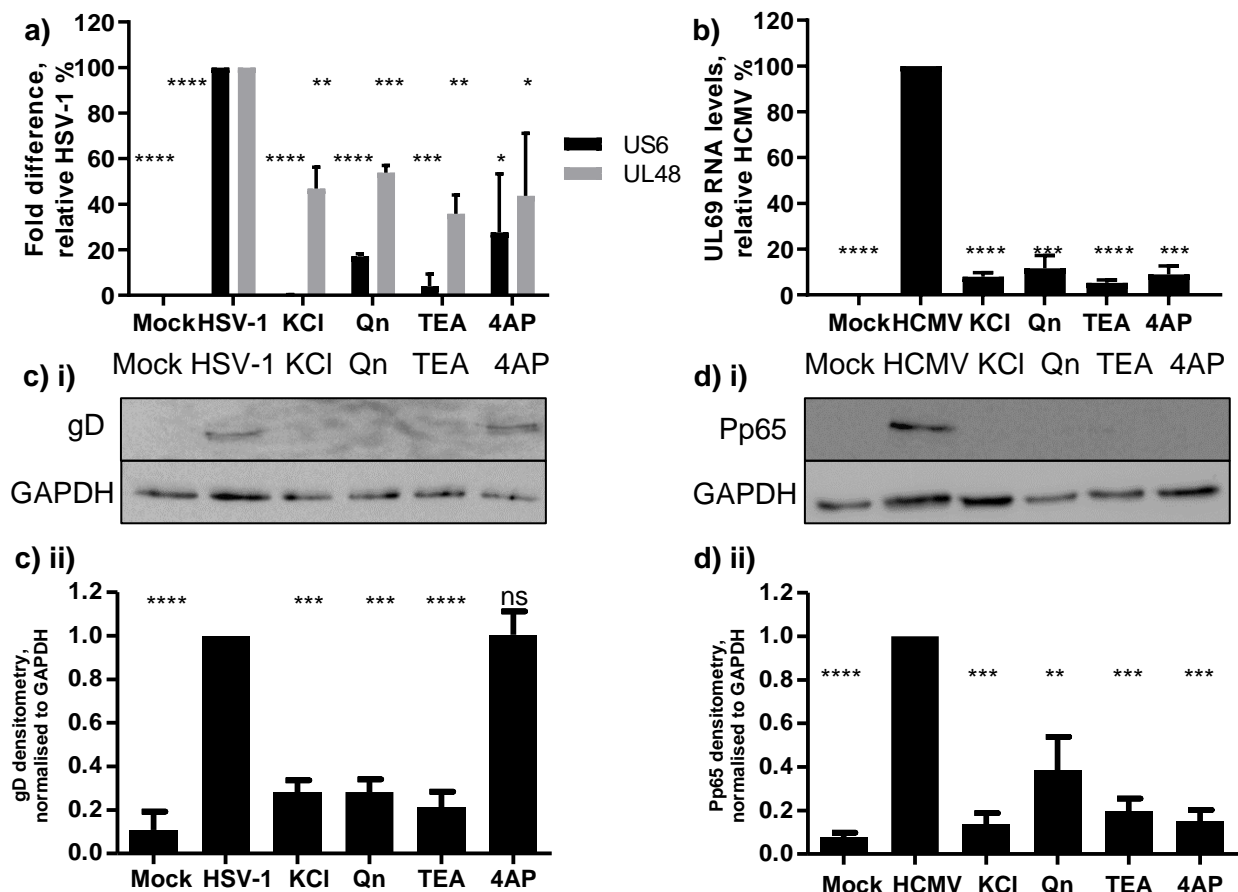


Figure 5.3 Viral expression levels after pre-treatment with general K⁺ blockers in HFFs. HSV-1 late genes US6 and UL48 (a) were used to assess HSV-1 mRNA expression and HCMV UL69 (b) was used to assess HCMV mRNA expression. HSV-1 late protein gD (c) and HCMV Pp65 (d) were used to assess protein expression. Densitometry of gD (c)ii) and Pp65 levels (d)ii) normalised to GAPDH are also shown. Asterisks correspond to P-values of ≤0.05 (*), ≤0.01 (**), ≤0.001 (***), and ≤0.0001 (****), respectively; ns denotes a P-value of > 0.05.

To determine whether the reductions in viral RNA and protein levels observed under K^+ inhibitor treatment led to reduced HSV-1 and HCMV virion production, re-infection assays were performed. Results showed reduced viral RNA levels in naïve HFFs infected with media from infected HFFs that were pre-treated with the various inhibitors (Figure 5.4). Interestingly, 4AP was shown to inhibit HCMV infectious virion production, further indicating HCMV lytic replication requires a K_v channel, however, 4AP had no effect on HSV-1 virion production, suggesting HSV-1 may utilize an alternative K^+ channel, not from the K_v family. The schematic in Figure 5.4c shows how re-infection assays are performed.

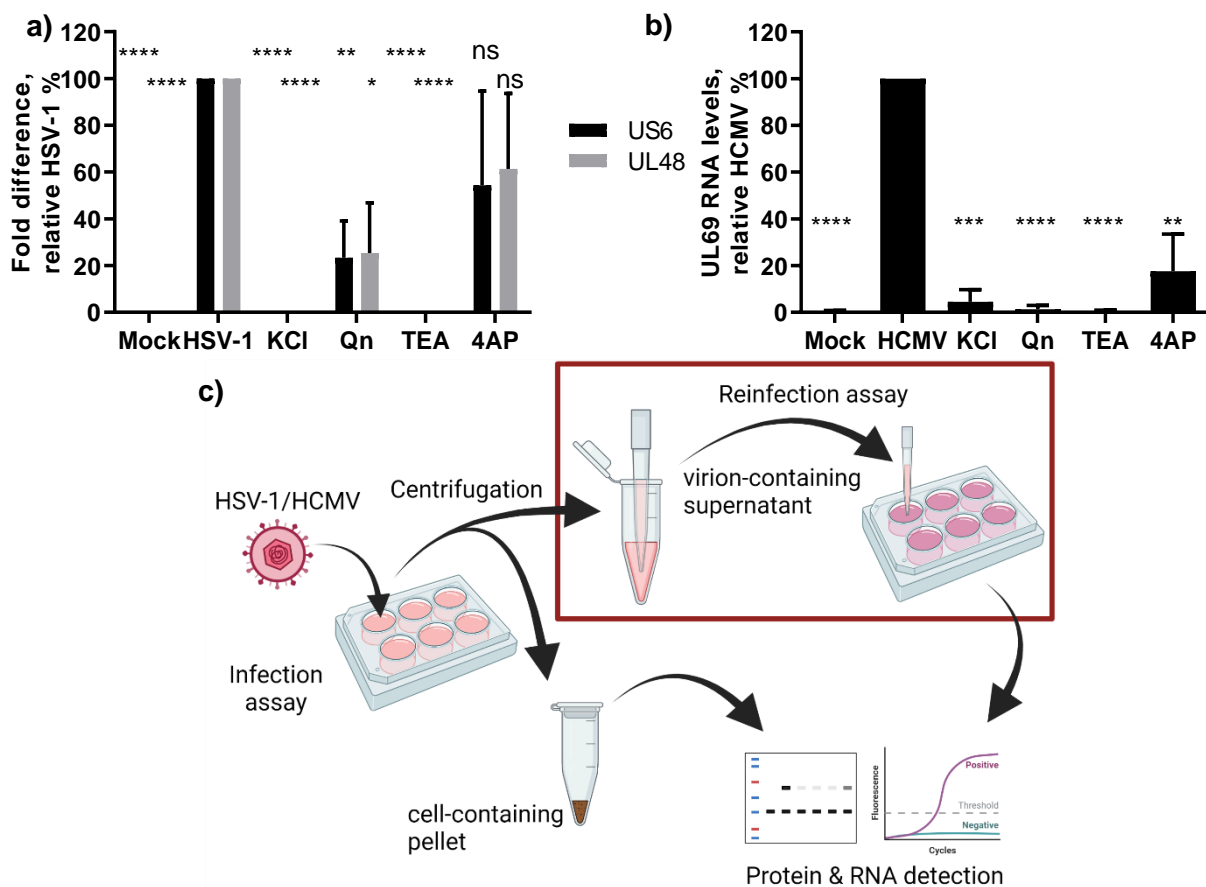


Figure 5.4 RNA levels of viral genes in general K^+ channel inhibitor re-infection assays. HFFs were pre-treated with general K^+ blockers prior to infection with HSV-1 or HCMV. Virion containing media from these infections was then used to re-infect naïve HFFs; HSV-1 late genes US6 and UL48 (a) and HCMV UL69 (b). Schematic of infection, and subsequent re-infection assay. Asterisks correspond to P-values of ≤ 0.05 (*), ≤ 0.01 (**), ≤ 0.001 (***), and ≤ 0.0001 (****), respectively; ns denotes a P-value of > 0.05 .

5.4. HSV-1 lytic replication requires $K_{Ca}3.1$ channel activity

As 4AP was unsuccessful in inhibiting HSV-1 lytic replication and infectious virion production, it suggests a non-voltage gated channel is required for HSV-1 lytic replication. To determine whether K_{Ca} channels were required for HSV-1 lytic replication, charybdotoxin (CTX) a BK_{Ca}

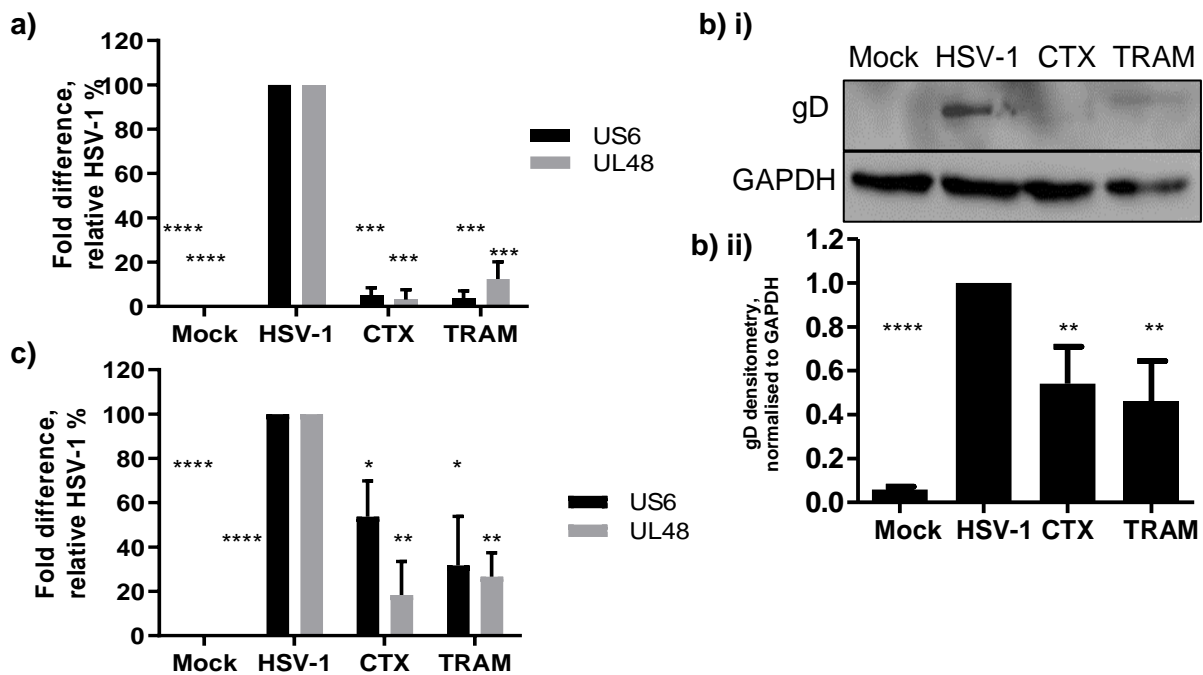


Figure 5.5 HSV-1 RNA (a) and protein (b) levels after pre-treatment with CTX or TRAM in HFFs or in a reinfection assay (c). HFFs were treated with CTX or TRAM prior to HSV-1 infection, cells were harvested after 24 hours. Densitometry for viral protein levels were normalised to GAPDH (b ii). Asterisks correspond to P-values of ≤ 0.05 (*), ≤ 0.01 (**), ≤ 0.001 (***), and ≤ 0.0001 (****), respectively; ns denotes a P-value of > 0.05 .

and $K_{Ca}3.1$ inhibitor was used to further elucidate which potassium channel could be essential for lytic HSV-1 replication. TRAM-34 (TRAM), a $K_{Ca}3.1$ inhibitor was also used in parallel. Both CTX and TRAM successfully inhibited HSV-1 lytic replication at RNA and protein level (Figure 5.5a and 5.5b). Similarly, a reduction in infectious virion production was also observed in reinfection assays (Figure 5.5c). Together, these results indicate a requirement for $K_{Ca}3.1$ during HSV-1 lytic replication.

To further support a potential role of $K_{Ca}3.1$ in HSV-1 lytic replication, $K_{Ca}3.1$ RNA levels were determined to assess whether HSV-1 lytic replication induced $K_{Ca}3.1$ expression. $K_{Ca}3.1$ was upregulated in the presence of HSV-1 lytic replication, however $K_v1.3$ expression was unaffected (Figure 5.6), further suggesting $K_{Ca}3.1$ is required during HSV-1 lytic replication.

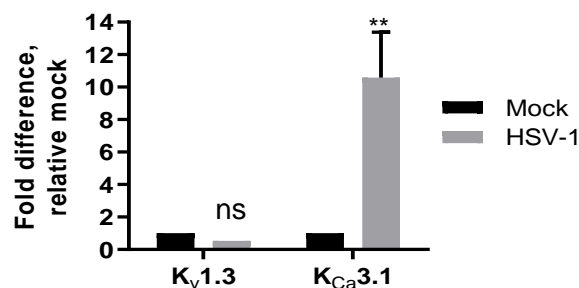


Figure 5.6 K^+ channel expression in mock- and HSV-1 infected HFFs. $K_{Ca}3.1$ and $K_v1.3$ mRNA levels were assessed in HFFs 24-hours after infection. Asterisks correspond to P-values of ≤ 0.01 ; ns denotes a P-value of > 0.05 .

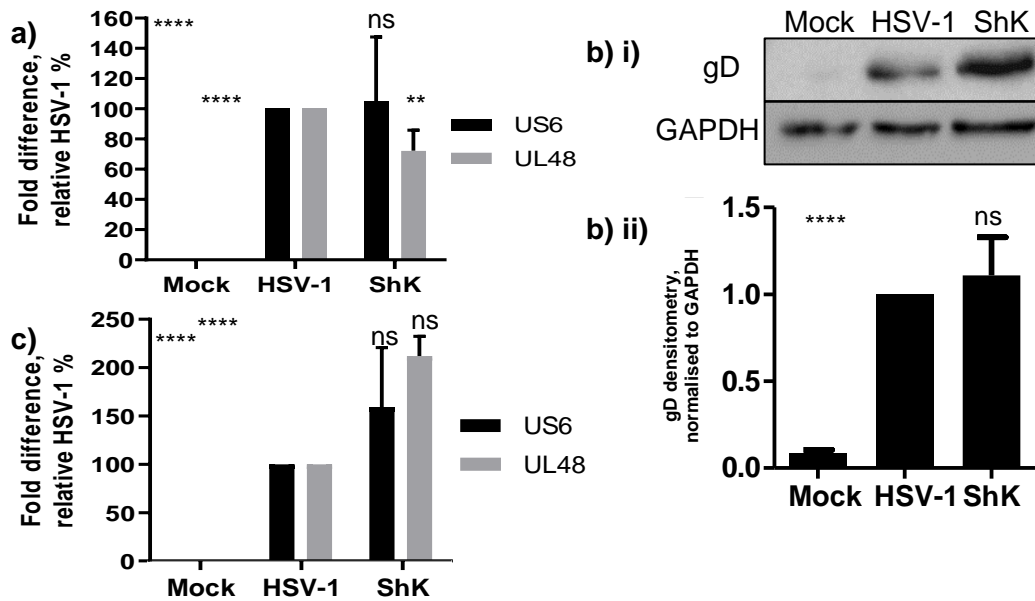


Figure 5.7 HSV-1 RNA (a) and protein (b) levels after pre-treatment with ShK in HFFs or in a reinfection assay (c). HFFs were treated with ShK prior to HSV-1 infection, cells were harvested after 24 hours. Densitometry for viral protein levels were normalised to GAPDH (d). Asterisks correspond to P-values of ≤ 0.05 (*), ≤ 0.01 (**), ≤ 0.001 (***), and ≤ 0.0001 (****), respectively; ns denotes a P-value of > 0.05 .

To confirm $K_{Ca}3.1$ inhibition was specifically required by HSV-1, ShK, the $K_v1.3$ inhibitor previously used during KSHV experiments was used to treat HFFs prior to HSV-1 infection. Results showed that HSV-1 lytic replication was unaffected by ShK treatment, suggesting HSV-1 lytic replication is not dependent upon $K_v1.3$ activity (Figure 5.7).

5.5. HCMV lytic replication requires $K_v3.4$ channel activity

4AP successfully inhibited HCMV replication, therefore ShK treatment was used to determine whether $K_v1.3$ dependency was conserved during KSHV and HCMV lytic replication. However,

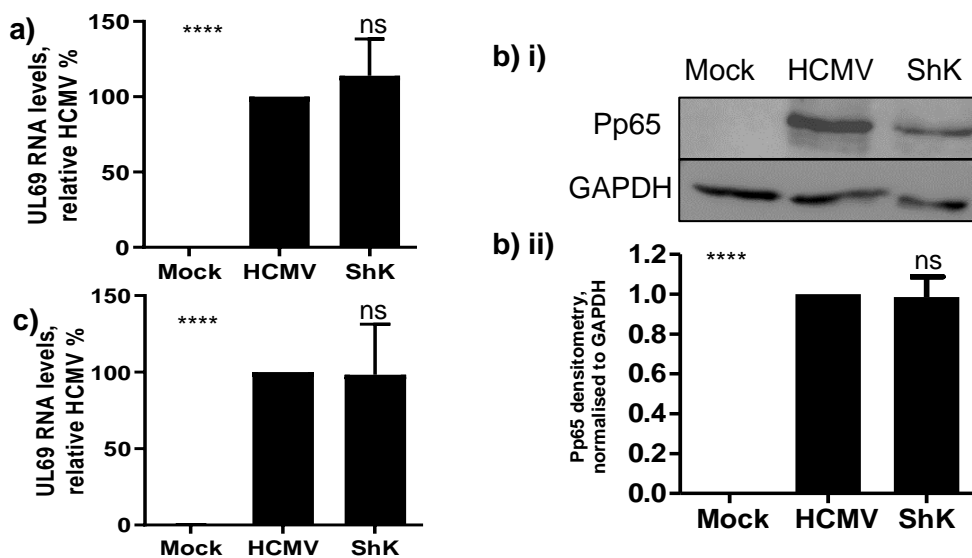


Figure 5.8 HCMV RNA (a) and protein (b) levels after pre-treatment with ShK in HFFs or in a reinfection assay (c). HFFs were treated with ShK prior to HCMV infection, cells were harvested after 7 days. Densitometry for Pp65 levels were normalised to GAPDH (b ii). Asterisks correspond to P-values of ≤ 0.05 (*), ≤ 0.01 (**), ≤ 0.001 (***), and ≤ 0.0001 (****), respectively; ns denotes a P-value of > 0.05 .

in contrast to KSHV, HCMV lytic replication was unaffected by ShK treatment (Figure 5.8). Therefore, HCMV lytic replication relies upon an alternative K_v channel, not $K_v1.3$.

Given the sensitivity of HCMV infection to 4AP, five other 4AP-sensitive channels, which are known to be upregulated during HCMV infection, were assessed for their expression in HFF via qRT-PCR. Only $K_v3.4$ and $K_v9.3$ were expressed in HFFs (Figure 5.9a), suggesting these may be important in the HCMV lytic replication cycle. Notably, $K_v3.4$ was upregulated throughout HCMV lytic replication over a 7-day period (Figure 5.9b).

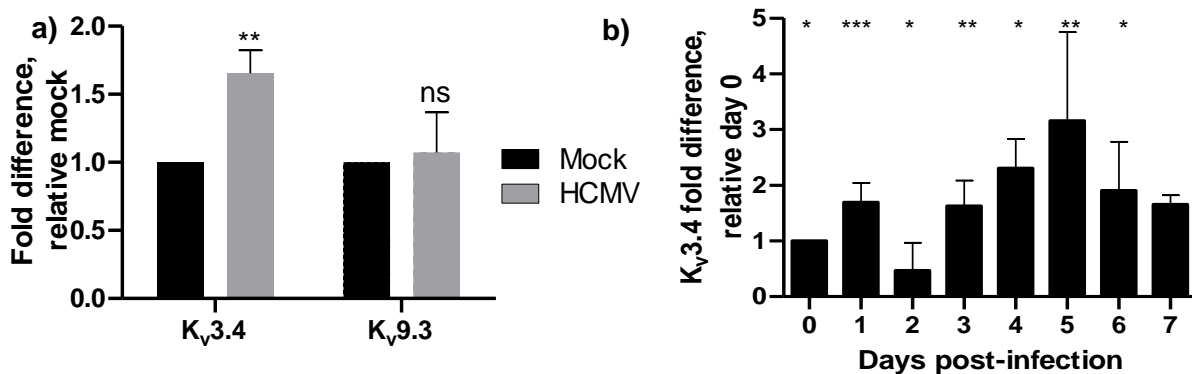


Figure 5.9 HCMV RNA (a) and protein (b) levels after pre-treatment with BDS I in HFFs or in a reinfection assay (c). HFFs were treated with BDS I prior to HCMV infection, cells were harvested after 7 days. Densitometry for Pp65 levels were normalised to GAPDH (d). Asterisks correspond to P-values of ≤ 0.05 (*), ≤ 0.01 (**), ≤ 0.001 (***), and ≤ 0.0001 (****), respectively; ns denotes a P-value of > 0.05 .

To determine whether $K_v3.4$ is required during HCMV lytic replication, a specific $K_v3.4$ inhibitor, Blood Depressing Substance I (BDS I), was used in pre-treatment studies in HFFs at non-toxic concentrations (Appendix, supplementary figure 8j). Both UL69 RNA levels and Pp65 protein levels were reduced when compared to the DMSO-treated control (Figure 5.10a & b), indicating $K_v3.4$ activity is essential for HCMV lytic replication. This was further supported by reinfection assays, which also showed HCMV infectious virion production was reduced upon BDS I treatment. Together, this suggests that $K_v3.4$ is essential for HCMV lytic replication.

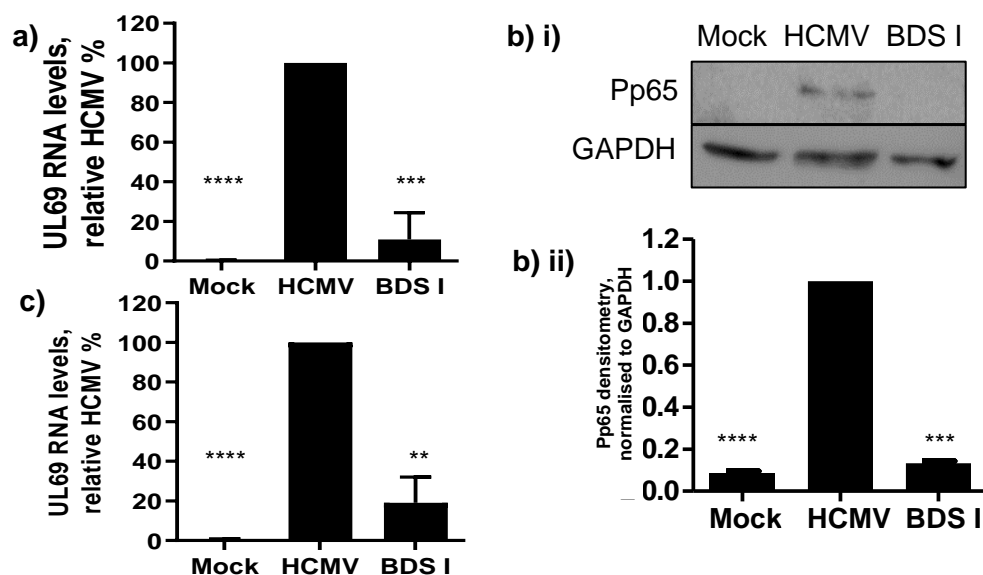


Figure 5.10 K^+ channel expression in mock- and HCMV infected HFFs (a) and during an HCMV lytic replication time-course (b). $K_v3.4$ and $K_v9.3$ mRNA levels were assessed after 7 days post-infection. As $K_v3.4$ mRNA levels were increased, a time-course to assess $K_v3.4$ levels throughout HCMV infection was performed. Asterisks correspond to P-values of ≤ 0.05 (*), ≤ 0.01 (**), ≤ 0.001 (***), and ≤ 0.0001 (****), respectively; ns denotes a P-value of > 0.05 .

5.6. Membrane hyperpolarisation occurs during both HSV-1 and HCMV lytic replication cycles

As $K_{Ca}3.1$ and $K_v3.4$ were upregulated during HSV-1 and HCMV lytic replication, respectively, increased expression could lead to an increase in channel activity, resulting in K^+ efflux and membrane hyperpolarisation, in a similar manner as described for KSHV lytic replication in the previous chapters.

Given the replication cycles of each virus have different timespans, the timepoints for each DiBAC₄(3) hyperpolarisation experiment were altered accordingly. HSV-1 infected HFFs were hyperpolarised throughout the first 24-hours of infection, with dramatic hyperpolarisation

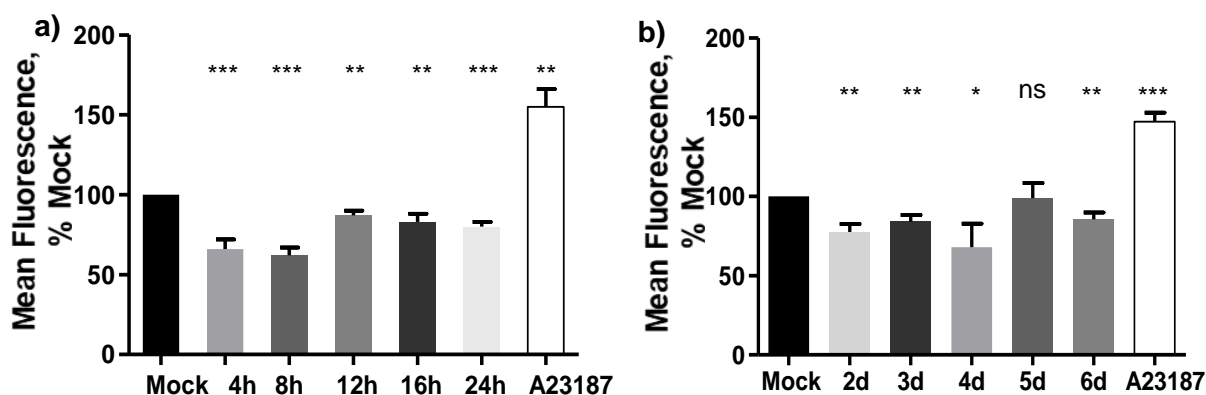


Figure 5.11 DiBAC₄(3) mean fluorescence of HFFs, as measured by flow cytometry. DiBAC₄(3) mean fluorescence, over a reactivation time-course in HSV-1-infected (a) and HCMV-infected HFFs, displayed as a percentage, relative to mock infected cells. Asterisks correspond to P-values of ≤ 0.05 (*), ≤ 0.01 (**), ≤ 0.001 (***), and ≤ 0.0001 (****), respectively; ns denotes a P-value of > 0.05 .

observed within 4-8 hours post-infection (Figure 5.11a). As with membrane polarisation experiments in TReX BCBL1-Rta cells, A23187 results in depolarisation of the HFF cell membranes. In accord with the slower replication cycle, HCMV infected HFFs were hyperpolarized 2-4 days post-infection (Figure 5.11b). This confirms K⁺ channel-mediated membrane hyperpolarisation is conserved throughout HSV-1, HCMV and KSHV lytic replication, although specific channels required for K⁺ efflux vary.

5.7. Calcium influx occurs during HSV-1 and HCMV lytic replication

As hyperpolarisation is observed during both HSV-1 and HCMV lytic replication, it was determined whether this membrane hyperpolarisation induces a calcium influx, as observed in KSHV lytic replication. To this end, investigations into the calcium ratio of HFFs during HSV-1 and HCMV lytic replication were performed using Fura Red as a ratiometric indicator via flow cytometry, as described in chapter four. Results showed increased intracellular calcium levels compared to mock-infected cells from 4 hours post-infection with HSV-1 and 2 days post-infection for HCMV (Figure 5.12). This indicates a calcium influx occurs during HSV-1 and HCMV lytic replication.

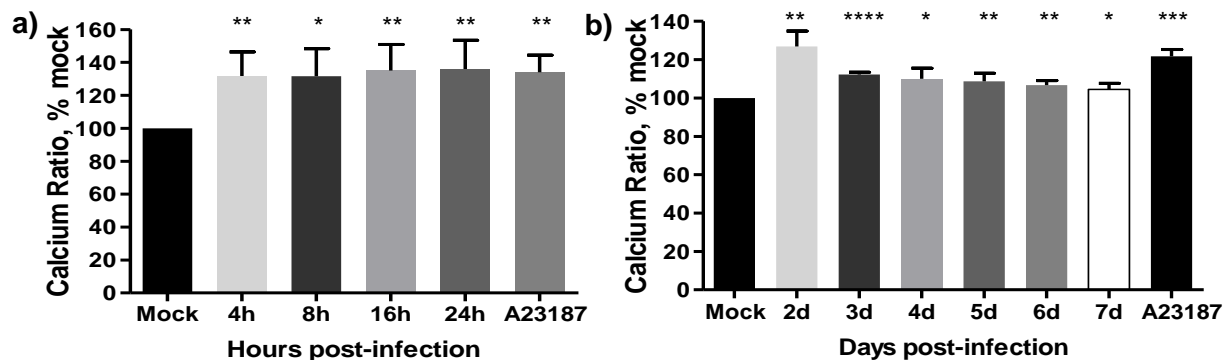


Figure 5.12 Calcium ratio in HSV-1 infected (a) and HCMV-infected (b) HFFs, measured via flow cytometry. Cells were harvested at various time-points, depending upon the viral replication cycle, and incubated with Fura Red for 30 minutes at 37°C, before fluorescence was measured. Asterisks correspond to P-values of ≤0.05 (*), ≤0.01 (**), ≤0.001 (***), and ≤0.0001 (****), respectively; ns denotes a P-value of > 0.05.

Experiments to elucidate which calcium channel is responsible for the calcium influx were performed. Given the conservation of the hyperpolarisation-mediated calcium influx, PNG was first used to assess for channel conservation between *Herpesviridae*. Both HSV-1 and HCMV RNA (Figure 5.13a & b) and protein (Figure 5.13c & d) levels were reduced after PNG treatment, indicating Ca_v3.2 activity is essential for both HCMV and HSV-1 lytic replication. Furthermore, reinfection assays showed that infectious virion production was reduced to

around 10% of the positive control after pre-treatment with PNG for both viruses (Figure 5.13e & f). This further confirms $Ca_v3.2$ activity is required during HCMV and HSV-1 lytic replication.

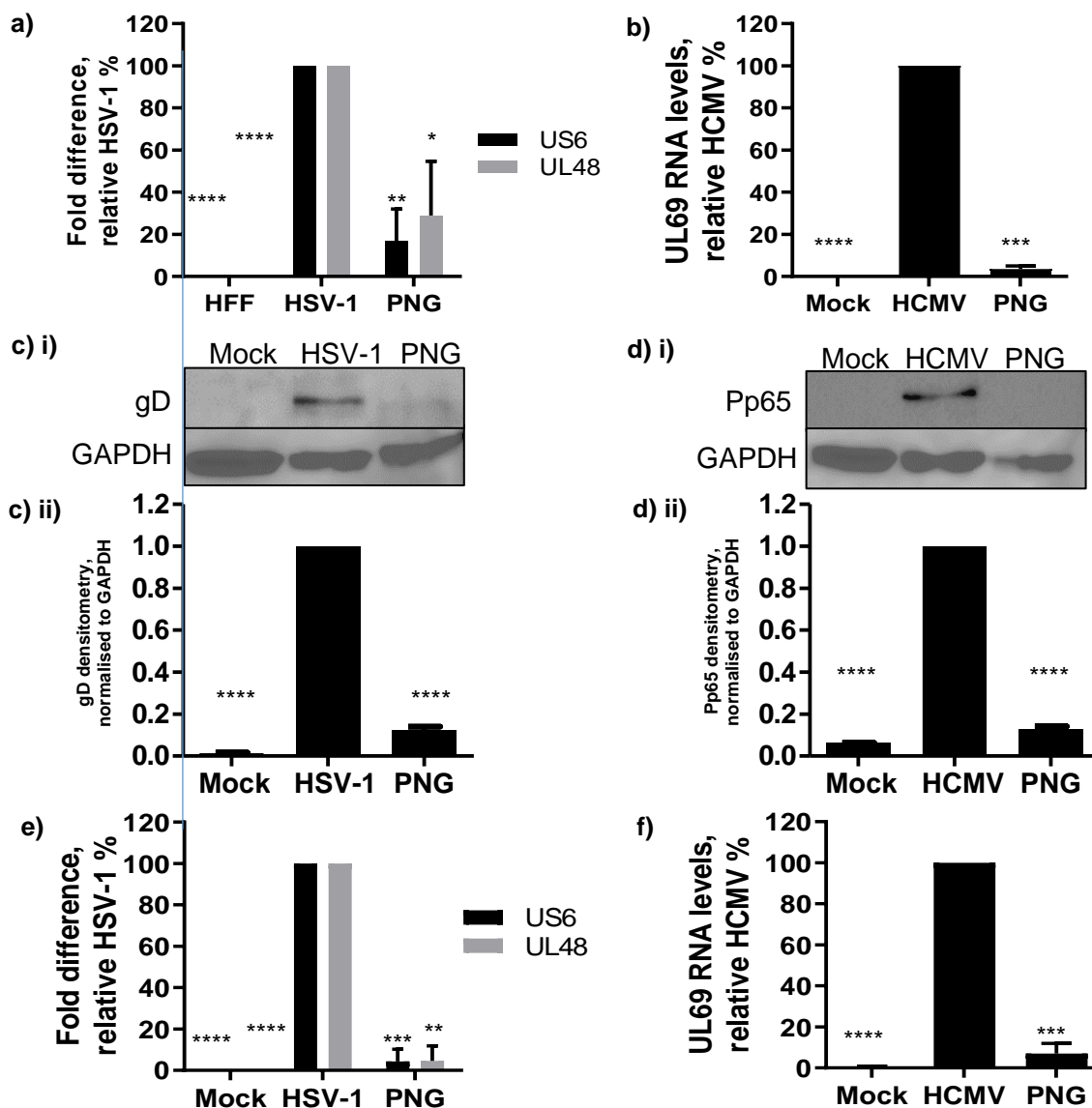


Figure 5.13 Viral gene expression after pre-treatment with PNG in HFFs. HSV-1 late genes US6 and UL48 (a) were used to assess HSV-1 infection and HCMV UL69 (b) was used to assess HCMV infection via qRT-PCR. HSV-1 late protein gD (c) and HCMV Pp65 (d). Densitometries normalised to GAPDH are also shown (ii). HFFs were pre-treated with PNG prior to infection with HSV-1 or HCMV. Virion containing media from these infections was then used to reinfect naïve HFFs; HSV-1 late genes US6 and UL48 (e) and HCMV UL69 (f). Asterisks correspond to P-values of ≤ 0.05 (*), ≤ 0.01 (**), ≤ 0.001 (***), and ≤ 0.0001 (****), respectively.

5.8. Calcineurin activity is required during HSV-1 and HCMV lytic replication

As previously reported, CsA can be used to prevent reactivation of symptomatic HSV-1 or HCMV infection in latently infected patients (Columbo et al., 2014). To determine whether CsA prevents HSV-1 or HCMV lytic replication in HFF cells, reinfection assays were performed.

Both US6 and UL48 RNA levels were reduced after CsA treatment, when compared to the DMSO treated control (Figure 5.14a). CsA also reduced RNA levels of UL69 in HCMV infected cells (Figure 5.14b). Therefore, CsA reduces infectious virion production during both HSV-1 or HCMV lytic replication cycles, leading to the lower RNA levels seen in reinfection assays. These results suggest calcineurin activity is required during HSV-1 and HCMV lytic replication.

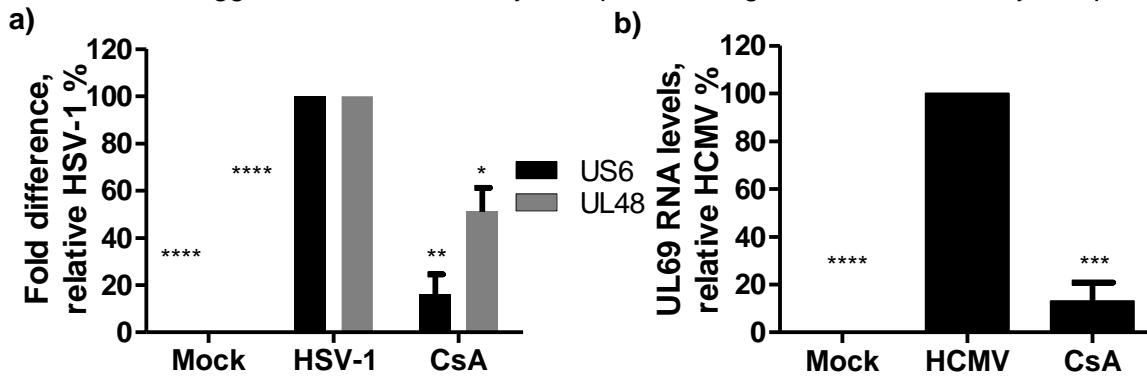


Figure 5.14 RNA levels of viral genes in CsA pre-treatment reinfection assays. HFFs were pre-treated with CsA prior to infection with HSV-1 or HCMV. Virion containing media from these infections was then used to reinfect naïve HFFs; HSV-1 late genes US6 and UL48 (a) and HCMV UL69 (b). Asterisks correspond to P-values of ≤ 0.05 (*), ≤ 0.01 (**), ≤ 0.001 (***), and ≤ 0.0001 (****), respectively.

5.9. Discussion

The rise of acyclovir resistant HSV-1 strains is threatening current therapeutic methods. Furthermore, acyclovir and its derivatives have limited effect on VZV and HCMV lytic replication and have no effect on either KSHV or EBV lytic replication due to the variation within the thymidine kinase encoded by each family member. Generating a pan-herpes antiviral utilising ion channel inhibition would therefore have many advantages for *Gammapherpesvirinae* infections. Virally induced K^+ efflux mediated hyperpolarisation occurs during both HSV-1 and HCMV lytic replication, both leading to Ca^{2+} influx and NFAT1 upregulation, suggesting the mechanism itself is conserved. Figure 5.15 shows the conserved virally mediated hyperpolarisation-driven calcium influx mechanism. However, each virus investigated requires a different potassium channel to drive K^+ -mediated hyperpolarisation. This has implications for pan-herpesvirus inhibitors targeting K^+ channels. Targeting $Ca_v3.2$ or calcineurin could present an alternative approach, as both HSV-1 and HCMV lytic replication was reduced by specific inhibition of $Ca_v3.2$ or CsA treatment, as well as KSHV lytic replication (chapter 4).

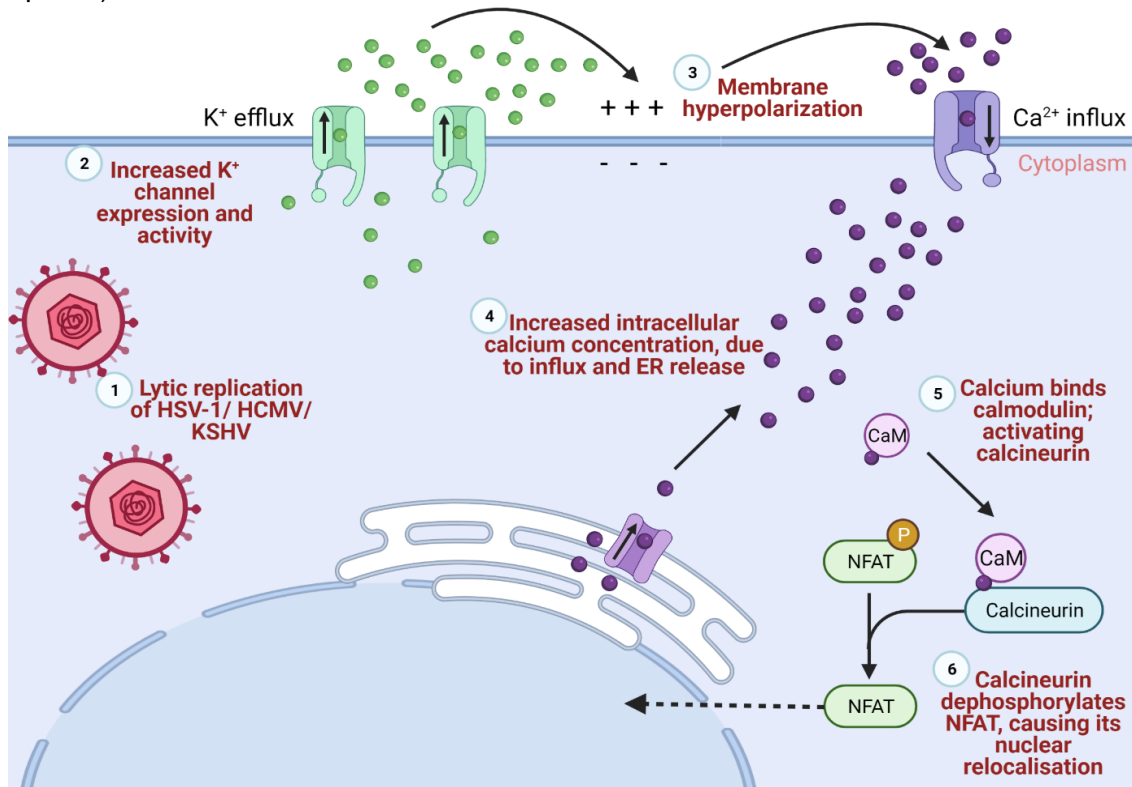


Figure 5.15 Schematic of hyperpolarisation-mediated calcium influx mechanism, conserved during HSV-1, HCMV or KSHV lytic replication. Created with Biorender.com.

The generation of knockdown $K_{Ca}3.1$, $K_v3.4$ and $Ca_v3.2$ cell lines using HFFs would have further supported the role of these channels during HSV-1 and HCMV lytic replication, however, attempts at $K_{Ca}3.1$ knockdown in HFFs were unsuccessful and, as mentioned, $Ca_v3.2$ is essential in TREx BCBL1-Rta cells. Additionally, other studies have already shown the potential of using ion channel blockers to target herpesvirus infection and replication. Most recently, Ding et al (2021) investigated the effect of Ca_v channel inhibitors on HSV-2, finding that Ca^{2+} influx caused by Ca_v3 channels were required during the later stages of HSV-2 lytic replication and that Ca_v3 inhibition via channel blockers was sufficient to prevent HSV-2 replication.

Zhang et al (2017) found that HSV-1 causes a reduction in $Ca_v3.2$ protein levels and thus channel activity during early phases of replication in a murine neuroblastoma cell line. This appears to contradict the effect of PNG on HSV-1 infection, however, the paper also found that HSV-1 upregulates $Ca_v3.2$ mRNA levels.

Other investigations into host channels during HSV-1 infection showed a requirement for chloride channels during an early stage of replication (Zheng et al., 2014). Using tamoxifen to target Cl^- channels for HSV-1 successfully reduced lytic replication; potentially targeting viral entry. However, this avenue does present an issue regarding early detection of primary infection or lytic reactivation and would therefore require rapid access to any potential treatment. Although tamoxifen and other chloride channel blockers may not be the way forward for acyclovir resistant HSV-1 treatment, there is a proof of principle and further investigation into the role of ion channels in HSV-1 replication could provide a more suitable drug target. Tamoxifen itself also increases IFN γ levels, raising the implications for affecting innate immunity, which could already be compromised during HSV-1 lytic replication.

Due to observed channel specificity, investigations into the role of each channel in other Human herpesviruses within the three sub-families could determine whether specific potassium channels are conserved throughout sub-families and thus enable the investigation into utilising ion channel inhibitors as pan-herpes therapeutics.

Chapter 6

Discussion

6 Discussion

Ion channels regulate the intracellular concentration of various ions, including Ca^{2+} and other divalent ions which function as secondary messengers to regulate numerous pathways including cytokine production, differentiation, and cytotoxicity within lymphocytes (Hogan et al., 2010; Alexander et al., 2011). The movement of these cations across the plasma membrane depends on electrical gradients that are maintained by specific channels. Many viruses encode their own viroporin which participate in several viral functions, such as viral entry via membrane or vesicle modulation, glycoprotein trafficking, and virion release (Scott and Griffin, 2015). Ion channel modification has been shown to play vital roles in the replication of several viruses, with some success in targeting ion channels as an antiviral therapy (Hover et al., 2017; Charlton et al., 2020). This research has not been limited to host ion channels, with numerous antiviral treatments targeting virally-encoded viroporins, including several treatments against influenza A M2 viroporin, such as amantadine and its derivatives. General ion channel inhibitors such as verapamil, an antiarrhythmic which targets L-type calcium channels, has also been repurposed to treat classic swine fever virus via its p7 viroporin activity (Scott and Griffin, 2015). New studies also indicate verapamil and other calcium channel blockers already approved for clinical use could be repurposed to treat SARS-CoV 2 infection (Straus et al., 2020). These observations show promise for utilising ion channel modulators as antiviral targets in a variety of different infections and indicate a rapid response treatment avenue against novel infections, such as during the COVID-19 pandemic.

However, until now there has been little investigation into the relationship between KSHV and host ion channels. This research has been long overdue as treatments of KSHV-associated diseases are lacking, therefore repurposing a clinically approved ion channel inhibitor holds promise, particularly in Sub-Saharan Africa.

Therefore, key channel families were investigated for their requirement during KSHV lytic reactivation by assessing KSHV lytic replication in the presence of well characterized modulators of K^+ channels. This uncovered a novel K^+ efflux mediated hyperpolarisation

mechanism, which triggers calcium signalling and this mechanism was found to be conserved between subfamilies.

Chapter three revealed, for the first time, the dependence of KSHV on the function of a K^+ channel, endogenously expressed within B cells, to complete its lytic replication cycle. Specifically, the voltage-gated outwardly rectifying K^+ channel, $K_v1.3$, is activated during KSHV reactivation, leading to hyperpolarization of the cell membrane (Figure 6.1). This current can be inhibited utilising peptides derived from scorpion or sea anemone venom, MgTX and ShK-Dap²², respectively (Kalman et al., 1998; Bajaj and Han, 2019). When applied to reactivated cells, these compounds are detrimental to KSHV lytic induction. These highly stable venom-derived peptides already hold potential as a solution to the lack of treatment options for KS in remote regions which lack infrastructure systems necessary to provide traditional therapeutics. Given the abundance of natural sources for $K_v1.3$ -inhibition a safe, effective therapeutic based on these compounds is a promising target for prevention of lytic KSHV replication and thus KSHV-associated malignancies. Furthermore, A $K_v1.3$ inhibitor is currently undergoing clinical trials (Tarcha et al., 2017).

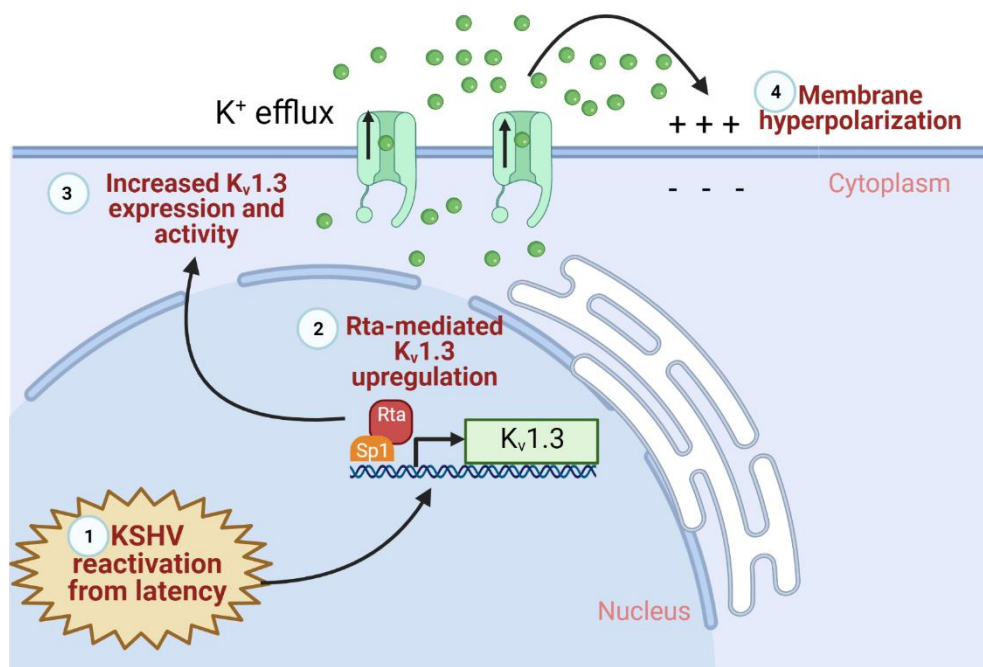


Figure 6.1 Schematic of KSHV-specific $K_v1.3$ -mediated hyperpolarisation mechanism which occurs upon reactivation of lytic viral replication. Utilising $K_v1.3$ or Sp1 inhibitors provides novel avenues of antiviral therapy research. Created with BioRender.com.

K_v upregulation has been associated with tumorigenesis in a variety of carcinomas. Notably, a correlation has been established between $K_v1.3$ abundance and the grade of tumour malignancy (Jang et al., 2011). The enhanced $K_v1.3$ currents observed during lytic replication may also promote KSHV mediated tumour development. Elucidating the potential role of $K_v1.3$ in KSHV oncogenesis could further assist targets for KSHV treatment using a $K_v1.3$ blocker. Notably, the results in chapter three not only presented an ion channel target for KSHV therapeutic research, initial upregulation of $K_v1.3$ was Rta and Sp1 mediated. This interaction could also present an avenue of therapeutics. For example, by small molecules or affimers which block the Rta-Sp1 binding domain.

Although KSHV latency is generally assumed to be the state leading to transformation by KSHV, lytic viral proteins are detectable in KSHV infected PEL, MCD, and KS cells, and have been implicated in tumorigenesis; oncogenic proteins encoded by KSHV lytic genes and KSHV lytic replication and successful KSHV infection can replenish episomes lost within highly proliferating tumour cells (Chatterjee et al., 2002; Katano et al., 2000; Katano et al., 2001; Parravicini et al., 2000). Successful treatment of KS patients with KSHV DNA replication blockers indicate that lytic replication is required for both initiation of KS and maintenance of the disease (Coen et al., 2014). KSHV requires $K_v1.3$ for lytic replication therefore targeting $K_v1.3$ activity in KSHV infected patients may hold promise as a future anti-KSHV drug development. Rituximab, an anti-CD20 monoclonal antibody, has recently been used to targeted KSHV-infected B-cells, this treatment substantially improved MCD patient outcomes (Uldrick et al., 2014). Notably, rituximab has been identified as a $K_v1.3$ inhibitor in Daudi human B-lymphoma cells; reducing $K_v1.3$ channel activity to 20% at concentrations of 100-200 $\mu\text{g/ml}$, which is greater than the concentration required for CD20 activation (Wang et al., 2012). $K_v1.3$ inhibition by rituximab is likely to contribute to the beneficial effects seen on KS tumours, thus highlighting the possibility of selective $K_v1.3$ blockers as potent anti-KSHV therapeutics. While compounds targeting $K_v1.3$ are in preclinical development only dalazatide (an ShK derivative) is currently undergoing clinical trials for immune-related disorders, such as plaque psoriasis treatment (Tarcha et al., 2017).

KSHV has no known viroporin, suggesting that it has evolved KSHV proteins to interfere with the normal cellular ion channel profile. This molecular piracy is well documented in KSHV, as the virus has acquired many genes from the host cell to establish a cellular environment that favours its pathogenesis (Choi et al., 2001). $K_v1.3$ plays vital roles in B lymphocytes, the location of the latent KSHV reservoir, including Ca^{2+} influx, cytokine production, cell proliferation, clonal expansion, and cell death (Wulff et al., 2004, Wulff and Zhorov, 2008; Wang et al., 2012; Chiang et al., 2017) therefore KSHV-mediated channel manipulation favours KSHV lytic replication due to the dependence of KSHV reactivation on intracellular Ca^{2+} mobilisation.

Furthermore, chapter four shows activation of $K_v1.3$ initiates Ca^{2+} influx through $Ca_v3.2$. This Ca^{2+} influx enhances the Ca^{2+} -driven nuclear localisation of NFAT1 and subsequent induction of NFAT-driven gene expression, required for lytic replication (Figure 6.2). This shows $K_v1.3$ and $Ca_v3.2$ channels are direct contributors to KSHV lytic replication. This $K_v1.3$ -mediated calcium influx mechanism has been highly studied in T cells, where T cell receptor binding induces $K_v1.3$ -mediated membrane hyperpolarisation, activating the NFAT-calcium signalling pathway and thus production of cytokines required during the immune response (Wulff et al.,

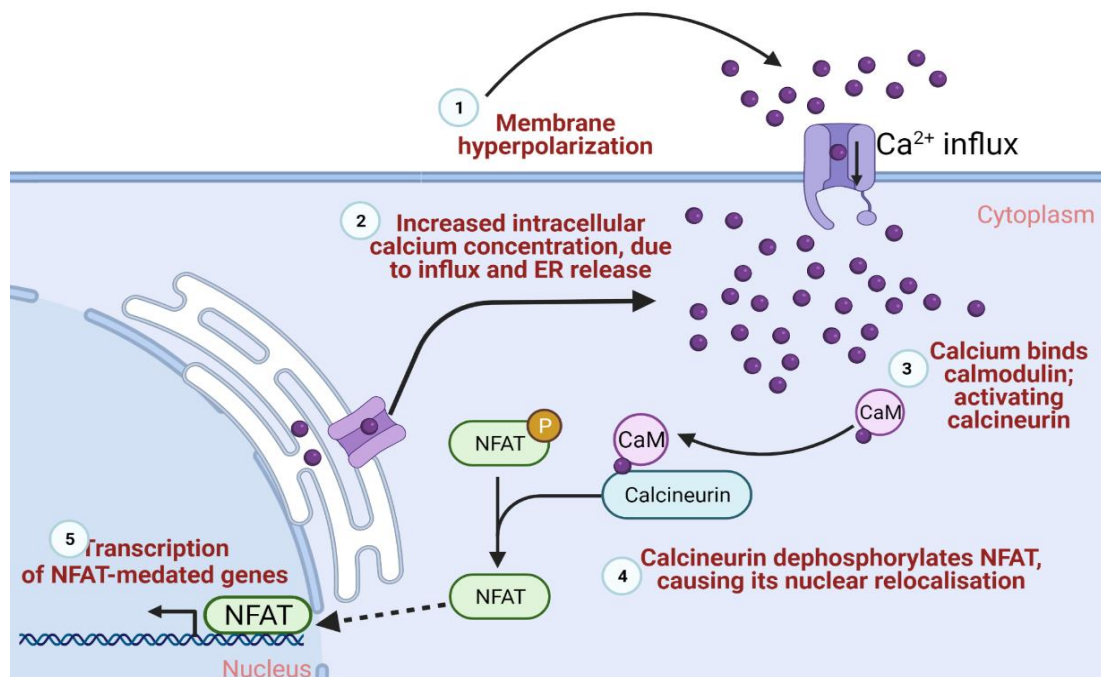


Figure 6.2 Schematic of KSHV-specific hyperpolarisation-mediated calcium influx and signalling mechanism which occurs upon reactivation of lytic viral replication. Drugs which target this pathway include cyclosporin, which is already clinically approved as an immunosuppressant. Created with BioRender.com.

2004, Wulff and Zhorov, 2008; Wang et al., 2012; Chiang et al., 2017). T_{EM} and class-switched B cells are dependent upon this mechanism to trigger the NFAT-calcium signalling cascade. Chapters three and four therefore reveal both K_v1.3 and Ca_v3.2 channels directly contribute to KSHV lytic replication. This dependence on host cell channels during KSHV lytic replication opens new insights into how *Herpesviridae* members manipulate susceptible cells during virus pathogenesis and uncovers novel avenues for pan-*Herpesviridae* treatments.

With the increased survival rate after the onset of AIDS, the increasing success rate of transplants, and the increasing global life expectancy (King et al., 2003); cases of AIDS-associated, Iatrogenic and Classic KS have the potential to increase (Rohner et al., 2014). At present, there is a lack of treatment that cannot be left to continue. Additionally, the rise of acyclovir resistant HSV-1 strains is threatening current therapeutic methods, thus generating a pan-herpes antiviral utilising ion channel inhibition would solve both issues (Piret and Boivin, 2010). Given the data showing that targeting K_v1.3 or Ca_v3.2 channel activity reduces the ability of KSHV to reactivate from latency, two avenues of drug discovery present themselves. Furthermore, targeting the downstream effects of this dysregulated channel activity using CsA or similar calcineurin inhibitors holds promise for rapid development as a novel KSHV, or even pan-herpes, treatment due to their current approved use. An additional benefit of preventing host mechanisms essential for herpesviral lytic replication lies in the reduced risk of antiviral resistance occurring as host genomic mutation rates are negligible in comparison to those of many viral genomes.

T-type channels, including Ca_v3.2, support a wide range of physiologic processes including vital roles in the firing of neurons and pacemaking within the sinoatrial node (Zamponi et al, 2015). Channel activation also triggers both the NFAT and CREB pathways to enable gene expression (Lin et al., 2014). Notably, regulation of potassium channels by Ca_v3.2 has also been shown to control firing within axons, through inhibition of K_v7 channel activity (Zamponi et al, 2015). In addition to the potential link of K_v1.3 and KSHV tumourigenesis, Ca_v3.2 channel activity has been implicated in proliferation of prostate cancer cells, in conjunction with BK

channel K⁺ efflux, however cell proliferation was inhibited using flunarizine (Gackière et al., 2013).

Calcium signalling has long been linked to the promotion of KSHV lytic replication, with ionomycin, a calcium ionophore inducing ORF50 expression, and thus triggering KSHV lytic replication (Chang et al, 2000; Zoetewij et al., 2001; Aneja and Yuan, 2017). This reactivation can be inhibited using calcineurin inhibitors, tacrolimus and CsA, indicating calcium signalling mediated KSHV reactivation is dependent upon calcineurin activity (Zoetewij et al., 2001). While calcineurin inhibitors are currently in clinical use as immunosuppressants, the use of such a broad-acting drug for inhibiting KSHV lytic replication presents the risk of potential off-target effects, therefore utilising this stage of the mechanism as a potential KSHV therapeutic would require the development of novel compounds. In addition to calcium mediated KSHV reactivation from latency, KSHV proteins have been shown to affect calcium movement within host cells (Feng et al., 2002; Chen et al., 2018). KSHV K7 targets calcium-modulating cyclophilin ligand to modulate calcium movement and thus prevent apoptosis of host cells, enabling completion of KSHV lytic replication and persistent infection (Feng et al., 2002). KSHV K15 interactions with SOCE channels directly contributing to pathogenesis, by enabling both cell proliferation and migration via increased Ca²⁺ influx caused by upregulation of Orai1 and thus SOCE channel formation and activity (Chen et al., 2018).

Furthermore, several inflammatory and angiogenic cytokines are expressed in KS tumours, enabling KSHV replication and pathogenesis; these cytokines have been linked to regulation of specific cell cycle phases and cell differentiation, along with contributing to oncogenesis (Balkwill, 2006; Sharma-Walia et al., 2010; Mojic et al., 2017; Agrawal et al., 2018; Giulianelli et al., 2019; Xu et al., 2019; Jary et al., 2020). As shown in chapter four, KSHV lytic replication induces expression of a variety of NFAT-regulated genes, many of which have been implicated in oncogenesis. ANGPT2, for example, is highly upregulated in tumour cells and has been linked to poor prognosis in cancer patients (Yu et al., 2016; Jary et al., 2020). A study into prevention of KSHV-induced ANGPT2 showed reductions in both angiogenesis and tumour

growth within a mouse model, indicating the role of ANGPT2 in KS tumour development and the potential of ANGPT2 inhibitors as a KS therapeutic (Yu et al., 2016).

Notably, induction of cyclooxygenase 2 (COX2) transcription occurs via several different ion-dependent processes, including the Ca^{2+} -dependent calcineurin-NFAT and CREB pathways, which is activated through phosphorylation after K^+ -dependent hyperpolarisation (Sharma-Walia et al., 2010). COX2 stimulation occurs during carcinogenesis, and as viral gene expression is required for continued COX2 expression, COX2 could be contributing to the oncogenic nature of KSHV (Sharma-Walia et al., 2010; George Paul et al., 2011). Therefore, COX2 inhibitors, currently used for their anti-inflammatory effects, could be repurposed as anti-cancer drugs and investigation into their effect on KSHV pathogenesis may present a novel therapeutic approach, initial *in vitro* investigations into the use of nimesulide, a COX2 inhibitor, as a KSHV treatment showed promise.

As shown in chapter five, human herpesviruses from other subfamilies did not require $\text{K}_v1.3$ during lytic viral replication, although further investigation into the role of $\text{K}_v1.3$ in animal *Gammaherpesvirinae* MHV-68 and HVS, along with the human *Gammaherpesvirinae* EBV, could determine whether specific potassium channels are conserved throughout sub-families. However, the specific K^+ channels required for both HSV-1 and HCMV lytic replication were

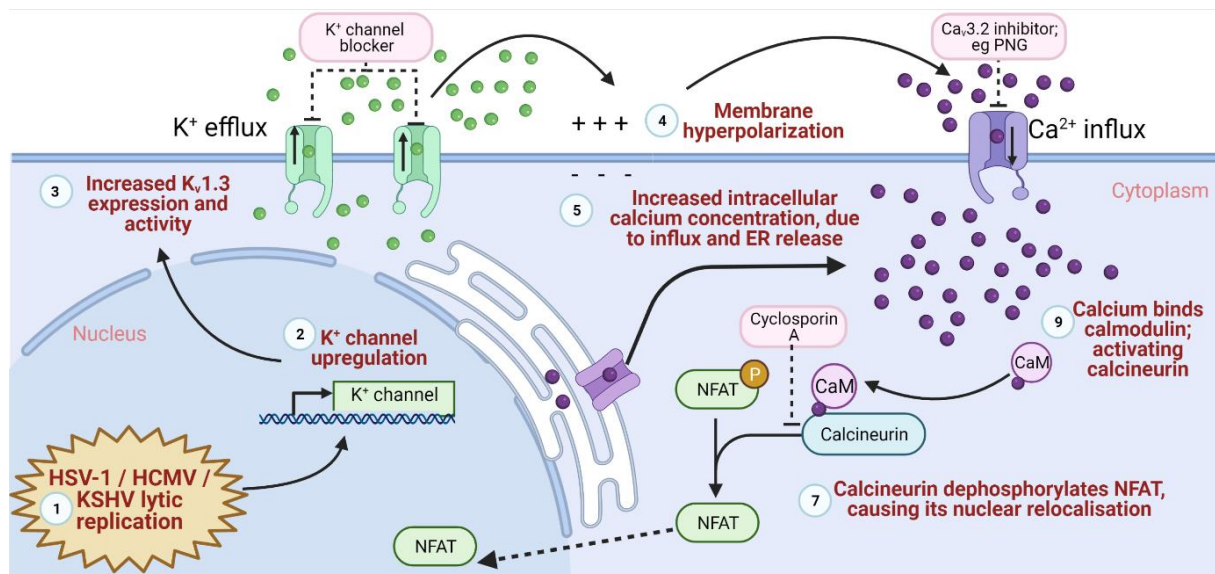


Figure 6.3 Schematic of general K^+ efflux and hyperpolarisation-mediated calcium influx and signalling mechanism which occurs during herpesviral lytic replication. Herpesviral lytic replication is dependent upon the calcium signalling cascade, each virus triggers the cascade by manipulating host ion channels. Drug targets are also indicated. Created with BioRender.com

identified and thus could be targeted by specific ion channel inhibitors to prevent diseases caused by the lytic replication of each virus. Notably, the hyperpolarisation-mediated calcium influx mechanism was conserved, indicating this mechanism could be targeted for novel pan-*Herpesviridae* antiviral treatments (Figure 6.3).

Furthermore, $Ca_v3.2$ successfully inhibited KSHV reactivation and HSV-1 or HCMV infection, suggesting $Ca_v3.2$ inhibition could present a novel target for pan-*Herpesviridae* antivirals. While Ding et al., (2020) showed that T-type calcium channels blockers could be utilised to inhibit HSV-2 infection, others have shown HSV-1 manipulates the activity of $Ca_v3.2$, via downregulation, although this can be rescued by IL-6 production (Zhang et al., 2019). Additionally, knockdown experiments into the effect of $Ca_v3.2$ on KSHV were unsuccessful as no cells survived the selection process, suggesting $Ca_v3.2$ is essential for cell survival. This hindered further investigation into the effect of $Ca_v3.2$ on lytic *Herpesviridae* replication.

Other studies show the potential of using ion channel inhibitors to prevent *Herpesviridae* infection and lytic replication (Kennedy et al., 2013; Zheng et al., 2014). Traditional treatments, such as acyclovir, have been used to help reduce pain of PHN, both during VZV lytic replication thus reducing the risk of PHN and during episodes of PHN (Kennedy et al., 2013). However, the drug has no effect on the host factors causing PHN and viral genes or proteins are not readily observed during PHN. When factoring in observed HSV-1 acyclovir resistance and the lower efficacy of acyclovir on VZV, there is already a heightened risk that this treatment will fail over long-term use. Two clinically approved Na^+ channel inhibitors lidocaine and carbamazepine, a local numbing agent and an anticonvulsant used to treat epilepsy, respectively hold promise as pain relief during PHN. Both have been shown to suppress Na_v channel activity which is thought to cause the neuropathic pain experienced during PHN. Moreover, repurposing tamoxifen to target Cl^- channels for HSV-1 treatment would hinder early stages of viral replication, potentially viral entry (Zheng et al., 2014). This could be used to reduce symptomatic HSV-1 infection as tamoxifen also increases IFN levels, thus boosting the innate immune system, when compromised this system can trigger HSV-1 lytic replication and symptomatic infection.

6.1. Future work

As mentioned, further investigation into Rta-Sp1-K_v1.3 promoter interactions could provide an upstream target to prevent K_v1.3-mediated KSHV lytic replication, and thus an avenue for development of therapeutics for KSHV-associated diseases. Additionally, the Rta-K_v1.3 ChIP and Rta transfection experiments could be modified for use in HFFs investigating the channel promoter binding to Rta homologs within HSV-1 and HCMV to determine whether the channel upregulation mechanism is conserved. Furthermore, Mithramycin can be used as a control in these experiments to determine whether channel upregulation is Sp1-mediated. While initial investigation into the effect of Mith A on HSV-1 and HCMV lytic replication was performed, showing reduction in RNA levels when compared to DMSO-treated HFFs, further experiments were prevented due to lab activity closures during the COVID-19 pandemic.

Whilst attempts to generate a stable Ca_v3.2-depleted cell line in TREx BCBL1-Rta cells failed, indicating the channel is essential for cell survival, experiments into Ca_v3.2 overexpression or treatment with a channel activator could balance the channel inhibitor experiments, as encouragement of lytic replication would confirm the channel is utilised by HSV-1, HCMV and KSHV during their lytic replication cycle. Further depletion HFF-based cell lines generated for K_{Ca}3.1 and K_v3.4, along with assessing whether Ca_v3.2 could be depleted in a different cell line, could have further confirmed these channels are essential for HSV-1 and HCMV lytic replication, respectively. Moreover, these depleted cell lines would enable further investigation into the downstream stages within the upregulation mechanism, for example NFAT1 relocalisation and subsequent upregulation of NFAT1-mediated genes.

As K⁺ channel dependence varied between the three *Herpesviridae* family members investigated, experiments into channel conservation within subfamilies were planned to determine whether K_v1.3 was essential for both KSHV and EBV lytic replication, along with closely related animal *Gammaherpesvirinae* members HVS and MHV-68. As ShK-Dap²² has been shown to effectively inhibit the mouse K_v1.3 homolog, experiments utilising the peptide as a pre-treatment prior to EBV, HVS and MHV-68 were planned, along with *in vivo* studies in mice. Furthermore, genetically modified mice with a humanised immune system could also be

utilised to study $K_v1.3$ inhibition as a potential KSHV therapeutic *in vivo*. However, the *in vivo* studies were dependent upon the success of ShK-Dap²² inhibiting MHV-68 *in vitro*.

Additional experiments into the effect of $K_{Ca}3.1$ and $K_v3.4$ inhibitors on *Alphaherpesvirinae* and *Betaherpesvirinae* lytic replication, respectively, would also elucidate whether K^+ channel conservation occurs within subfamilies.

References

- Abbott, B., Fukuda, D., Dorman, D., Occolowitz, J., Debono, M. and Farhner, L., 1979. Microbial transformation of A23187, a divalent cation ionophore antibiotic. *Antimicrobial Agents and Chemotherapy*, 16(6), pp.808-812.
- Agrawal, U., Kumari, N., Vasudeva, P., Mohanty, N. and Saxena, S., 2018. Overexpression of COX2 indicates poor survival in urothelial bladder cancer. *Annals of Diagnostic Pathology*, 34, pp.50-55.
- Aneja, K. and Yuan, Y., 2017. Reactivation and Lytic Replication of Kaposi's Sarcoma-Associated Herpesvirus: An Update. *Frontiers in Microbiology*, 8.
- Albà, M., Das, R., Orengo, C. and Kellam, P., 2001. Genomewide Function Conservation and Phylogeny in the Herpesviridae. *Genome Research*, 11(1), pp.43-54.
- Alexander, S., Mathie, A. and Peters, J., 2011. ION CHANNELS. *British Journal of Pharmacology*, 164, pp.S137-S174.
- Arias, C., Weisburd, B., Stern-Ginossar, N., Mercier, A., Madrid, A., Bellare, P., Holdorf, M., Weissman, J. and Ganem, D., 2014. KSHV 2.0: A Comprehensive Annotation of the Kaposi's Sarcoma-Associated Herpesvirus Genome Using Next-Generation Sequencing Reveals Novel Genomic and Functional Features. *PLOS Pathogens*, 10(1), p.e1003847.
- Bailey, S. and Macardle, P., 2006. A flow cytometric comparison of Indo-1 to fluo-3 and Fura Red excited with low power lasers for detecting Ca²⁺ flux. *Journal of Immunological Methods*, 311(1-2), pp.220-225.
- Bajaj, S. and Han, J., 2019. Venom-Derived Peptide Modulators of Cation-Selective Channels: Friend, Foe or Frenemy. *Frontiers in Pharmacology*, 10.
- Bakhramov A, Boriskin Y, Booth J, Bolton T. 1995. Activation and deactivation of membrane currents in human fibroblasts following infection with human cytomegalovirus. *Biochimica et Biophysica Acta (BBA) - Molecular Cell Research*. 1265(2-3):143-151.
- Balkwill, F., 2006. TNF- α in promotion and progression of cancer. *Cancer and Metastasis Reviews*, 25(3), pp.409-416.
- Birkmann, A. and Zimmermann, H., 2016. HSV antivirals – current and future treatment options. *Current Opinion in Virology*, 18, pp.9-13.
- Bower, M., Nelson, M., Young, A., Thirlwell, C., Newsom-Davis, T., Mandalia, S., Dhillon, T., Holmes, P., Gazzard, B. and Stebbing, J., 2005. Immune Reconstitution Inflammatory Syndrome Associated With Kaposi's Sarcoma. *Journal of Clinical Oncology*, 23(22), pp.5224-5228.
- Broussard, G. and Damania, B., 2020. KSHV: Immune Modulation and Immunotherapy. *Frontiers in Immunology*, 10.
- Brown, B., Nguyen, H. and Wulff, H., 2019. Recent advances in our understanding of the structure and function of more unusual cation channels. *F1000Research*, 8, p.123.
- Carter, J. and Saunders, V., 2008. *Virology, Principles and Applications*. Chichester: Wiley.
- Cesarman, E., Damania, B., Krown, S., Martin, J., Bower, M. and Whitby, D., 2019. Kaposi sarcoma. *Nature Reviews Disease Primers*, 5(1).

- Chang, J., Renne, R., Dittmer, D. and Ganem, D., 2000. Inflammatory Cytokines and the Reactivation of Kaposi's Sarcoma-Associated Herpesvirus Lytic Replication. *Virology*, 266(1), pp.17-25.
- Charlton, F., Pearson, H., Hover, S., Lippiat, J., Fontana, J., Barr, J. and Mankouri, J., 2020. Ion Channels as Therapeutic Targets for Viral Infections: Further Discoveries and Future Perspectives. *Viruses*, 12(8), p.844.
- Chatterjee, M., Osborne J., Bestetti G., Chang Y., Moore P.S., 2002. Viral IL-6-Induced Cell Proliferation and Immune Evasion of Interferon Activity. *Science*, 298(5597), pp.1432-1435.
- Chen, W., Xu, C., Wang, L., Shen, B. and Wang, L., 2018. K15 Protein of Kaposi's Sarcoma Herpesviruses Increases Endothelial Cell Proliferation and Migration through Store-Operated Calcium Entry. *Viruses*, 10(6), p.282.
- Cheshenko, N., Del Rosario, B., Woda, C., Marcellino, D., Satlin, L. and Herold, B., 2003. Herpes simplex virus triggers activation of calcium-signaling pathways. *Journal of Cell Biology*, 163(2), pp.283-293.
- Chiang, E., Li, T., Jeet, S., Peng, I., Zhang, J., Lee, W., DeVoss, J., Caplazi, P., Chen, J., Warming, S., Hackos, D., Mukund, S., Koth, C. and Grogan, J., 2017. Potassium channels Kv1.3 and KCa3.1 cooperatively and compensatorily regulate antigen-specific memory T cell functions. *Nature Communications*, 8(1).
- Choi, J., Means, R., Damania, B. and Jung, J., 2001. Molecular piracy of Kaposi's sarcoma associated herpesvirus. *Cytokine & Growth Factor Reviews*, 12(2-3), pp.245-257.
- Clapham, D., 2007. Calcium Signaling. *Cell*, 131(6), pp.1047-1058.
- Coen, N., Duraffour, S., Snoeck, R. and Andrei, G., 2014. KSHV Targeted Therapy: An Update on Inhibitors of Viral Lytic Replication. *Viruses*, 6(11), pp.4731-4759.
- Colombo, D., Chimenti, S., Grossi, P., Marchesoni, A., Di Nuzzo, S., Griseta, V., Gargiulo, A., Parodi, A., Simoni, L. and Bellia, G., 2014. Prevalence of Past and Reactivated Viral Infections and Efficacy of Cyclosporine A as Monotherapy or in Combination in Patients with Psoriatic Arthritis—Synergy Study: A Longitudinal Observational Study. *BioMed Research International*, 2014, pp.1-7.
- Connolly, S.A., Jardetzky, T.S. and Longnecker, R., 2021. The structural basis of herpesvirus entry. *Nature reviews Microbiology*, 19(2), pp.110-121.
- Das, D.K., Bulow, U., Diehl, W.E., Durham, N.D., Senjobe, F., Chandran, K., Luban, J. and Munro, J.B., 2020. Conformational changes in the Ebola virus membrane fusion machine induced by pH, Ca²⁺, and receptor binding. *PLoS biology*, 18(2), p.e3000626.
- de Lera Ruiz, M. and Kraus, R., 2015. Voltage-Gated Sodium Channels: Structure, Function, Pharmacology, and Clinical Indications. *Journal of Medicinal Chemistry*, 58(18), pp.7093-7118.
- Dellis, O., Arbabian, A., Papp, B., Rowe, M., Joab, I. and Chomienne, C., 2011. Epstein-Barr Virus Latent Membrane Protein 1 Increases Calcium Influx through Store-operated Channels in B Lymphoid Cells. *Journal of Biological Chemistry*, 286(21), pp.18583-18592.
- Deng, H., Chu, J., Rettig, M., Martinez-Maza, O. and Sun, R., 2002. Rta of the human herpesvirus 8/Kaposi sarcoma-associated herpesvirus up-regulates human interleukin-6 gene expression. *Blood*, 100(5), pp.1919-1921.

Ding, L., Jiang, P., Xu, X., Lu, W., Yang, C., Li, L., Zhou, P. and Liu, S., 2021. T-type calcium channels blockers inhibit HSV-2 infection at the late stage of genome replication. *European Journal of Pharmacology*, 892, p.173782.

D'Alessandro, S., Scaccabarozzi, D., Signorini, L., Perego, F., Ilboudo, D., Ferrante, P. and Delbue, S., 2020. The Use of Antimalarial Drugs against Viral Infection. *Microorganisms*, 8(1), p.85.

Feng, P., Park, J., Lee, B., Lee, S., Bram, R. and Jung, J., 2002. Kaposi's Sarcoma-Associated Herpesvirus Mitochondrial K7 Protein Targets a Cellular Calcium-Modulating Cyclophilin Ligand To Modulate Intracellular Calcium Concentration and Inhibit Apoptosis. *Journal of Virology*, 76(22), pp.11491-11504.

Foster, T.L., Verow, M., Wozniak, A.L., Bentham, M.J., Thompson, J., Atkins, E., Weinman, S.A., Fishwick, C., Foster, R., Harris, M. and Griffin, S., 2011. Resistance mutations define specific antiviral effects for inhibitors of the hepatitis C virus p7 ion channel. *Hepatology*, 54(1), pp.79-90.

Frishman, W., 1997. Mibefradil: A New Selective T-Channel Calcium Antagonist for Hypertension and Angina Pectoris. *Journal of Cardiovascular Pharmacology and Therapeutics*, 2(4), pp.321-330.

Gackière, F., Warnier, M., Katsogiannou, M., Derouiche, S., Delcourt, P., Dewailly, E., Slomianny, C., Humez, S., Prevarskaya, N., Roudbaraki, M. and Mariot, P., 2013. Functional coupling between large-conductance potassium channels and Cav3.2 voltage-dependent calcium channels participates in prostate cancer cell growth. *Biology Open*, 2(9), pp.941-951.

Gershon, A., Breuer, J., Cohen, J., Cohrs, R., Gershon, M., Gilden, D., Grose, C., Hambleton, S., Kennedy, P., Oxman, M., Seward, J. and Yamanishi, K., 2015. Varicella zoster virus infection. *Nature Reviews Disease Primers*, 1(1).

Giulianelli, S., Riggio, M., Guillardoy, T., Pérez Piñero, C., Gorostiaga, M., Sequeira, G., Pataccini, G., Abascal, M., Toledo, M., Jacobsen, B., Guerreiro, A., Barros, A., Novaro, V., Monteiro, F., Amado, F., Gass, H., Abba, M., Helguero, L. and Lanari, C., 2019. FGF2 induces breast cancer growth through ligand-independent activation and recruitment of ER α and PRBD4 isoform to MYC regulatory sequences. *International Journal of Cancer*.

Gradoville, L., Gerlach, J., Grogan, E., Shedd, D., Nikiforow, S., Metroka, C. and Miller, G., 2000. Kaposi's Sarcoma-Associated Herpesvirus Open Reading Frame 50/Rta Protein Activates the Entire Viral Lytic Cycle in the HH-B2 Primary Effusion Lymphoma Cell Line. *Journal of Virology*, 74(13), pp.6207-6212.

Grimm, C., Chen, C., Wahl-Schott, C. and Biel, M., 2017. Two-Pore Channels: Catalyzers of Endolysosomal Transport and Function. *Frontiers in Pharmacology*, 08.

Grinde, B., 2013. Herpesviruses: latency and reactivation—viral strategies and host response. *Journal of oral microbiology*, 5(1), p.22766.

Griffiths, P., Baraniak, I. and Reeves, M., 2014. The pathogenesis of human cytomegalovirus. *The Journal of Pathology*, 235(2), pp.288-297.

Gunaratne, G.S., Yang, Y., Li, F., Walseth, T.F. and Marchant, J.S., 2018. NAADP-dependent Ca²⁺ signaling regulates Middle East respiratory syndrome-coronavirus pseudovirus translocation through the endolysosomal system. *Cell calcium*, 75, pp.30-41.

- Hancock, M., Crawford, L., Perez, W., Struthers, H., Mitchell, J. and Caposio, P., 2021. Human Cytomegalovirus UL7, miR-US5-1, and miR-UL112-3p Inactivation of FOXO3a Protects CD34+ Hematopoietic Progenitor Cells from Apoptosis. *mSphere*, 6(1).
- Hogan, P., Lewis, R. and Rao, A., 2010. Molecular Basis of Calcium Signaling in Lymphocytes: STIM and Orai. *Annual Review of Immunology*, 28(1), pp.491-533.
- Hover, S., King, B., Hall, B., Loundras, E.A., Taqi, H., Daly, J., Dallas, M., Peers, C., Schnettler, E., McKimmie, C. and Kohl, A., 2016. Modulation of potassium channels inhibits bunyavirus infection. *Journal of Biological Chemistry*, 291(7), pp.3411-3422.
- Hover, S., Foster, B., Barr, J. and Mankouri, J., 2017. Viral dependence on cellular ion channels – an emerging anti-viral target?. *Journal of General Virology*, 98(3), pp.345-351.
- Hurt, A.C., Ho, H.T. and Barr, I., 2006. Resistance to anti-influenza drugs: adamantanes and neuraminidase inhibitors. *Expert review of anti-infective therapy*, 4(5), pp.795-805.
- ICTV, 2021. Taxonomy. [online] Talk.ictvonline.org. Available at: <<https://talk.ictvonline.org/taxonomy/>> [Accessed 18 March 2021].
- Iwata, M., Komori, S., Unno, T., Minamoto, N. and Ohashi, H., 1999. Modification of membrane currents in mouse neuroblastoma cells following infection with rabies virus. *British journal of pharmacology*, 126(8), pp.1691-1698.
- James, C., Harfouche, M., Welton, N., Turner, K., Abu-Raddad, L., Gottlieb, S. and Looker, K., 2020. Herpes simplex virus: global infection prevalence and incidence estimates, 2016. *Bulletin of the World Health Organization*, 98(5), pp.315-329.
- Jang, S., Byun, J., Jeon, W., Choi, S., Park, J., Lee, B., Yang, J., Park, J., O'Grady, S., Kim, D., Ryu, P., Joo, S. and Lee, S., 2015. Nuclear Localization and Functional Characteristics of Voltage-gated Potassium Channel Kv1.3. *Journal of Biological Chemistry*, 290(20), pp.12547-12557.
- Jang, S., Choi, S., Ryu, P. and Lee, S., 2011. Anti-proliferative effect of Kv1.3 blockers in A549 human lung adenocarcinoma in vitro and in vivo. *European Journal of Pharmacology*, 651(1-3), pp.26-32.
- Jary, M., Hasanova, R., Vienot, A., Asgarov, K., Loyon, R., Tirole, C., Bouard, A., Orillard, E., Klajner, E., Kim, S., Viot, J., Colle, E., Adotevi, O., Bouché, O., Lecomte, T., Borg, C. and Feugeas, J., 2020. Molecular description of ANGPT2 associated colorectal carcinoma. *International Journal of Cancer*, 147(7), pp.2007-2018.
- Kalman, K., Pennington, M., Lanigan, M., Nguyen, A., Rauer, H., Mahnir, V., Paschetto, K., Kem, W., Grissmer, S., Gutman, G., Christian, E., Cahalan, M., Norton, R. and Chandy, K., 1998. ShK-Dap22, a Potent Kv1.3-specific Immunosuppressive Polypeptide. *Journal of Biological Chemistry*, 273(49), pp.32697-32707.
- Kapoor, A., Cai, H., Forman, M., He, R., Shamay, M. and Arav-Boger, R., 2012. Human Cytomegalovirus Inhibition by Cardiac Glycosides: Evidence for Involvement of the hERG Gene. *Antimicrobial Agents and Chemotherapy*, 56(9), pp.4891-4899.
- Karsan, N., Palethorpe, D., Rattanawong, W., Marin, J., Bhola, R. and Goadsby, P., 2018. Flunarizine in migraine-related headache prevention: results from 200 patients treated in the UK. *European Journal of Neurology*, 25(6), pp.811-817.

- Katano H, Sato Y, Itoh H, Sata T. Expression of human herpesvirus 8 (HHV-8)-encoded immediate early protein, open reading frame 50, in HHV-8-associated diseases. *J Hum Virol*. 2001 Mar-Apr;4(2):96-102. PMID: 11437319.
- Katano, H., Sato, Y., Kurata, T., Mori, S. and Sata, T., 2000. Expression and Localization of Human Herpesvirus 8-Encoded Proteins in Primary Effusion Lymphoma, Kaposi's Sarcoma, and Multicentric Castleman's Disease. *Virology*, 269(2), pp.335-344.
- Kennedy P, Montague P, Scott F, Grinfeld E, Ashrafi G, Breuer J et al. 2013. Varicella-Zoster Viruses Associated with Post-Herpetic Neuralgia Induce Sodium Current Density Increases in the ND7-23 Nav-1.8 Neuroblastoma Cell Line. *PLOS ONE*. 8(1):e51570.
- Kennedy, P., Rovnak, J., Badani, H. and Cohrs, R., 2015. A comparison of herpes simplex virus type 1 and varicella-zoster virus latency and reactivation. *Journal of General Virology*, 96(7), pp.1581-1602.
- King, J., Justice, A., Roberts, M., Chang, C. and Fusco, J., 2003. Long-Term HIV/AIDS Survival Estimation in the Highly Active Antiretroviral Therapy Era. *Medical Decision Making*, 23(1), pp.9-20.
- Kostopoulou, O., Wilhelmi, V., Raiss, S., Ananthaseshan, S., Lindström, M., Bartek, J. and Söderberg-Naucler, C., 2017. Human cytomegalovirus and Herpes Simplex type I virus can engage RNA polymerase I for transcription of immediate early genes. *Oncotarget*, 8(57), pp.96536-96552.
- Krasznai, Z., Márián, T., Balkay, L., Emri, M. and Trón, L., 1995. Flow cytometric determination of absolute membrane potential of cells. *Journal of Photochemistry and Photobiology B: Biology*, 28(1), pp.93-99.
- Kshatri, A., Gonzalez-Hernandez, A. and Giraldez, T., 2018. Physiological Roles and Therapeutic Potential of Ca²⁺ Activated Potassium Channels in the Nervous System. *Frontiers in Molecular Neuroscience*, 11.
- Lin, S., Tzeng, B., Lee, K., Smith, R., Campbell, K. and Chen, C., 2014. Cav3.2 T-type calcium channel is required for the NFAT-dependent Sox9 expression in tracheal cartilage. *Proceedings of the National Academy of Sciences*, 111(19), pp.E1990-E1998.
- Liu, J., 2009. Calmodulin-dependent phosphatase, kinases, and transcriptional corepressors involved in T-cell activation. *Immunological Reviews*, 228(1), pp.184-198.
- Liu, R., Zhi, X., Zhou, Z., Zhang, H., Yang, R., Zou, T. and Chen, C., 2018. Mithramycin A suppresses basal triple-negative breast cancer cell survival partially via down-regulating Krüppel-like factor 5 transcription by Sp1. *Scientific Reports*, 8(1).
- Mankouri, J., Dallas, M.L., Hughes, M.E., Griffin, S.D., Macdonald, A., Peers, C. and Harris, M., 2009. Suppression of a pro-apoptotic K⁺ channel as a mechanism for hepatitis C virus persistence. *Proceedings of the National Academy of Sciences*, 106(37), pp.15903-15908.
- Mathie, A., Veale, E., Cunningham, K., Holden, R. and Wright, P., 2021. Two-Pore Domain Potassium Channels as Drug Targets: Anesthesia and Beyond. *Annual Review of Pharmacology and Toxicology*, 61(1), pp.401-420.
- Matsumura, S., Persson, L.M., Wong, L. and Wilson, A.C., 2010. The latency-associated nuclear antigen interacts with MeCP2 and nucleosomes through separate domains. *Journal of virology*, 84(5), pp.2318-2330.

- Mesri, E.A., Cesarman, E. and Boshoff, C., 2010. Kaposi's sarcoma and its associated herpesvirus. *Nat Rev Cancer*. 10 (10), pp.707-719.
- Mojic, M., Takeda, K. and Hayakawa, Y., 2017. The Dark Side of IFN- γ : Its Role in Promoting Cancer Immuno-evasion. *International Journal of Molecular Sciences*, 19(1), p.89.
- Monteith, G., Prevarskaya, N. and Roberts-Thomson, S., 2017. The calcium–cancer signalling nexus. *Nature Reviews Cancer*, 17(6), pp.373-380.
- Müller, M., Slivinski, N., Todd, E.J., Khalid, H., Li, R., Karwatka, M., Merits, A., Mankouri, J. and Tuplin, A., 2019. Chikungunya virus requires cellular chloride channels for efficient genome replication. *PLoS neglected tropical diseases*, 13(9), p.e0007703.
- Narkhede, M., Arora, S. and Ujjani, C., 2018. Primary effusion lymphoma: current perspectives. *OncoTargets and Therapy*, Volume 11, pp.3747-3754.
- Oberstein, A. and Shenk, T., 2017. Cellular responses to human cytomegalovirus infection: Induction of a mesenchymal-to-epithelial transition (MET) phenotype. *Proceedings of the National Academy of Sciences*, 114(39), pp.E8244-E8253.
- Ou, X., Liu, Y., Lei, X., Li, P., Mi, D., Ren, L., Guo, L., Guo, R., Chen, T., Hu, J. and Xiang, Z., 2020. Characterization of spike glycoprotein of SARS-CoV-2 on virus entry and its immune cross-reactivity with SARS-CoV. *Nature communications*, 11(1), pp.1-12.
- O'Grady, S. and Lee, S. (2005). Molecular diversity and function of voltage-gated (Kv) potassium channels in epithelial cells. *The International Journal of Biochemistry & Cell Biology*, 37(8), pp.1578-1594.
- Panou, M.M., Antoni, M., Morgan, E.L., Loundras, E.A., Wasson, C.W., Welberry-Smith, M., Mankouri, J. and Macdonald, A., 2020. Glibenclamide inhibits BK polyomavirus infection in kidney cells through CFTR blockade. *Antiviral research*, 178, p.104778.
- Parravicini, C., Chandran, B., Corbellino, M., Berti, E., Paulli, M., Moore, P. and Chang, Y., 2000. Differential Viral Protein Expression in Kaposi's Sarcoma-Associated Herpesvirus-Infected Diseases. *The American Journal of Pathology*, 156(3), pp.743-749.
- Piotrowski, I., Kulcenty, K. and Suchorska, W., 2020. Interplay between inflammation and cancer. *Reports of Practical Oncology & Radiotherapy*, 25(3), pp.422-427.
- Piret J, Boivin G. Resistance of Herpes Simplex Viruses to Nucleoside Analogues: Mechanisms, Prevalence, and Management. *Antimicrobial Agents and Chemotherapy*. 2010;55(2):459-472.
- Poole, C. and James, S., 2018. Antiviral Therapies for Herpesviruses: Current Agents and New Directions. *Clinical Therapeutics*, 40(8), pp.1282-1298.
- Rohner, E., Valeri, F., Maskew, M., Prozesky, H., Rabie, H., Garone, D., Dickinson, D., Chimbetete, C., Lumano-Mulenga, P., Sikazwe, I., Wyss, N., Clough-Gorr, K., Egger, M., Chi, B. and Bohlius, J., 2014. Incidence Rate of Kaposi Sarcoma in HIV-Infected Patients on Antiretroviral Therapy in Southern Africa. *JAIDS Journal of Acquired Immune Deficiency Syndromes*, 67(5), pp.547-554.
- Rossier, M., 2016. T-Type Calcium Channel: A Privileged Gate for Calcium Entry and Control of Adrenal Steroidogenesis. *Frontiers in Endocrinology*, 7.
- Scott, C. and Griffin, S., 2015. Viroporins: structure, function and potential as antiviral targets. *Journal of General Virology*, 96(8), pp.2000-2027.

- Shannon-Lowe, C. and Rickinson, A., 2019. The Global Landscape of EBV-Associated Tumors. *Frontiers in Oncology*, 9.
- Sharma-Walia, N., George Paul, A., Patel, K., Chandran, K., Ahmad, W. and Chandran, B., 2010. NFAT and CREB Regulate Kaposi's Sarcoma-Associated Herpesvirus-Induced Cyclooxygenase 2 (COX-2). *Journal of Virology*, 84(24), pp.12733-12753.
- Shou, J., Jing, J., Xie, J., You, L., Jing, Z., Yao, J., Han, W. and Pan, H., 2015. Nuclear factor of activated T cells in cancer development and treatment. *Cancer Letters*, 361(2), pp.174-184.
- Stankus, S. J., Dlugopolski, M., & Packer, D., 2000. Management of herpes zoster (shingles) and postherpetic neuralgia. *American family physician*, 61(8), 2437–2448.
- Stauffer, S., Feng, Y., Nebioglu, F., Heilig, R., Picotti, P. and Helenius, A., 2014. Stepwise priming by acidic pH and a high K⁺ concentration is required for efficient uncoating of influenza A virus cores after penetration. *Journal of virology*, 88(22), pp.13029-13046.
- Strange, K., Yamada, T. and Denton, J., 2019. A 30-year journey from volume-regulated anion currents to molecular structure of the LRRC8 channel. *Journal of General Physiology*, 151(2), pp.100-117.
- Straus, M., Bidon, M., Tang, T., Whittaker, G. and Daniel, S., 2020. FDA approved calcium channel blockers inhibit SARS-CoV-2 infectivity in epithelial lung cells. *Cold Spring Harbor Laboratory (COVID-19 SARS-CoV-2 preprints from medRxiv and bioRxiv)* [online] Available from: <https://www.biorxiv.org/content/10.1101/2020.07.21.214577v3>
- Tarcha, E., Olsen, C., Probst, P., Peckham, D., Muñoz-Elías, E., Kruger, J. and Iadonato, S., 2017. Safety and pharmacodynamics of dalazatide, a Kv1.3 channel inhibitor, in the treatment of plaque psoriasis: A randomized phase 1b trial. *PLOS ONE*, 12(7), p.e0180762.
- Uldrick, T., Polizzotto, M., Aleman, K., Wyvill, K., Marshall, V., Whitby, D., Wang, V., Pittaluga, S., O'Mahony, D., Steinberg, S., Little, R. and Yarchoan, R., 2014. Rituximab plus liposomal doxorubicin in HIV-infected patients with KSHV-associated multicentric Castleman disease. *Blood*, 124(24), pp.3544-3552.
- Vaeth, M. and Feske, S., 2018. NFAT control of immune function: New Frontiers for an Abiding Trooper. *F1000Research*, 7, p.260.
- Walsh, K., 2020. Screening Technologies for Inward Rectifier Potassium Channels: Discovery of New Blockers and Activators. *SLAS DISCOVERY: Advancing the Science of Drug Discovery*, 25(5), pp.420-433.
- Wang, L., Wang, N., Lu, X., Liu, B., Yanda, M., Song, J., Dai, H., Sun, Y., Bao, H., Eaton, D. and Ma, H., 2012. Rituximab inhibits Kv1.3 channels in human B lymphoma cells via activation of FcγRIIB receptors. *Biochimica et Biophysica Acta (BBA) - Molecular Cell Research*, 1823(2), pp.505-513.
- Wendt, E., Ferry, H., Greaves, D. and Keshav, S., 2015. Ratiometric Analysis of Fura Red by Flow Cytometry: A Technique for Monitoring Intracellular Calcium Flux in Primary Cell Subsets. *PLOS ONE*, 10(4), p.e0119532.
- Woodward, M., Marko, A., Galea, S., Egel, B. and Straus, W., 2019. Varicella Virus Vaccine Live: A 22-Year Review of Postmarketing Safety Data. *Open Forum Infectious Diseases*, 6(8).

Wu, L., Lin, W., Liao, Q., Wang, H., Lin, C., Tang, L., Lian, W., Chen, Z., Li, K., Xu, L., Zhou, R., Ding, Y. and Zhao, L., 2020. Calcium Channel Blocker Nifedipine Suppresses Colorectal Cancer Progression and Immune Escape by Preventing NFAT2 Nuclear Translocation. *Cell Reports*, 33(4), p.108327.

Wulff, H., Knaus, H., Pennington, M. and Chandy, K. (2004). K⁺ Channel Expression during B Cell Differentiation: Implications for Immunomodulation and Autoimmunity. *The Journal of Immunology*, 173(2), pp.776-786.

Wulff, H. and Zhorov, B., 2008. K⁺ Channel Modulators for the Treatment of Neurological Disorders and Autoimmune Diseases. *Chemical Reviews*, 108(5), pp.1744-1773.

Xu, Z., Zhang, Y., Xu, M., Zheng, X., Lin, M., Pan, J., Ye, C., Deng, Y., Jiang, C., Lin, Y., Lu, X. and Chi, P., 2019. Demethylation and Overexpression of CSF2 are Involved in Immune Response, Chemotherapy Resistance, and Poor Prognosis in Colorectal Cancer. *OncoTargets and Therapy*, Volume 12, pp.11255-11269.

Yoast, R., Emrich, S. and Trebak, M., 2020. The anatomy of native CRAC channel(s). *Current Opinion in Physiology*, 17, pp.89-95.

Yu, X., Sha, J., Xiang, S., Qin, S., Conrad, P., Ghosh, S., Weinberg, A. and Ye, F., 2016. Suppression of KSHV-induced angiopoietin-2 inhibits angiogenesis, infiltration of inflammatory cells, and tumor growth. *Cell Cycle*, 15(15), pp.2053-2065.

Zamponi, G., Striessnig, J., Koschak, A. and Dolphin, A., 2015. The Physiology, Pathology, and Pharmacology of Voltage-Gated Calcium Channels and Their Future Therapeutic Potential. *Pharmacological Reviews*, 67(4), pp.821-870.

Zanella, M., Cordey, S. and Kaiser, L., 2020. Beyond Cytomegalovirus and Epstein-Barr Virus: a Review of Viruses Composing the Blood Virome of Solid Organ Transplant and Hematopoietic Stem Cell Transplant Recipients. *Clinical Microbiology Reviews*, 33(4).

Zhang, L., Sun, Y., Zeng, H., Wang, Q., Jiang, X., Shang, W., Wu, Y., Li, S., Zhang, Y., Hao, Z., Chen, H., Jin, R., Liu, W., Li, H., Peng, K. and Xiao, G., 2020. Calcium channel blocker amlodipine besylate therapy is associated with reduced case fatality rate of COVID-19 patients with hypertension. *Cell Discovery*, 6(1).

Zhang, Q., Hsia, S. and Martin-Caraballo, M., 2019. Regulation of T-type Ca²⁺ channel expression by interleukin-6 in sensory-like ND7/23 cells post-herpes simplex virus (HSV-1) infection. *Journal of Neurochemistry*, 151(2), pp.238-254.

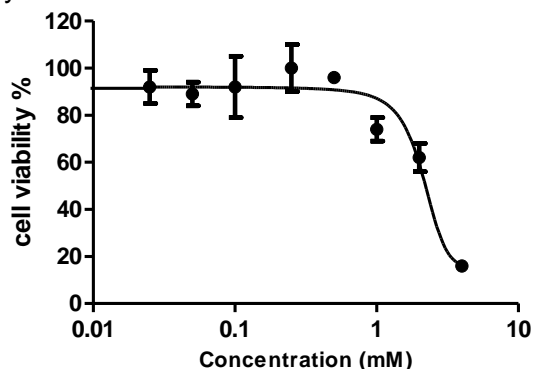
Zhang, W., Fujii, N. and Naren, A., 2012. Recent advances and new perspectives in targeting CFTR for therapy of cystic fibrosis and enterotoxin-induced secretory diarrheas. *Future Medicinal Chemistry*, 4(3), pp.329-345.

Zheng, K., Chen, M., Xiang, Y., Ma, K., Jin, F., Wang, X., Wang, X., Wang, S. and Wang, Y., 2014. Inhibition of herpes simplex virus type 1 entry by chloride channel inhibitors tamoxifen and NPPB. *Biochemical and Biophysical Research Communications*, 446(4), pp.990-996.

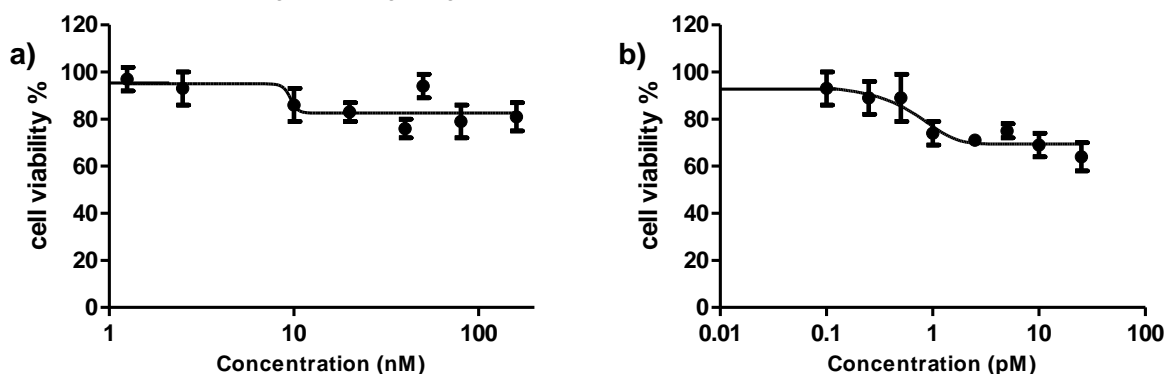
Zoetewij JP, Moses AV, Rinderknecht AS, Davis DA, Overwijk WW, Yarchoan R, Orenstein JM, Blauvelt A. 2001. Targeted inhibition of calcineurin signaling blocks calcium-dependent reactivation of Kaposi sarcoma-associated herpesvirus. *Blood*. 97(8):2374-2380.

Appendix

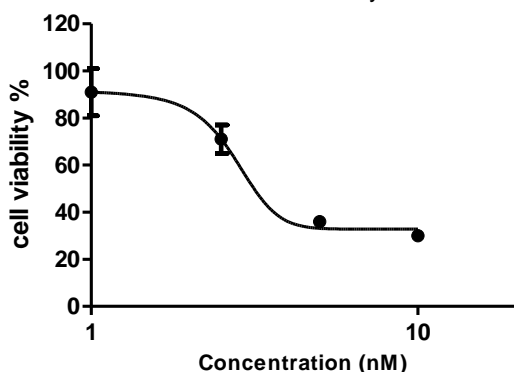
Prior to use in reactivation and infection experiments, each compound was used to determine cell viability post-treatment in an MTS assay, thus enabling subsequent experiments at non-cytotoxic concentrations.



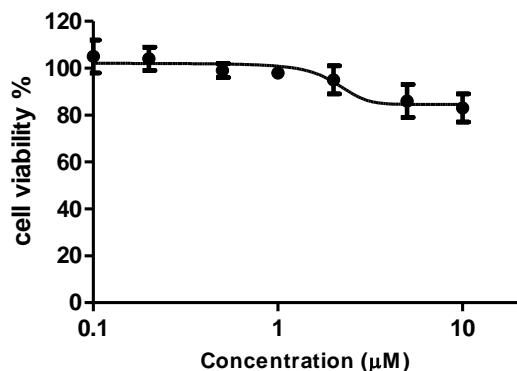
Supplementary Figure 1 Cell viability of TREx BCBL1-Rta in the presence 4AP. TREx BCBL1-Rta cells were treated with varying concentrations of 4AP for 24 hours before cell survival was assessed via MTS assay. Results are presented on an XY-graph using a log-scale.



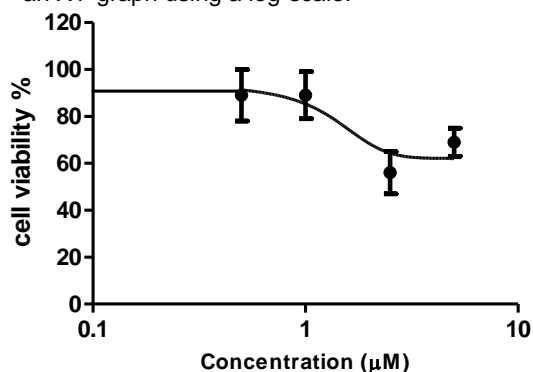
Supplementary Figure 2 Cell viability of TREx BCBL1-Rta in the presence of MgTX (a) or ShK (b). TREx BCBL1-Rta cells were treated with varying concentrations of MgTX for 24 hours or ShK for 48 hours before cell survival was assessed via MTS assay. Results are presented on an XY-graph using a log-scale.



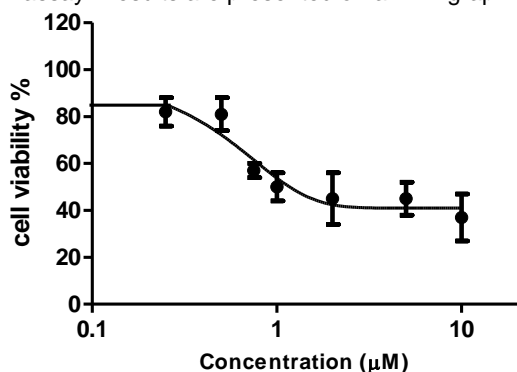
Supplementary Figure 3 Cell viability of TREx BCBL1-Rta in the presence of TRAM. TREx BCBL1-Rta cells were treated with varying concentrations of TRAM for 24 hours before cell survival was assessed via MTS assay. Results are presented on an XY-graph using a log-scale.



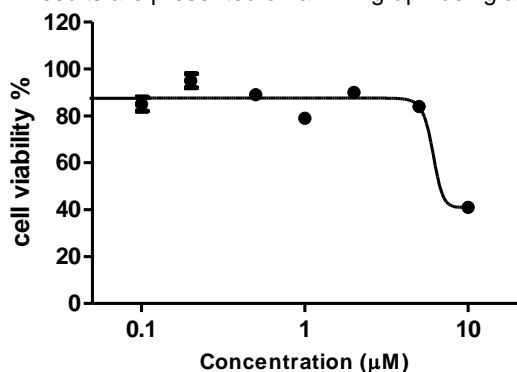
Supplementary Figure 4 Cell viability of U87 in the presence of Mith A. U87 cells were treated with varying concentrations of Mith A for 24 hours before cell survival was assessed via MTS assay. Results are presented on an XY-graph using a log-scale.



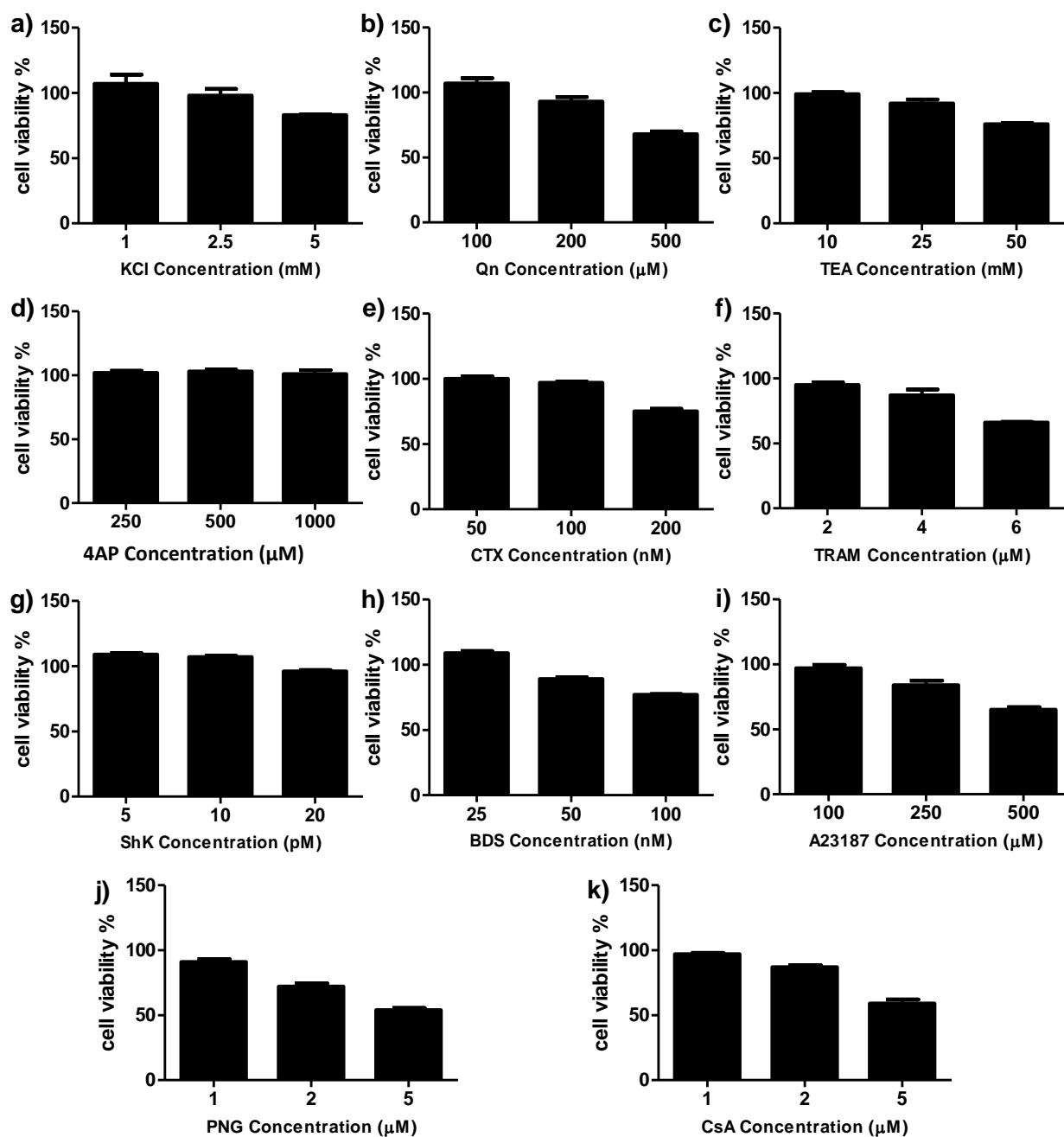
Supplementary Figure 5 Cell viability of TREx BCBL1-Rta in the presence of A23187. TREx BCBL1-Rta cells were treated with varying concentrations of A23187 for 24 hours before cell survival was assessed via MTS assay. Results are presented on an XY-graph using a log-scale.



Supplementary Figure 6 Cell viability of TREx BCBL1-Rta in the presence of PNG. TREx BCBL1-Rta cells were treated with varying concentrations of PNG for 24 hours before cell survival was assessed via MTS assay. Results are presented on an XY-graph using a log-scale.



Supplementary Figure 7 Cell viability of TREx BCBL1-Rta in the presence of MgTX (a) or ShK (b). TREx BCBL1-Rta cells were treated with varying concentrations of MgTX for 24 hours or ShK for 48 hours before cell survival was assessed via MTS assay. Results are presented on an XY-graph using a log-scale.



Supplementary Figure 8 Cell viability of HFF in the presence of various inhibitors and ionophores. HFF cells were treated with varying concentrations of KCl (a), Qn (b), TEA (c), 4AP (d), CTX (e), TRAM (f), ShK (g), BDS (h), A23187 (i), PNG(j) and CsA (k) for 1 week before cell survival was assessed via MTS assay. Results are presented on an XY-graph using a log-scale.